NASA-CR-202202

FINAL REPORT

Submitted to:	NASA Marshall Space Flight Center
Grant Title:	THEORY AND COMPUTATION OF OPTIMAL LOW- AND MEDIUM-THRUST ORBIT TRANSFERS
Grant Number:	NAG8-921
Principal Investigator / Project Director:	Dr. Jason C.H. Chuang School of Aerospace Engineering Georgia Institute of Technology Atlanta, GA 30332-0150 Phone: (404)894-3075 Fax: (404)894-2760 E-mail: ch.chuang@aerospace.gatech.edu
Research Assistants:	Troy D. Goodson Laura A. Ledsinger School of Aerospace Engineering Georgia Institute of Technology
Period Covered:	July 7, 1992 to June 30, 1996
Date of Submission:	July 26, 1996

TABLE OF CONTENTS

LIST OF ILLUSTRATIONS

LIST OF SYMBOLS

Bold type always indicates a vector quantity

For variables, italics indicates a scalar quantity

Vectors with Greek symbols are indicated by plain text with no italics

Unless otherwise specified, subscripts refer to partial derivatives with respect to the subscripted variable.

$\mathbf{a}_{\times}$ denotes the skew symmetric matrix representation of the cross product:

$$\mathbf{a}_{\times} = \begin{bmatrix} 0 & -a_z & a_y \\ a_z & 0 & -a_x \\ -a_y & a_x & 0 \end{bmatrix} \text{ where } \mathbf{a} = \begin{bmatrix} a_x \\ a_y \\ a_z \end{bmatrix}$$

c	Characteristic velocity of the rocket motor. $c=g_o J_{sp}$.
C_D	The drag coefficient of the spacecraft, see Eq. (1.4)
C^i	Denotes the set of i-dimensional vector functions continuous with respect all arguments, vector and/or scalar
$diag\{z_1,\ldots z_N\}$	An NxN matrix where the jth diagonal element is z_j
$\mathbf{e}_T(t)$	Rocket motor thrust direction at time t (a unit vector)
e_x	The component of the eccentricity vector in the X-direction of OXYZ
e_y	The component of the eccentricity vector in the Y-direction of OXYZ
e_z	The component of the eccentricity vector in the Z-direction of OXYZ
$\mathbf{F}$	A Force acting on the spacecraft; cause of force denoted by subscript
g_o	Earth's gravitational acceleration at sea-level
G	An auxiliary function defined for derivation of the necessary conditions
H	The Hamiltonian, defined in the usual manner for bang-bang optimal control problems
H_T	The switching function, defined in the usual manner for bang-bang optimal control problems
h_x	The component of the angular momentum vector in the X-direction of OXYZ
h_y	The component of the angular momentum vector in the Y-direction of OXYZ

h_z	The component of the angular momentum vector in the Z-direction of OXYZ
$\mathbf{I}$	The identity matrix - if subscripts are given they denote its dimensions
I_{sp}	Specific impulse of the rocket motor
J	A cost functional or performance index
J_2	The constant describing the mass distribution of the central body; for Earth it is often taken as $J_2=1082.61\times10^{-6}$
$m(t)$	Total spacecraft mass at time t
$\overline{\mathbf{N}}$	The 3×3 matrix $diag\{1,1,3\}$
OXYZ	This is a Rectangular Cartesian inertial reference frame. Here O is fixed at the gravitational center. The directions X,Y,Z form a right-handed system; X and Y are in the equatorial plane. Z completes the right-handed system.
R_e	The equatorial radius of the gravitating body - for oblateness effects
R^i	Denotes the set of i-dimensional real numbers
$\mathbf{r}(t)$	Radius vector from origin O of OXYZ to spacecraft's location at time t
$r(t)$	Magnitude of $\mathbf{r}(t)$
r_o	Reference altitude for reference atmospheric density (ρ_o) in atmospheric model, see Eq. (1.4)
S	The cross sectional area of spacecraft used in computing drag, see Eq. (1.4)
$T_{\max}$	The upper bound on rocket motor thrust magnitude
t	Time
t_f	Transfer time, the total length of time required to execute the transfer
$T(t)$	Rocket motor thrust magnitude at time t
U	The gravitational potential function, see Eq. (1.5). This definition only holds in Section I
U	Denotes the set of piece-wise continuous scalar functions with one scalar argument. This definition does not hold in Section I
$\mathrm{u}(t)$	The component of $\mathbf{v}$ in the X-direction of OXYZ
$\mathrm{v}(t)$	The component of $\mathbf{v}$ in the Y-direction of OXYZ
$\mathbf{v}(t)$	Velocity vector in OXYZ at time t
$v(t)$	Magnitude of $\mathbf{v}(t)$
$\mathrm{w}(t)$	The component of $\mathbf{v}$ in the Z-direction of OXYZ
W_o	Weight of spacecraft at initial point of transfer.

$\mathbf{x}(t)$	The component of $\mathbf{r}$ in the X-direction of OXYZ
$\mathbf{x}(t)$	Vector $\left[\mathbf{r}^T(t) \quad \mathbf{v}^T(t) \quad m(t)\right]^T$; this definition changes in Section III
$\mathbf{y}(t)$	The component of $\mathbf{r}$ in the Y-direction of OXYZ
$\mathbf{z}(t)$	The component of $\mathbf{r}$ in the Z-direction of OXYZ
$\mathbf{z}$	State used in numerical computation
α_o, α_f	These vectors contain the orbital elements which are used to specify the initial and final orbits of the transfer, respectively.
α_i	A vector containing the orbital elements of the *i*th transfer orbit. For an N burn transfer the zeroth orbit is the initial orbit and the Nth orbit is the final orbit. This only applies for numeric subscripts.
β	Constant from the atmosphere model describing air density variation in the prescribed altitude region, see Eq. (1.4); this definition changes in Section III
Γ	Dummy nonsquare matrix used for generality in Lemma III.1
$\Gamma(\mathbf{x})$	Dummy matrix function used for generality in Lemma III.2
θ	The latitude angle of the current position from the equator; thrust angle in plane; this definition changes in Section III
λ_e	The Lagrange multiplier associated with the constraint on $\mathbf{e}_T$ magnitude
λ_m	The Lagrange multiplier associated with m
$\lambda_r(t)$	The Lagrange multiplier associated with $\mathbf{r}$
$\lambda_v(t)$	The Lagrange multiplier associated with $\mathbf{v}$
μ	The gravitational constant for the central body
ν_o, ν_f	Lagrange multipliers associated with boundary conditions at initial and final points
ρ_0	Atmospheric density at reference altitude (r_0) for atmospheric model, see Eq. (1.4)
τ	The independent variable used in numerical computation, represents normalized time
$\psi(\mathbf{x})$	Vector function that calculates the orbital elements for the state $\mathbf{x}$

Symbol Definitions Applying Only to Section III, Subsection III.2.2

t_{fj}	Transfer time for the *j*th burn

$\mathbf{e}_{T_j}(t)$	Thrust direction function for the *j*th burn
$\boldsymbol{\lambda}_j(t)$	Lagrange multiplier functions for the *j*th burn
ν_j	A vector containing the Lagrange multipliers associated with the respective boundary condition. Even indices indicate association with the final orbit; odd indices indicate association with the initial orbit.
β_j	The initial condition for the mass of the *j*th burn
ξ_j	The Lagrange multiplier associated with the initial mass constraint of the *j*th burn
$m_j(t)$	The mass as a function of time for the *j*th burn
$\mathbf{f}(\mathbf{x}_j(t), \mathbf{e}_{T_j}(t))$	Represents the state dynamics with the thrust always on, as in the one-burn problem.
$\bar{J}_j$	Adjoined cost functional for the *j*th burn of an approximate discretized problem; application of a direct optimization method is anticipated
$\overline{m}_{j,i}$	Final mass from the discrete problem, *j*th burn, at the *i*th time node
η_j	Same as ν_j except that these are for the discrete problem's boundary conditions
$\zeta_1(\mathbf{y}_{j,1})$	Function that computes the initial orbital elements associated with the initial state $\mathbf{y}_{j,1}$ for the discretized problem
$\zeta_2(\mathbf{y}_{j,M})$	Function that computes the initial orbital elements associated with the initial state $\mathbf{y}_{j,M}$ for the discretized problem
σ_j	The Lagrange multiplier associated with the initial mass constraint of the *j*th burn for the discretized problem
$\mu_{j,i}$	Lagrange multipliers associated with the state $\mathbf{y}_{j,i}$ for the *j*th burn at time node *i*, discretized problem
$\omega_{j,i}$	Thrust direction at time node *i*, for the *j*th burn, discretized problem
$\Delta_i(\mathbf{y}_{j,i}, \omega_{j,i})$	Constraint at time node *i* for the *j*th burn that enforces implicit integration, discretized problem

Symbol Definitions Applying Only to Section III, except Subsection III.2.2

$\mathbf{f}(\mathbf{x}(t))$	Defined in problem $\{P\}$, the state dynamics without control
$\mathbf{g}(y(t), \mathbf{v}(t))$	Defined in problem $\{P\}$, the controlled portion of the state dynamics

$\{I\}$	Defines a set of necessary conditions that represent a typical application of optimal control theory, excluding Pontryagin's Minimum Principle; defined in subsection III.2.4.
$\{II\}$	Defines a set of necessary conditions that represent the Patched method; defined in subsection III.2.4.
$\{III\}$	Defines a set of necessary conditions that represent the Modified Patched method; defined in subsection III.3.1.
$\{P\}$	A definition for an optimal control problem that generalizes the optimal orbit transfer problem; defined in subsection III.2.4.
t_o	The fixed initial time for the problem $\{P\}$
t_f	The free final time for the problem $\{P\}$
t_{si}	The switching times defined as variables in the conditions $\{I\}$
t_i	For conditions $\{II\}$ and $\{III\}$, the initial time of burn i
t_{fi}	For conditions $\{II\}$ and $\{III\}$, the final time of burn i
$u(t)$	Defined in problem $\{P\}$, the scalar control that appears linearly in the Hamiltonian; this is assumed to be a bang-bang control
u_{max}	The maximum value allowed for the control $u(t)$
$\mathbf{v}(t)$	Defined in problem $\{P\}$, the control vector that optimal control determines to be a continuous function of time.
$\mathbf{x}(t)$	State vector in problem $\{P\}$ that contains all states except $y(t)$. In problem $\{P\}$, conditions $\{I\}$, $\{II\}$, and $\{III\}$ these states are defined for the time interval $[t_o,t_f]$
$y(t)$	One of the states in problem $\{P\}$, separated from the rest of the state vector so that it may be treated separately. In $\{P\}$ and $\{I\}$ this state is Defined for the time interval $[t_o,t_f]$
$\hat{\lambda}(t)$	Defined in conditions $\{I\}$, Lagrange multiplier vector functions associated with the whole state vector - it is partitioned as $\left[\hat{\lambda}_x^T(t) \quad \hat{\lambda}_y(t)\right]^T$
$\bar{\lambda}_i(t)$	Defined in conditions $\{II\}$, Lagrange multiplier vector functions associated with the whole state vector on the ith $u=u_{max}$ arc, which is the interval $t \in \left[t_i, t_{fi}\right]$ for $i=1,..N$ - it is partitioned as $\left[\bar{\lambda}_{xi}^T(t) \quad \bar{\lambda}_{yi}(t)\right]$
$\hat{\lambda}_x(t)$	Defined in conditions $\{I\}$, Lagrange multiplier vector functions associated with the state vector $\mathbf{x}(t)$

$\hat{\lambda}_y(t)$	Defined in conditions $\{I\}$, Lagrange multiplier vector functions associated with the state $y(t)$
$\bar{\lambda}_{xi}(t)$	Defined in conditions $\{II\}$, Lagrange multiplier vector functions associated with the state vector $\mathbf{x}(t)$ on the ith $u=u_{max}$ arc, which is the interval $t \in [t_i, t_{fi}]$ for $i=1,..N$
$\bar{\lambda}_{yi}(t)$	Defined in conditions $\{II\}$, Lagrange multiplier vector functions associated with the state $y(t)$ on the ith $u=u_{max}$ arc, which is the interval $t \in [t_i, t_{fi}]$ for $i=1,..N$
$\hat{\nu}_o$	Defined in conditions $\{I\}$, the Lagrange multipliers associated with the boundary conditions at the initial time
$\hat{\nu}_f$	Defined in conditions $\{I\}$, the Lagrange multipliers associated with the boundary conditions at the final time
$\bar{\nu}_{oi}$	Defined in conditions $\{II\}$, the Lagrange multipliers associated with the boundary conditions at the time t_i for $i=1,...N$
$\bar{\nu}_{fi}$	Defined in conditions $\{II\}$, the Lagrange multipliers associated with the boundary conditions at the time t_{fi} for $i=1,...N$
$\lambda(t)$	Defined in conditions $\{III\}$, the Lagrange multiplier associated with the state $\mathbf{x}$ and $\lambda = [\lambda_r{}^T \quad \lambda_v{}^T]^T$
$\lambda_r(t)$	Defined in conditions $\{III\}$, the Lagrange multiplier associated with $\mathbf{r}$
$\lambda_v(t)$	Defined in conditions $\{III\}$, the Lagrange multiplier associated with $\mathbf{v}$
ν_i	Defined in conditions $\{III\}$, Lagrange multipliers associated with boundary conditions at i; $i=0,N+1$

Symbol Definitions Applying Only to Section IV

Lagrange multiplier symbols are the same as above, however, here they refer to a minimization problem.

$\mathbf{A}(t)$	Matrix in the differential equations for the linear correction to the state and Lagrange multipliers, control correction accounted for
$\mathbf{B}(t)$	Matrix in the differential equations for the linear correction to the state as depending on the Lagrange multiplier corrections, control correction accounted for

$\mathbf{C}(t)$	Matrix in the differential equations for the linear correction to the Lagrange multipliers as depending on the state corrections, control correction accounted for
dt_f	Correction to final time
H	The Hamiltonian
$\mathbf{P}(t)$, $\mathbf{S}(t)$, $\mathbf{V}(t)$	Sweepback matrices used to compute $\overline{\mathbf{P}}(t)$, $\overline{\mathbf{S}}(t)$, $\overline{\mathbf{V}}(t)$
$\overline{\mathbf{P}}(t)$, $\overline{\mathbf{S}}(t)$, $\overline{\mathbf{V}}(t)$	Sweepback matrices for free final time
$\mathbf{m}(t)$, $\mathbf{n}(t)$	Sweepback vectors used to compute $\overline{\mathbf{P}}(t)$, $\overline{\mathbf{S}}(t)$, $\overline{\mathbf{V}}(t)$
$\{t_1,\ldots,t_i,\ldots t_N\}$	Time nodes for discrete guidance with time-to-go
Δt_{s_i}	Length of guidance time interval i
dt_{f_i}	Correction to final time, computed at start of guidance time interval i
$\delta\mathbf{x}(t)$	Linear correction for the state of the nominal trajectory, control correction accounted for
$\alpha(t)$	Sweepback scalar
$\delta\theta(t)$	Control (thrust direction angle) correction
$\theta(t)$	Thrust direction angle (control)
$\delta\lambda(t)$	Linear correction for the Lagrange multipliers of the nominal trajectory, control correction accounted for
$d\nu$	Linear correction for the constant Lagrange multipliers, control correction accounted for
$\phi(\mathbf{x})$	Cost function for minimization problem
$\delta\psi$	Linear correction to boundary conditions, control correction accounted for
$\Omega(\mathbf{x},\nu,t)$	Hamiltonian for minimization problem

SUMMARY

This report presents new theoretical results which lead to new algorithms for the computation of fuel-optimal multiple-burn orbit transfers of low and medium thrust. Theoretical results introduced herein show how to add burns to an optimal trajectory and show that the traditional set of necessary conditions may be replaced with a much simpler set of equations. Numerical results are presented to demonstrate the utility of the theoretical results and the new algorithms.

Two indirect methods from the literature are shown to be effective for the optimal orbit transfer problem with relatively small numbers of burns. These methods are the Minimizing Boundary Condition Method (MBCM) and BOUNDSCO. Both of these methods make use of the first-order necessary conditions exactly as derived by optimal control theory.

Perturbations due to Earth's oblateness and atmospheric drag are considered. These perturbations are of greatest interest for transfers that take place between low Earth orbit altitudes and geosynchronous orbit altitudes. Example extremal solutions including these effects and computed by the aforementioned methods are presented.

It is a commonly accepted notion in the field of optimal orbit transfer that the more burns an optimal transfer executes, the lower the cost. Unfortunately, many numerical methods are not robust enough to simply "jump" from an N-burn solution to an N+1 burn solution. A new algorithm is presented which greatly eases this process. The method is just as easily implemented in the framework of MBCM as BOUNDSCO, any indirect method, or a hybrid method.

Using this algorithm and the indirect methods mentioned above, the phenomena of multiple solutions is demonstrated for the optimal orbit transfer problem. A simple empirical guideline is proposed which chooses between two or more multiple solutions when using this algorithm. It is not claimed that the algorithm will obtain the globally optimal solution.

Intuitively, one might want to think of an optimal multiple-burn transfer not as one large trajectory, but as a sequence of optimal one-burn transfers between transfer orbits that are optimally chosen. For ideal gravity, a strong relationship is shown to exist between these two problems. Based on this relationship, two new numerical methods are presented which iteratively compute optimal orbit transfers. The first method, named the Patched Method, appears to be very robust yet sluggish in convergence. The second method, named the Modified Patched Method (MPM) seems somewhat less robust but much faster in convergence. For optimal orbit transfers in ideal gravity with large numbers of burns, MPM seems to be superior to the other methods investigated in this report.

Finally, an investigation is made into a suboptimal multiple-burn guidance scheme. This scheme is, in fact, seen to have somewhat less than desirable terminal error. This terminal error is improved through a time-to-go indexing scheme. Future directions for multiple-burn guidance are suggested.

The FORTRAN code developed for this study has been collected together in a package named ORBPACK. ORBPACK and a user manual are provided. The manual is included as an appendix to this report.

SECTION I

THE ORBIT TRANSFER PROBLEM

I.1. Introduction

The most popular motor today for performing orbit transfers is of high thrust and usually a solid, sometimes a liquid rocket motor. These typically have a specific impulse, or I_{sp}, in the lower hundreds of seconds (250s-450s) and thrust in the thousands of Newtons[1] and up. In this range, they can be considered impulsive[2], applying changes in velocity on a time scale much shorter than the orbit period. For many years the study of optimal orbit transfer has focused on these impulsive motors.

With the hopes of lower fuel consumption due to an I_{sp} typically in the thousands of seconds, electric propulsion has recently grown in popularity and many studies have been performed to develop the motors; a major satellite manufacturer is already designing satellites which use a Xenon Ion Propulsion System (XIPS)[3]. The thrust produced by these motors is in the tens to thousandths of Newtons; for example, XIPS produces 18 thousandths of a Newton with an I_{sp} just under 3,000 sec. Obviously, orbit transfer maneuvers with such electric propulsion will take more time and practical transfers can no longer be modeled as impulsive. Since it is necessary to specify the maneuver with continuous functions as opposed to discrete impulsive events, the optimal transfer problem has been too complicated for exact analytical solutions.

[1]Hertz, J. R.., and Arson, W. J., *Space Mission Analysis and Design*, Kluwer Academic Publishers, Boston, 1991.
[2]Robbins, H. M., "An Analytical Study of the Impulsive Approximation," *AIAA Journal*, Vol. 4, No. 8, 1966, pp. 1417-1423
[3]Christensen, R. A., ed., "Space Propulsion's Latest Thrust," *Vectors*, Vol 37, No. 1, 1995, Hughes Electronics, Los Angeles.

Numerical methods for the computation of optimal orbit transfers have been widely studied. These numerical methods fall into three categories: direct, indirect, and hybrid methods. Direct methods parameterize the thrust program and then attempt to optimize these parameters while satisfying boundary conditions. Indirect methods employ the mathematics of optimal control to formulate a Two-Point Boundary Value Problem (TPBVP) which can then be approached with a variety of numerical methods. Hybrid methods are a combination of the two. These methods are often formed by simply removing difficult conditions from the TPBVP and optimizing some equivalent cost function over the released parameters.

The main objective of this research was the computation of fuel-optimal low and medium thrust orbit transfers. Here, medium thrust was taken as $1 > T/W_o \geq 0.01$ and low-thrust as $0.01 > T/W_o \geq 0.001$. This particular definition has been made because it is the initial acceleration which the rocket motor produces compared with the gravitational acceleration at that point that determines how easily changes in the initial orbit will be made. In contrast, comparing the initial rocket motor acceleration with the weight of the spacecraft as it would measure on the planet's surface does not directly indicate the motor's ability to move the spacecraft away from a very high orbit.

Of the utmost interest was the ability to compute highly efficient transfers for the ideal case. This will provide mission planners with the ability to compute a "best" transfer which can be used to judge more practical schemes. However, the ideal case does not quite represent reality; the ability to handle orbit perturbations is desirable as this would produce more realistic "best" transfers. For trajectories that spend much time near or beyond geosynchronous orbit, the dominant orbit perturbations will result from either Earth oblateness effects or atmospheric drag.[1]

Software using multiple-point shooting and modified-shooting techniques were used and produced many solutions. Using these, some characteristics of the solution have been observed and studied. Identification of these characteristics has resulted in the development of a new method for improving optimal orbit transfers. The method introduces additional burns to optimal ideal-gravity orbit transfers using an under-exploited property of the switching function. A set of improved transfers were constructed and these uncovered new properties of optimal transfers.

Furthermore, two new methods have been developed. The first is a new hybrid approach called the Patched Method. This method combines the robustness of a direct approach and the greater convergence speed of the multiple-shooting approach in a configuration that can handle transfers with large numbers of burns. However, the Patched Method pays for its robustness with speed.

The second new method is the Modified Patched Method (MPM). MPM trades back some of the sluggishness of the Patched Method for a small loss in robustness. This trade-off is accomplished by making use of properties specific to the orbit transfer problem. Some of these properties appear to be new, developed here for the first time. Overall, MPM seems to be superior to any of the other methods applied in this report.

The other objective of this research was the examination of a capable guidance algorithm for multiple-burn orbit transfer. Work on this has produced a one-burn guidance algorithm using neighboring optimal feedback control. This guidance algorithm could be used on a burn-by-burn basis to produce a sub-optimal trajectory.

I.2. Orbit Transfer Modeling

The spacecraft is represented by a point mass and assumed to be a thrusting craft acted upon by the aerodynamic drag and oblate-body gravity forces of a central body.

The central body, or planet, is also represented as a point mass positioned at its own center of gravity. Furthermore, the problem is restricted to crafts of mass much smaller than that of the central body; therefore, the planet is assumed fixed in inertial space. This inertial space is described with a rectangular Cartesian inertial reference frame (OXYZ). The central body is fixed at the center O of this frame and the z-axis is perpendicular to that body's equator. All motion within this frame agreeing with the above assumptions must satisfy Newton's Second Law:

$$\sum \mathbf{F} = \frac{d(m\mathbf{v})}{dt} \tag{1.1}$$

where m is the spacecraft's mass, $\mathbf{v}$ is its velocity with respect to the reference frame, and $\Sigma\mathbf{F}$ represents the sum of forces on the craft.

In this case, gravity, drag, and thrust make up the total force acting on the craft. This gives

$$m\dot{\mathbf{v}} = T\mathbf{e}_T - \mathbf{F}_{drag} - \mathbf{F}_{gravity} \tag{1.2}$$

in which the thrust is some time-varying function $T(t)$ independent of a time-varying direction $\mathbf{e}_T(t)$. This is most clearly derived by considering a momentum balance of the spacecraft as it expells mass to produce thrust; absorbing the dm/dt term into the thrust term produces Equation (1.2).

The thrust direction is expressed as the unit vector $\mathbf{e}_T(t)$. For a three-dimensional thrust vector the control requires a magnitude and three components or two angles. For two dimensional problems, the one magnitude and only two independent control components or one angle is required.

It is assumed that the fuel consumption of the motor is represented by

$$\dot{m} = -\frac{T}{g_o I_{sp}} \tag{1.3}$$

where g_o is Earth's gravitational acceleration at sea level and I_{sp} is the motor's specific impulse.

It is assumed that the atmosphere surrounding the central body can be described by an exponential model as in the standard atmosphere[4] resulting in the following aerodynamic drag force:

$$\mathbf{F}_{drag} = \frac{1}{2}\rho_o e^{-\beta(r-r_o)} S C_D v \mathbf{v} \tag{1.4}$$

where β is a constant from the atmosphere model describing air density variation in the prescribed altitude region, ρ_o is the atmosphere density at the altitude r_o, S is the cross-sectional area of the craft, C_D is the craft's drag coefficient, v is the magnitude of the velocity $\mathbf{v}$, and r is the magnitude of the position vector $\mathbf{r}$.

The gravitational potential energy to the second harmonic is[5]

$$U = \frac{\mu m}{r} + \frac{1}{2} J_2 R_e^2 \frac{\mu m}{r^3}\left(1 - 3cos^2(\theta)\right) \tag{1.5}$$

where R_e is the equatorial radius of the central body, θ is the latitude angle of the current position from the equator, μ is the gravitational constant for the central body, and J_2 is a constant describing the mass distribution of the central body; for Earth J_2=1082.61×10^{-6}. There are additional mass distribution terms, but the series is truncated here. θ is

[4]Anderson, J. D., *Fundamentals of Aerodynamics*, New York: McGraw-Hill Book Co., 1984.

[5]Space Technology Laboratories, *Flight Performance Handbook for Orbital Operations*, New York: Wiley, 1963.

described with Cartesian coordinates by $z=r\cos(\theta)$. This gravitational potential exerts the following force on the spacecraft:

$$\mathbf{F}_{gravity} = \frac{\partial U}{\partial \mathbf{r}} = -\left\{ \frac{\mu}{r^3}\mathbf{I} + \frac{3}{2}\mu J_2 \frac{R_e^2}{r^5}\left(\overline{\mathbf{N}} - 5\left(\frac{z}{r}\right)^2 \mathbf{I} \right) \right\} \mathbf{r} \tag{1.6}$$

where $\overline{\mathbf{N}}$ =diag{1,1,3} and $\mathbf{I}$ is the identity matrix.

The equations of motion for the spacecraft are

$$\dot{\mathbf{x}}(t) = \mathbf{f}(\mathbf{x}(t), T(t), \mathbf{e}_T(t)) \tag{1.7}$$

where

$$\mathbf{x}(t) = \left[\mathbf{r}^{\mathrm{T}}(t) \quad \mathbf{v}^{\mathrm{T}}(t) \quad m(t) \right]^{\mathrm{T}} \tag{1.8}$$

and

$$\mathbf{f}(\mathbf{x}(t), T(t), \mathbf{e}_T(t)) = \left\{ \begin{array}{c} \mathbf{v} \\ \frac{T}{m}\mathbf{e}_T - \frac{\mu}{r^3}\mathbf{r} - \left\{ \frac{3}{2}\mu J_2 \frac{R_e^2}{r^5}\left(\overline{\mathbf{N}} - 5\left(\frac{z}{r}\right)^2 \right) \right\} \mathbf{r} - \frac{1}{2}\frac{\rho_o}{m} e^{-\beta(r-r_o)} S C_D v \mathbf{v} \\ -T/(g_o I_{sp}) \end{array} \right\} \begin{array}{r} (1.9a) \\ (1.9b) \\ (1.9c) \end{array}$$

The thrust magnitude has both an upper and a lower bound. The upper bound is called $T_{\max}$, the lower bound is zero. Therefore, the following inequality constraint must be satisfied for all time $t \in [0, t_f]$:

$$0 \le T \le T_{max} \tag{1.10}$$

For the purposes of this study a simple atmosphere model was chosen. The model was not intended to accurately represent the Earth's atmosphere, or any other planet for that matter. It is implemented only for the purpose of demonstrating the methods used herein and to allow examination of its effects on the optimal transfer.

The model was defined from a reference altitude of 450 km above the planet's equator. The entire atmosphere region was assumed isothermal with a temperature of 1,000K. The density at the definition altitude was defined to be 1.184×10^{-12} kg/m^3. The definition point for this model was taken from the 1976 U.S. Standard Atmosphere[6]. Also, it was assumed that C_D=2, a common approximation for spacecraft[7], and the cross sectional area of the satellite was arbitrarily chosen to be 4π m^2.

For problems in which the ideal gravity assumption is acceptable, coasting trajectories are well understood and can be analytically represented. Therefore, it is simplest to optimize the exit, or "thrust on," point on the initial orbit and the entry, or "thrust off," point on the final orbit. A real spacecraft implementing the orbit transfer could simply wait in the initial orbit until arrival at the initial orbit exit point, indicating that the maneuver should begin.

Hence, the boundary conditions must determine all orbital elements except position on orbit, and are written as

$$\psi\left(x(t_o)\right)=\alpha_o \tag{1.11a}$$
$$\psi\left(x(t_f)\right)=\alpha_f \tag{1.11b}$$

where the function ψ determines these orbital elements for the state in question and α_o and α_f are vectors containing the desired values at the initial and final points, respectively. Such a determination could be accomplished several different ways.

[6]United States. COESA. *U.S. Standard Atmosphere, 1976*, Washington: GPO, 1976.
[7]King-Hele, D. *Theory of Satellite Orbits in an Atmosphere*, London, Butterworths, 1964.

However, using the angular momentum and eccentricity vectors is perhaps the simplest.[8] For planar transfers, all motion can be placed in X-Y plane and the components of the ψ function are

$$\begin{aligned}\psi_1 &= h = \mathrm{xv} - \mathrm{yu} \\ \psi_2 &= \mu e_x = \left[\left(v^2 - \mu/r\right)\mathrm{x} - \left(\mathbf{r}^T\mathrm{v}\right)\mathrm{u}\right] \\ \psi_3 &= \mu e_y = \left[\left(v^2 - \mu/r\right)\mathrm{y} - \left(\mathbf{r}^T\mathrm{v}\right)\mathrm{v}\right]\end{aligned} \tag{1.12}$$

Where h is the angular momentum, e_x is the X-component of the eccentricity vector, and e_y is the Y-component of the eccentricity vector.

In the three-dimensional case, these vectors will compose six components. Since the angular momentum and eccentricity vectors are always perpendicular, one of these components will be redundant and thus removable. There is one restriction on which component is removed; it can be seen clearly by considering the property that the vectors are always orthogonal, expressed as

$$h_x e_x + h_y e_y + h_z e_z = 0 \tag{1.13}$$

A component of one of the two vectors can be removed if it can be computed using Equation (1.13). In other words, since Eq. (1.13) always holds, knowledge of the removed component is implied and it is unnecessary to explicitly compute it. Another way to state this is to say that the six components are linearly dependent. Therefore, if for the orbit transfer problem in question, $h_z \neq 0$ on a terminal orbit, then the ψ function components can be written as

[8]Kaplan, M. H. *Modern Spacecraft Dynamics and Control*, New York, John Wiley & Sons, 1976.

$$\psi_1 = h_x = \mathrm{yw} - \mathrm{zv} \tag{1.14a}$$
$$\psi_2 = h_y = \mathrm{zu} - \mathrm{xw} \tag{1.14b}$$
$$\psi_3 = h_z = \mathrm{xv} - \mathrm{yu} \tag{1.14c}$$
$$\psi_4 = \mu e_x = \left[\left(v^2 - \mu/r\right)\mathrm{x} - \left(\mathbf{r}^{\mathrm{T}}\mathbf{v}\right)\mathrm{u}\right] \tag{1.14d}$$
$$\psi_5 = \mu e_y = \left[\left(v^2 - \mu/r\right)\mathrm{y} - \left(\mathbf{r}^{\mathrm{T}}\mathbf{v}\right)\mathrm{v}\right] \tag{1.14e}$$

where x,y, and z are the components of **r** in OXYZ and u,v, and w are the components of **v** in OXYZ.

If the initial or final portion of a transfer traverses altitudes where ideal gravity is not a valid assumption, then the boundary conditions likely need to be reformulated. For example, a trajectory that begins at a very low Earth-altitude cannot truly coast with zero cost because energy would be lost due to atmospheric drag. For such a transfer, it would be more realistic to fix the initial point. Likewise, some missions may be more interested in delivering the spacecraft to a specific point in space, in which case the final condition should be a rendezvous condition.

Anticipating numerical applications, note that the problem can be nondimensionalized. This aided by making all states roughly the same order. In the presentation of example solutions, the hat (^) notation will be dropped and solutions are assumed nondimensionalized unless stated otherwise. The non-dimensionalizations follow:

$$\hat{\mathbf{r}} \equiv \mathbf{r}/r^{\star} \qquad \hat{m} \equiv m/m^{\star} \tag{1.15a-b}$$
$$\hat{t} \equiv t\Big/\sqrt{r^{\star 3}/\mu} \tag{1.15c}$$

and they require the following:

$$\hat{\mathbf{v}} \equiv \mathbf{v}\Big/\sqrt{\mu/r^{\star}} \qquad \hat{t}_f \equiv t_f\Big/\sqrt{r^{\star 3}/\mu} \tag{1.15d-e}$$

$$\hat{r}_o \equiv r_o/r^{\star} \qquad \hat{\beta} \equiv \beta r^{\star} \tag{1.15f-g}$$

$$\left(\hat{\rho}_o \hat{S}\hat{C}_D\right) \equiv \rho_o S C_D\left(r^{\star}/m^{\star}\right) \qquad \left(\hat{g}_o \hat{I}_{sp}\right) \equiv g_o I_{sp}\sqrt{r^{\star}/\mu} \tag{1.15h-i}$$

$$\hat{T} \equiv \left(T/m^{\star}\right)/\left(\mu/r^{\star 2}\right) \qquad \hat{R}_e \equiv R_e/r^{\star} \tag{1.15j-k}$$

The choices of $r^{☆}$ and $m^{☆}$ are completely arbitrary. However, it needs to be said that after a problem is solved by these nondimensionalizations rescaling must be exercised with caution; rescaling changes the atmosphere model and changes the equatorial radius used for the oblateness terms. For example, a given transfer with nondimensionalized parameters must specify the value for $\hat{R}_e$ if oblateness effects were considered. If, after rescaling, one intends this transfer to represent a maneuver about Earth then $r^{\star}$ must be such that R_e is the radius of Earth by Equation (1.15k). Similar arguments may be made concerning the nondimensionalized parameters for atmospheric drag effects.

Substitution of Eqs. (1.15a-k) into Eqs. (1.9a-c) shows that the nondimensional dynamic equations are equivalent to Eqs. (1.9a-c) with μ=1 (the value of J_2, however, has no dimensions and is not changed). In Eq. (1.9a), choosing the scalings for **r** and t, shows that the only consistent scaling for **v** is Eq. (1.15d). Then, in Eq. (1.9b) it is clear that Eqs. (1.15a-h) and (1.15j-k) are required for consistency. Substitution into Eq. (1.9b) also shows that the factor μ appears on both sides of Eq. (1.9b), in the numerator of every term; therefore, it may be dropped from both sides. Finally, substitution into Eq. (1.9c) reveals that Eq. (1.15i) is required for consistent scaling.

SECTION II

COMPUTATION OF OPTIMAL ORBIT TRANSFERS

II.1. Literature Review

One of the earliest and most notable applications of the calculus of variations to the orbit transfer problem was by Lawden[9]. His work established the now widely-used pointer vector theory. Lawden also derived many useful analytical results including an analytical solution for the Lagrange multipliers over coast arcs in ideal gravity[10]; his expression is easily configured to trajectories where the transfer time is unconstrained. He went on to conclude that for the case of escape from a circular orbit, tangential thrusting would be nearly optimal[11]; however, he noted that this thrust program may not fare so well in other cases. Lawden studied the possibility that, in addition to arcs of maximum thrust and null thrust, arcs of intermediate-thrust may exist in an optimal transfer[12]. He later wrote a general review of rocket trajectory optimization[13] and stated that issue of the existence of intermediate-thrust arcs was still unresolved.

After Lawden's formulation was published, many other researchers produced solutions to the Lagrange multipliers over coast arcs in ideal gravity. A set of

[9]Lawden, D. F., *Optimal Trajectories for Space Navigation*, London, Butterworths, 1963.
[10]Lawden, D. F., "Fundamentals of Space Navigation," *Journal of the British Interplanetary Society*, Vol. 13, No. 2, 1954, pp. 87-101, 1954.
[11]Lawden, D. F., "Optimal Escape from a Circular Orbit," *Astronautica Acta*, Vol. 4, No. 3, 1958, pp. 218-233.
[12]Lawden, D. F., "Optimal Intermediate-Thrust Arcs in a Gravitational Field," *Astronautica Acta*, Vol. 8, No. 2, pp. 106-123.
[13]Lawden, D. F., "Rocket Trajectory Optimization: 1950-1963," *Journal of Guidance, Control, and Dynamics*, Vol. 14, No. 4, 1991, pp. 705-711.

expressions derived by Danby[14] appear to be the earliest such work. This was actually for the equivalent problem of determining the matrizant. At almost the same time, Pines published work which derived constants of integration[15], some which apply during any part of the trajectory, even intermediate-thrust arcs, and some in restricted cases. Later, both Eckenwiler[16] and Hempel[17] produced formulations valid in a two-dimensional system. Lion and Handelsman[18] derived equations for a three-dimensional system. Glandorf[19] produced a very useful form for the Lagrange multiplier's that used the current radius, velocity, and angular momentum vectors as reference directions. Vinh[20] developed equations which reduced the solution of the Lagrange multipliers for any central force field to a problem of simple quadratures.

These analytical results have all proved useful in many studies of optimal orbit transfers. However, to date no closed-form expressions have been obtained for optimal orbit transfers, including the fuel-optimal thrust-limited case considered in this report. Therefore, numerical methods are used to produce exact solutions for this problem which has challenged the most sophisticated algorithms. These methods are traditionally divided into three types: indirect, direct, and hybrid.

---

[14]Danby, J. M. A, "The Matrizant of Keplerian Motion," *AIAA Journal*, Vol. 2, No. 1, 1964, pp. 16-19.
[15]Pines, S., "Constants of the Motion for Optimum Thrust Trajectories in a Central Force Field," *AIAA Journal*, Vol. 2, No. 11, 1964, pp. 2010-2014.
[16]Eckenwiler, M. W., "Closed-Form Lagrangian Multipliers for Coast Periods of Optimum Trajectories," *AIAA Journal*, Vol.3, No. 6, June 1965, pp. 1149-1151.
[17]Hempel, P. R., "Representation of the Lagrangian Multipliers for Coast Periods of Optimum Trajectories," *AIAA Journal*, Vol. 4, No. 4, June 1966, pp. 720-730.
[18]Lion, P. M., and Handelsman, M., "Primer Vector on Fixed-Time Impulsive Trajectories," *AIAA Journal*, Vol. 6, No. 1, 1968, pp. 127-132.
[19]Glandorf, D. R., "Lagrange Multipliers and the State Transition Matrix for Coasting Arcs," *AIAA Journal*, Vol. 7, No. 2, 1969, pp. 363-365.
[20]Vinh, N. X., "Integration of the Primer Vector in a Central Force Field," *Journal of Optimization Theory and Applications*, Vol. 9, No. 1, 1972, pp. 51-58.

II.1.1. Indirect Methods

Indirect methods convert the optimization problem into a TPBVP though optimal control theory. The most popular indirect methods by far seem to be the shooting and multiple-point shooting methods.

Among the studies using indirect methods, the work by Brown, Harrold, and Johnson[21] produced an indirect method named OPGUID/SWITCH which handles rendezvous trajectories or free entry/exit points and free final time using a modified set of boundary conditions. Results with OPGUID/SWITCH were presented for medium thrust levels and two to three burns.

Another indirect method, developed by McAdoo, Jezewski, and Dawkins[22] and dubbed OPBURN, was actually a combination of two approaches. The first approximated ideal gravity using a model for gravitational accelerations linearly varying with altitude. This assumption results in a linear steering law and was used to simplify low-accuracy calculation of the transfer. The data from this approach were used as the starting iterate of another, more accurate code. Results with this method were presented for medium thrust acceleration levels and two to three burns.

Edelbaum, Sackett, and Malchow[23] produced computer code to solve minimum time transfers (one burn) using equinoctial orbital elements as state variables. Constraints on exposure to solar radiation were considered. This method relied heavily upon the

[21]Brown, K. R., Harrold, E. F., and Johnson, G. W., "Rapid Optimization of Multiple-Burn Rocket Flights," *NASA CR-1430*, Sept., 1969.

[22]McAdoo, S., Jr., Jezewski, D. J., and Dawkins, G. S., "Development of a Method for Optimal Maneuver Analysis of Complex Space Missions," *NASA TN D-7882*, April, 1975.

[23]Edelbaum, T.N., Sackett, L. L., and Malchow, H. L., "Optimal Low Thrust Geocentric Transfer" AIAA Paper 73-1074, *Proceedings of the AIAA 10th Electric Propulsion Conference*, Lake Tahoe, Nevada, November 1973.

method of averaging and was named SECKSPOT. Horsewood, Suskin, and Pines[24] modified SECKSPOT to produce a code for the optimization of multiple-burn rendezvous orbit transfers with plane changes between circular orbits with low-thrust in an ideal gravity field. The transfer times for these trajectories were fixed.

A study by Redding[25] handled point-to-point, or rendezvous, low-thrust transfers with plane changes. The method presented in the study includes the reduced set of boundary conditions established earlier by Brown, et. al.[21] It was limited to transfers to geosynchronous orbits in an ideal gravity field and no results are discussed for elliptical terminal orbits. Solutions with low-thrust were obtained for transfers with two to six burns.

II.1.2. Direct Methods

The most common technique for direct methods is to discretize the control and possibly the state, then optimize the performance index by varying the control and state at each node of the independent variable. This optimization is usually subject to some constraints. In orbit transfer optimization, it obviously makes sense to use any helpful results from the application of optimal control theory. Almost universally, direct methods for orbit transfer optimization make use of a bang-bang assumption which eliminates the possibility of intermediate-thrust arcs. The control is then taken as a combination of switching times and directions.

The Direct Collocation with Nonlinear Programming (DCNLP) technique makes use of polynomial approximation to both perform integration and approximate the control

[24]Horsewood, J.L., Suskin, M.A., and Pines, S., "Moon Trajectory Computational Capability Development," *NASA Lewis TR-90-51*, Cleveland, Ohio 44135, July 1990.

[25]Redding, D.C., "Optimal Low-Thrust Transfers to Geosynchronous Orbit," *NASA Lewis SUDAAR 539*, Cleveland, Ohio 44135, Sept. 1983.

at nodes. Dickmanns and Wells[26] made a significant contribution using a DCNLP method based on piece-wise Hermite polynomial approximations for the state and Lagrange multipliers. More recently, Hargraves and Paris[27] used this technique in their OTIS (Optimal Trajectories by Implicit Simulation) program. The Direct Transcription and Nonlinear Programming (DTNLP) technique is very similar to DCNLP, with transcription replacing collocation for implicit integration.

Using DCNLP once then DTNLP later, Enright and Conway[28,29] examined circular, point-to-point planar transfers with ideal gravity. The methods demonstrated in these studies were shown effective for two- and three-burn trajectories. In using the DTNLP method, a technique was developed for calculating the Lagrange multipliers so that Pontryagin's Minimum Principle could be checked. In some cases, it was found that this principle had been violated.

Vulpetti and Montreali[30] used nonlinear programming to optimize transfers between circular orbits with inclinations. They did include oblateness and drag in their gravity model; their thrust acceleration level was about 0.0019*g*. Example transfers included from two to four burns. Pourtakdoust and Jalali[31] used DTNLP for three-

[26]Dickmanns, F.D., and Well, K.H., "Approximate Solution of Optimal Control Problems Using Third Order Hermite Functions," *IFIP-TC7, VI Technical Conference on Optimization Techniques*, Novosibirsh Springer, 1974.

[27]Hargraves, C.R., Paris, S.W., Vlases, W.G., "OTIS Past, Present, and Future," *Proceedings of the 1992 AIAA conference of Guidance, Navigation, and Control*, Hilton Head, S.C. 1992

[28]Enright, P.J. and Conway, B.A., "Optimal Finite-Thrust Spacecraft Trajectories Using Collocation and Nonlinear Programming," *Journal of Guidance, Control, and Dynamics*, Vol. 14, No. 5, 1991, pp. 981-985.

[29]Enright, P.J. and Conway, B.A., "Discrete Approximations to Optimal Trajectories Using Direct Transcription and Nonlinear Programming," *Journal of Guidance, Control, and Dynamics*, Vol. 15, No. 4, 1992, pp. 994-1002.

[30]Vulpetti, G. and Montereali, R.M., "High-Thrust and Low-Thrust Two-Stage LEO-LEO Transfer" *Acta Astronautica*, Vol. 15, No. 12, 1987, pp. 973-979 (84-354)

[31]Pourtakdoust, S.H. and Jalali, M.A., "Optimal Three-Dimensional Orbital Transfer Using Direct Optimization Methods," *Engineering Systems Design and Analysis*, Vol. 64-6, ASME, 1994, pp. 53-58.

dimensional two-burn transfers with a medium thrust level. All these studies mentioned above either used fixed final time, fixed entry/exit positions in orbits, or both.

Another direct method that is gaining in popularity makes use of a technique called differential inclusion.[32] Coverstone-Carroll, V. and Williams, S.N.[33] used differential inclusion concepts in a direct optimization scheme that produced one- and two-burn planar interplanetary rendezvous trajectories. The title of the study states that these trajectories are for low-thrust, but the thrust levels fit in the medium thrust range defined for this report.

II.1.3. Hybrid Methods

Methods are called hybrid if they don't fit neatly into either of the above categories. Typically, hybrid methods for the orbit transfer problem involve some use of the Lagrange multipliers and the Euler-Lagrange equations but also use direct optimization to determine other parameters of the trajectory.

Zondervan, Wood, and Caughey[34] used a hybrid method to study three-burn transfers with plane changes in ideal gravity and for thrust levels in the medium and low-thrust range. Their approach was to take the indirect setup and release the switching function constraint. The switching points were then optimized directly.

---

[32]Kisielewicz., M., *Differential Inclusions and Optimal Control*, Kluwer Academic Publishers, Boston, 1991.

[33]Coverstone-Carroll, V. and Williams, S.N., "Optimal Low Thrust Trajectories Using Differential Inclusion Concepts," *Proceedings of the AAS Rocky Mountain Guidance Conference*, Colorado, 1994.

[34]Zondervan, K.P., Wood, L.J., and Caughey, T.K., "Optimal Low-Thrust, Three-Burn Orbit Transfers with Large Plane Changes," *Journal of the Astronautical Sciences*, Vol. 32, No. 3, 1984, pp. 407-427.

Ilgen[35] used a hybrid scheme called HYTOP to compute low-thrust transfers for an Orbit Transfer Vehicle (OTV) study. The HYTOP algorithm uses the fact from optimal control theory that the pointer vector function is continuous for the duration of the transfer. The pointer vector function, and only this function, is discretized into piece-wise linear functions. The state was represented by equinoctial orbital elements. The final mass was then optimized over the choice of the pointer vector function parameters subject to the TPBVP constraints.

Each hybrid method is unique, these two are by no means representative of all that have been attempted. To date, there does not appear to be any standard hybrid methodology.

II.2. Using Indirect Methods and Homotopy to Compute Solutions

The following subsections describe work in this research effort using indirect methods and homotopy to compute solutions. Modified forms of both shooting and multiple-point shooting were found capable of computing medium thrust transfers with small numbers of burns and some low-thrust transfers. In this domain, a new method for increasing the number of burns in a transfer was developed and is based a new property of the switching function. This new method was used to demonstrate that optimal orbit transfers may have multiple solutions. Also, when using this method there is a rule-of-thumb that may help compute the more efficient of the multiple solutions, thus, avoiding the need to compute all possible transfers and comparing the cost directly. However, there is no guarantee of a global minimum.

II.2.1. Application of Optimal Control

For this problem the choice of performance index is clear:

[35]Ilgen, M.R., "A Hybrid Method for Computing Optimal Low-Thrust OTV Trajectories," *Proceedings of the AAS Rocky Mountain Guidance Conference*, Colorado, 1994 (AAS 94-129).

$$J = m(t_f) \tag{2.1}$$

where $m(t_f)$ represents the mass of the spacecraft including its fuel at the end of the orbit transfer. The intention, then, is to maximize the performance index, *viz.* maximize the mass at the end of the transfer.

The TPBVP is constructed using the necessary conditions in the usual manner.[36] Include the steering direction vector constraint in the Hamiltonian, which can be defined for the optimization problem as

$$H(\mathbf{x}(t), T(t), \mathbf{e}_T(t), \boldsymbol{\lambda}(t)) = \boldsymbol{\lambda}^{\mathrm{T}}(t)\mathbf{f}(\mathbf{x}(t), T(t), \mathbf{e}_T(t)) + \lambda_e(\mathbf{e}_T^{\mathrm{T}}(t)\mathbf{e}_T(t) - 1) \tag{2.2a}$$

$$\begin{aligned} H = \boldsymbol{\lambda}_r^{\mathrm{T}}\mathbf{v} + \boldsymbol{\lambda}_v^{\mathrm{T}}\Bigg(\frac{T}{m}\mathbf{e}_T - \frac{\mu}{r^3}\mathbf{r} - \left\{\frac{3}{2}\mu J_2\frac{R_e^2}{r^5}\left[\overline{\mathbf{N}} - 5\left(\frac{z}{r}\right)^2\right]\right\}\mathbf{r} \\ - \frac{1}{2}\frac{\rho_o}{m}e^{-\beta(r-r_o)}SC_D v\mathbf{v}\Bigg) - \lambda_m\frac{T}{g_o I_{sp}} + \lambda_e(\mathbf{e}_T^{\mathrm{T}}\mathbf{e}_T - 1) \end{aligned} \tag{2.2b}$$

from which the Euler-Lagrange equations are obtained as ODEs governing the Lagrange multipliers

$$\begin{aligned} \dot{\boldsymbol{\lambda}}_r = -\left(\frac{\partial H}{\partial \mathbf{r}}\right)^{\mathrm{T}} = \mu\left[\frac{\boldsymbol{\lambda}_v}{r^3} - 3\frac{(\boldsymbol{\lambda}_v^{\mathrm{T}}\mathbf{r})\mathbf{r}}{r^5}\right] - \frac{1}{2}\frac{\rho_o}{m}\frac{\beta}{r}e^{-\beta(r-r_o)}SC_D v(\boldsymbol{\lambda}_v^{\mathrm{T}}\mathbf{v})\mathbf{r} \\ + \frac{3}{2}\mu J_2 R_e^2\left[\frac{\overline{\mathbf{N}}\boldsymbol{\lambda}_v}{r^5} - 5\frac{(\boldsymbol{\lambda}_v^{\mathrm{T}}\overline{\mathbf{N}}\mathbf{r})\mathbf{r}}{r^7}\right] - \frac{15}{2}\mu J_2 R_e^2\left[\frac{\mathrm{z}^2}{r^7}\boldsymbol{\lambda}_v - (\boldsymbol{\lambda}_v^{\mathrm{T}}\mathbf{r})\left(\frac{7\mathrm{z}^2}{r^9}\mathbf{r} - \frac{2\mathrm{z}}{r^7}\begin{bmatrix}0\\0\\1\end{bmatrix}\right)\right] \end{aligned} \tag{2.3a}$$

$$\dot{\boldsymbol{\lambda}}_v = -\left(\frac{\partial H}{\partial \mathbf{v}}\right)^{\mathrm{T}} = -\boldsymbol{\lambda}_r + \frac{1}{2}\frac{\rho_o}{m}e^{-\beta(r-r_o)}SC_D\left[\boldsymbol{\lambda}_v v + \frac{(\boldsymbol{\lambda}_v^{\mathrm{T}}\mathbf{v})\mathbf{v}}{v}\right] \tag{2.3b}$$

[36]Bryson, A.E. and Ho, Y.-C., *Applied Optimal Control*, New York: Hemisphere Publishing Corporation.

$$\dot{\lambda}_m = -\frac{\partial H}{\partial m} = \frac{T}{m^2}\lambda_v{}^{\mathrm{T}}\mathbf{e}_T - \frac{1}{2}\frac{\rho_o}{m^2}e^{-\beta(r-r_o)}SC_D v\lambda_v{}^{\mathrm{T}}\mathbf{v} \tag{2.3c}$$

The next Euler-Lagrange equation is easily derived as

$$\frac{\partial H}{\partial \mathbf{e}_T} = \frac{\partial}{\partial \mathbf{e}_T}\left(\frac{T}{m}\lambda_v{}^{\mathrm{T}}\mathbf{e}_T + \lambda_e\left(\mathbf{e}_T{}^{\mathrm{T}}\mathbf{e}_T - 1\right)\cdots\right) = \frac{T}{m}\lambda_v{}^{\mathrm{T}} + 2\lambda_e\mathbf{e}_T{}^{\mathrm{T}} = 0 \tag{2.4}$$

so that the necessary condition is satisfied if $\mathbf{e}_T = \lambda_v/|\lambda_v|$ and $\lambda_e = (T|\lambda_v|)/(2m)$; in other words, the thrust direction is parallel to λ_v, which Lawden thus referred to as the pointer vector. This choice is further supported by a sufficient condition; note that

$$\frac{\partial H}{\partial \mathbf{e}_T \partial \mathbf{e}_T} = 2\lambda_e\mathbf{I} = \frac{T}{m}|\lambda_v|\mathbf{I} > 0 \tag{2.5}$$

when $|\lambda_v| > 0$, $T>0$, and m finite. Also, note that if any one of these is violated during a burn, the trajectory is immediately indeterminate. The choice for the Lagrange multiplier λ_e has been made and does not need to be solved for.

The switching function is derived by an application of the maximum principle. The thrust magnitude, which has bounds T_{max} and 0, will give H its maximum value if it is at its maximum value when $H_T > 0$ and at its minimum when $H_T < 0$. The switching function is

$$H_T = \frac{|\lambda_v|}{m} - \frac{\lambda_m}{g_o I_{sp}} \tag{2.6}$$

and the switching law is

$$\begin{aligned} H_T > 0, &\quad T = T_{max} \\ H_T < 0, &\quad T = 0 \end{aligned} \tag{2.7}$$

If H_T were to be zero for a finite time the control would be singular. Higher-order derivatives of H_T would then be needed to calculate T. In subsection II.1., it was noted that this singular control has been investigated by many different researchers but no conclusions are widely accepted as to when, or if, it will be part of the optimal control.

Many authors[21,34,25,37] have identified the switching law, and associated switching function, as a source of strong sensitivity in numerical solutions.

To complete the TPBVP, the methods of optimal control supply a set of natural boundary conditions

$$\lambda(t_f) = \left[\frac{\partial G}{\partial \mathrm{x}(t_f)}\left(\mathrm{x}(t_o), \mathrm{x}(t_f), \mathrm{v}_o, \mathrm{v}_f\right)\right]^{\mathrm{T}} \tag{2.8a}$$

$$\lambda(t_o) = -\left[\frac{\partial G}{\partial \mathrm{x}(t_o)}\left(\mathrm{x}(t_o), \mathrm{x}(t_f), \mathrm{v}_o, \mathrm{v}_f\right)\right]^{\mathrm{T}} \tag{2.8b}$$

where G is defined as

$$G\left(\mathrm{x}(t_o), \mathrm{x}(t_f), \mathrm{v}_o, \mathrm{v}_f\right) = m(t_f) + \mathrm{v}_f^{\mathrm{T}}\left[\psi\left(\mathrm{x}(t_f)\right) - \alpha_f\right] + \mathrm{v}_o^{\mathrm{T}}\left[\psi\left(\mathrm{x}(t_o)\right) - \alpha_o\right] \tag{2.9}$$

and $\psi(\mathrm{x})$ was defined in Equations (1.12). Therefore, the natural boundary conditions can be expressed as

[37]Chuang, C.-H. and Goodson, T.D. "Optimal Trajectories of Low- and Medium- Thrust Orbit Transfers with Drag and Oblateness," *Submitted to the Journal of the Astronautical Sciences.*

$$\begin{bmatrix}\lambda_r(t_f)\\ \lambda_v(t_f)\end{bmatrix}=\left[\frac{\partial\psi}{\partial \mathrm{x}}(\mathrm{x}(t_f))\right]^T \mathrm{v}_f$$
$$\begin{bmatrix}\lambda_r(t_o)\\ \lambda_v(t_o)\end{bmatrix}=-\left[\frac{\partial\psi}{\partial \mathrm{x}}(\mathrm{x}(t_o))\right]^T \mathrm{v}_o \tag{2.10}$$
$$\lambda_m(t_f)=1$$

where

$$\left[\frac{\partial\psi}{\partial \mathrm{x}}(\mathrm{x})\right]^T=\begin{bmatrix}[\mathrm{r}_\times] & \left[2\mathrm{r}\mathrm{v}^T-(\mathrm{r}^T\mathrm{v})\mathrm{I}-\mathrm{v}\mathrm{r}^T\right]^T\\ [-\mathrm{v}_\times] & \left[(\mathrm{v}^T\mathrm{v})\mathrm{I}-\mathrm{v}\mathrm{v}^T+\frac{\mu}{(\mathrm{r}^T\mathrm{r})^{3/2}}\left(\mathrm{r}\mathrm{r}^T-(\mathrm{r}^T\mathrm{r})\mathrm{I}\right)\right]\end{bmatrix} \tag{2.11}$$

and the subscript "X" denotes the skew symmetric matrix representation of the cross product.

The last condition deals with the final time. For free transfer time the transversality condition must be satisfied

$$H(\mathrm{x}(t_f),\mathrm{u}(t_f),\lambda(t_f))=-\frac{\partial G}{\partial t_f}=0 \tag{2.12}$$

II.2.2. BOUNDSCO

One method used here to solve the TPBVP is a modification of the multiple-point shooting method. The specific algorithms are those given by H. J. Oberle in the subroutine BOUNDSCO[38], written in FORTRAN.

The state defined for the optimal control problem differs slightly from the state used in BOUNDSCO. The state used in BOUNDSCO for numerical computation is

[38]Oberle, H. J., "BOUNDSCO - Hinweise zur Benutzung des Mehrzielverfahrens für die numerische Lösung von Randwerproblemen mit Schaltbedingungen", Hamburger Beiträge zur Angewandten Mathematik, Berichte 6, 1987.

$$z(\tau)=\left[x^T(\tau)\quad \lambda^T(\tau)\quad t_f\quad \nu_o^T\quad \nu_f^T\right]^T$$

and includes a state denoting the transfer time, t_f, and the ν_o and ν_f vectors, from the natural boundary conditions. BOUNDSCO does not allow user-defined parameters that are determined in the iteration process, only functions of time; therefore, these last quantities must be included in the state **z** and specified to have zero derivatives with respect to time. Also, BOUNDSCO is restricted to problems with a fixed partition of the independent variable; therefore, the independent variable has been defined as $\tau \in [0,1]$ with $t = \tau t_f$. This requires that the system dynamics be properly transformed to the independent variable τ so that

$$\frac{d}{d\tau}\begin{bmatrix} x(\tau) \\ \lambda(\tau) \\ t_f \\ \nu_o \\ \nu_f \end{bmatrix} = \begin{bmatrix} \dot{x}(\tau) \\ \dot{\lambda}(\tau) \\ 0 \\ 0 \\ 0 \end{bmatrix} t_f d\tau$$

and these derivatives with respect to t are Eqs. (1.9a)-(1.9c) and (2.3a)-(2.3c). If **x** had N components, then the BOUNDSCO state, **z**, has $2N$+2(N-2)+1 components.

BOUNDSCO addresses the switching function sensitivity problem by the explicit inclusion of switching points in the problem formulation. The number of switching points is not changed by BOUNDSCO. It iteratively drives the guessed switching points to be zeros of the switching function, Eq. (2.6). The user must then decide in which intervals to have the thrust on and in which to have thrust off. Unfortunately, with this scheme the switching law, Eq. (2.7), may not be satisfied and must be checked after BOUNDSCO claims convergence to a solution.

II.2.3. The Minimizing-Boundary-Condition Method

The second method used herein is called the Minimizing-Boundary-Condition Method (MBCM)[39]. MBCM is a modified shooting algorithm in which the switching structure of the optimal control is implicit. The program checks the switching function and the switching law to ensure that Eqs. (2.6) and (2.7) are satisfied at each integration step.

As a modification to the simple shooting method, MBCM, expands the set of available solutions by removing one boundary condition while keeping the same number of unknowns. The choice of this boundary condition is arbitrary. With the number of unknowns unchanged, the solutions become a one-dimensional family. Since this gives a much larger set of solutions, it is much easier to solve the resulting boundary-value problem. Once that is accomplished, the search for the solution that incorporates the final boundary conditions is treated as a minimization problem. The gradient is numerically calculated and used to update the initial state until the last boundary condition is satisfied. This method is about as effective as BOUNDSCO in solving the two-point boundary-value problems for the solved optimal orbit transfers.

II.2.4. Example Two-Burn Extremal

A solution is presented in this subsection, obtained by both BOUNDSCO and MBCM. It is nondimensionalized and assumes ideal gravity. The transfer is made between two planar, aligned orbits. The solution's trajectory is shown in Figure 2.1. The transfer time has been optimized and is 19.05. The initial mass is 1.608. The initial semimajor axis is 3.847 and eccentricity is 0.02378. The final orbit semimajor axis is 1.5 and eccentricity is 0.333. The product $g_o J_{sp}$ is 1.313 and the thrust level is 0.03.

[39]Chuang, C.-H., and Speyer, J.L., "Periodic Optimal Hypersonic SCRAMjet Cruise," *Optimal Control Applications and Methods*, Vol. 8, 1987, pp. 231-242.

Since initial altitude for the transfer is 3.905, the initial T/W_o is 0.2845 and the transfer may be categorized as a medium thrust transfer by the definition stated earlier. With the initial orbit higher than the final orbit, this transfer may be viewed as an optimal descent transfer. However, since atmospheric drag has not been considered, it should not be viewed as an optimal de-orbiting transfer, where the spacecraft would be intentionally placed in an orbit low enough for drag to eventually destroy it.

Two burns are used to complete the transfer. Most of the change in energy occurs in the longer second burn, but most of the change in angular momentum occurs in the first burn.

II.2.5. Example Three-Burn Extremal Considering Perturbation Effects

In this subsection, another example transfer is presented. This transfer was also obtained with both BOUNDSCO and MBCM. However, this is a three-burn transfer whose terminal orbits are not planar. The initial orbit has the same semimajor axis and eccentricity as the transfer from Fig. 1 except now the orbit is inclined 20°, has a right ascension of 13°, and an argument of perigee at 15°. The final orbit is also identical but inclined 1° with 0° right ascension and an argument of perigee at 0°. The thrust level and specific impulse are also the same. This solution includes oblateness effects but excludes drag effects. For the computation of oblateness effects, Earth's value for J_2 (1082.61×10^{-6}) was used along with R_e=0.9696. Since this transfer is intended to be about the earth, $r^{☆}$=6578 *km* must be specified as it ensures the correct equatorial radius scaling.

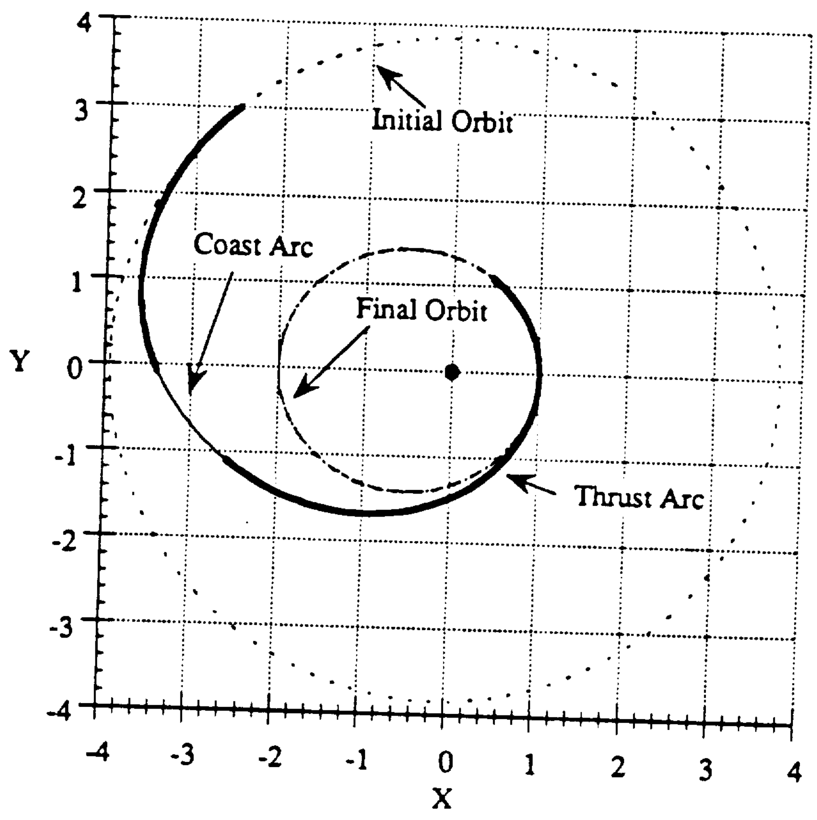

Figure 2.1 Two-Burn Extremal Orbit Transfer Solution with Free Final Time.

The trajectory is shown in Figs. 2.2-2.3. This is a fixed transfer time transfer with t_f=28.75. Recall that this is a descent trajectory; the initial orbit is higher than the final orbit. It is interesting to look at this transfer in terms of the normalized time, τ, the energy, E, the angular momentum, h, the semimajor axis, a, the eccentricity, e, the right ascension, Ω, the argument of perigee, ω, and inclination, i, for certain segments and points on the trajectory. For the first burn $\Delta\tau$=0.3616, ΔE=-0.07760, and Δh=-0.6566. The burn ends at what would be an orbit of a=2.409, e=0.5420, Ω=8.320°, ω=1.123°, and i=1.665°. For the second burn $\Delta\tau$=0.1450, ΔE=-0.1048, and Δh=-0.1310. The second burn ends at what would be an orbit of a=1.601, e=0.3742, Ω=-1.073°, ω=0.3892°, and

i=1.202°. For the third burn $\Delta\tau$=0.02420, ΔE=-0.02101, and Δh=-0.01865. The final mass for this transfer is 1.1656, the initial mass was 1.527. As a result of the oblateness effects, this transfer has poorer performance than if it could be performed in ideal gravity, where it's final mass would be 1.1659.

If drag is considered in the trajectory, performance improves and the final mass is 1.1663. This is consistent with a descending transfer whose final orbit is rather low. The altitude of perigee for the final orbit is 6578 *km* where drag needs to be considered; therefore, atmospheric drag can be used to improve performance. Obviously, with the consideration of atmospheric drag, this transfer could be considered as an optimal de-orbiting transfer.

The loss in performance caused by the oblateness effect is expected. The terminal orbits have their apses aligned; since the oblateness effect causes the line of nodes to regress, the optimal thrust program must fight this effect to return the orientation to that of the initial orbit. The improvement caused by drag is also expected for this is a descending trajectory and drag encourages descending trajectories.

It is interesting to note that the change in right ascension was almost exactly divided between the first two burns while the change in both inclination and argument of perigee happened almost entirely in the first burn. The change in inclination can be most dramatically seen in Fig. 2.3. The burn at the top of the figure is the first burn. The next two burns are difficult to distinguish but not very interesting from this vantage point. The second coasting orbit, or transfer orbit, is quite similar to the final orbit; fittingly, the third burn imparts the least energy of any of the burns.

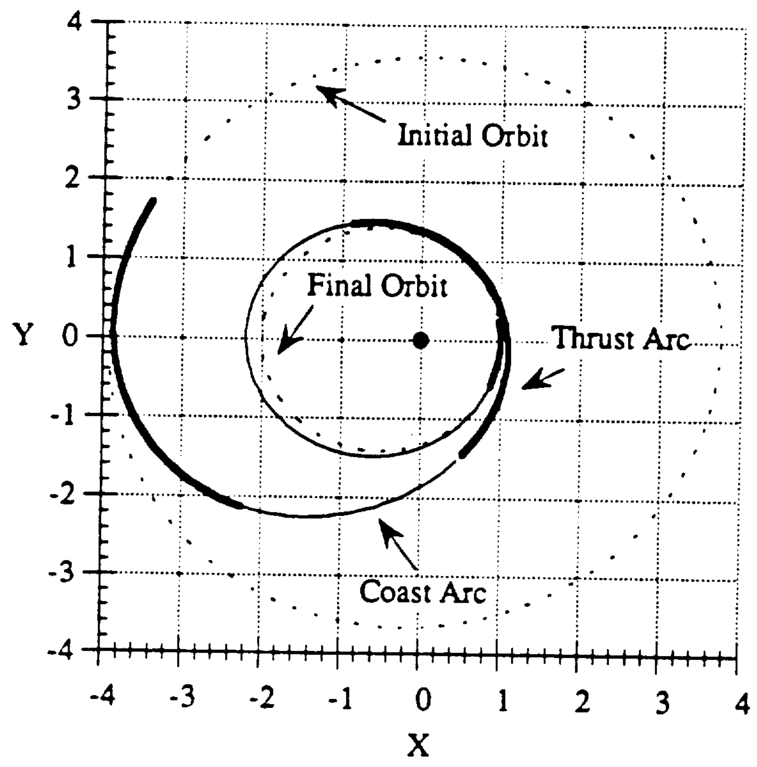

Figure 2.2 Projection into X-Y Plane of Three-Burn Transfer in Ideal Gravity

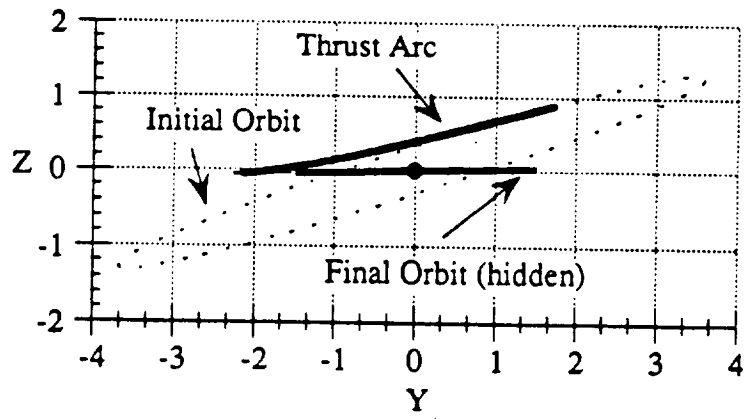

Figure 2.3 Projection into Z-Y Plane of Three-Burn Transfer in Ideal Gravity

This example demonstrates the ability of these methods to obtain exact solutions to the orbit transfer problem for nonplanar trajectories that include perturbing effects. BOUNDSCO typically can obtain such trajectories within the desired tolerance if given the solution under ideal gravity as the initial guess. However, performance usually becomes unacceptable if the number of burns was increased beyond six; this is an empirical observation and by no means constitutes an absolute limitation of BOUNDSCO. There may well be certain cases in which BOUNDSCO can compute transfers with more than six burns quite easily; however, experience indicates that these cases are uncommon.

II.3 A New Property of the Optimal Switching Function

A very interesting property of the optimal control solution under ideal gravity is that the initial and final values of the switching function are equal. Even more interesting is that for the free transfer time problem they are both equal to zero at the initial and final times.

This property may be explained with the following theorem. In the following, C_i^0 denotes the set of i-dimensional vector functions that are continuous with respect to all arguments, vector and/or scalar, and U denotes the set of piece-wise continuous scalar functions with one scalar argument.

Theorem II.1 : Given a bang-bang optimal control problem of the form:

$$J = \int_{t_i}^{t_f} \left[L(\mathbf{x}(t),t) + M(\mathbf{x}(t),t)u(t) \right] dt \text{ where } L(\mathbf{x}(t),t) \in C_1^0 \text{ and } M(\mathbf{x}(t),t) \in C_1^0$$

and subject to the following:

$$\dot{\mathbf{x}}(t) = \mathbf{f}(\mathbf{x}(t),t) + \mathbf{g}(\mathbf{x}(t),\mathbf{v}(t),t)u(t),\ \mathbf{x}(t) \in C_n^0,\ \mathbf{v}(t) \in C_m^0;$$
$$u_{min} \le u(t) \le u_{max}, u(t) \in U\ ;$$
$$\psi_i(\mathbf{x}(t_i)) = 0,\ \psi_f(\mathbf{x}(t_f)) = 0,\ \psi_i(\mathbf{x}(t_i)) \in C_{q_1}^0,\ \psi_f(\mathbf{x}(t_f)) \in C_{q_2}^0\ ;$$

t_i and t_f are free for optimization and satisfying the following assumptions:

(i) $L(\mathbf{x}(t_i),t_i) = L(\mathbf{x}(t_f),t_f)$;
(ii) $[\partial\psi_i(\mathbf{x}(t))/\partial\mathbf{x}(t)]\mathbf{f}(\mathbf{x}(t),t) = \mathbf{0}, [\partial\psi_f(\mathbf{x}(t))/\partial\mathbf{x}(t)]\mathbf{f}(\mathbf{x}(t),t) = \mathbf{0}$;
(iii) $u(t_i)=u(t_f)\neq 0$

then, considering the usual optimal control formulation, introduction of the $\lambda(t)$ functions, and the Hamiltonian $H(\mathbf{x}(t),\mathbf{v}(t),u(t),\lambda(t),t)$ function[36], the following statements are true:

(1) The switching function, $S(\mathbf{x}(t),\lambda(t),t) = \lambda(t)^{\mathrm{T}}\mathbf{g}(\mathbf{x}(t),\mathbf{v}(t),t) + M(\mathbf{x}(t),t)$, satisfies $S(\mathbf{x}(t_i),\lambda(t_i)) = S(\mathbf{x}(t_f),\lambda(t_f)) = -L(\mathbf{x}(t_f),t_f)/u(t_f)$ if and only if $H(\mathbf{x}(t_i),\mathbf{v}(t_i),u(t_i),\lambda(t_i),t_i) = 0$ and $H(\mathbf{x}(t_f),\mathbf{v}(t_f),u(t_f),\lambda(t_f),t_f) = 0$.
(2) If the Hamiltonian is autonomous with t_i and t_f fixed, then $S(\mathbf{x}(t_i),\lambda(t_i)) = S(\mathbf{x}(t_f),\lambda(t_f))$ and $S(\mathbf{x}(t_f),\lambda(t_f)) = [H(\mathbf{x}(t_f),\mathbf{v}(t_f),u(t_f),\lambda(t_f)) - L(\mathbf{x}(t_f))]/u(t_f)$.

Proof:

In the usual optimal control formulation, the boundary conditions at t_i and t_f result in the familiar natural boundary conditions on the Lagrange multipliers, written as

$$\lambda(t_i) = -(\partial\psi_i/\partial\mathbf{x})^{\mathrm{T}}\mathrm{v}_i \in R^n$$
$$\lambda(t_f) = (\partial\psi_f/\partial\mathbf{x})^{\mathrm{T}}\mathrm{v}_f \in R^n$$

which involve the constant Lagrange multiplier vectors $\mathrm{v}_i \in R^{q_1}$ and $\mathrm{v}_f \in R^{q_2}$, where R^i denotes the set of i-dimensional vectors with real-valued components. Now, consider the dot product of $\lambda(t_i)$ and $\lambda(t_f)$ with vectors called$\mathbf{n}_1 \in R^n$ and $\mathbf{n}_2 \in R^n$, respectively:

$$\lambda(t_i)^{\mathrm{T}}\mathbf{n}_1 = -\mathbf{v}_i^{\mathrm{T}}(\partial\psi_i/\partial\mathbf{x})\mathbf{n}_1$$
$$\lambda(t_f)^{\mathrm{T}}\mathbf{n}_2 = -\mathbf{v}_f^{\mathrm{T}}(\partial\psi_f/\partial\mathbf{x})\mathbf{n}_2$$

This shows that, at both the initial and final times, any vector in the null space of the relevant constraint gradient matrix is perpendicular to the corresponding Lagrange multiplier vector. Assumption (ii) indicates appropriate choices for $\mathbf{n}_1$ and $\mathbf{n}_2$ as

$$\mathbf{n}_1 = \mathbf{f}(\mathbf{x}(t_i),t_i)$$
$$\mathbf{n}_2 = \mathbf{f}(\mathbf{x}(t_f),t_f)$$

With these choices, the Hamiltonian at either terminal time may be written in the following form:

$$H(\mathbf{x}(t),\mathbf{v}(t),u(t),\lambda(t),t) = \left[\lambda(t)^{\mathrm{T}}\mathbf{g}(\mathbf{x}(t),\mathbf{v}(t),t) + M(\mathbf{x}(t),t)\right]u(t) + L(\mathbf{x}(t),t)$$

Statements (1) and (2) follow immediately. ■

The theorem is useful because it leads to a method for finding time-optimal extremals with additional u_{max} arcs when u_{min}=0. Although not attempted in this work, it may also lead to a method for finding extremals with fewer u_{max} arcs.

Applied to the orbit transfer problem with ideal gravity and free transfer time, condition (1) implies the switching function must be zero at the entry/exit points. A similar condition was successfully used in the place of Eqs. (2.10) by Brown, et. al.[21] for free transfer time problems in ideal gravity. In that work, however, the condition was used as a boundary condition in order to reduce the number of variables in the problem.

One may make more use of this property of equal switching function values than a boundary condition; it can be used to help add burns, improving the performance of extremal orbit transfers as shall be seen in the following subsections.

II.3.1 Family of Extremals

Exploitation of the property described earlier by Theorem II.1, along with the favorable performance of these indirect methods allowed the study of the characteristics of families of solutions. Herein a family of solutions is defined as a set of solutions whose transfer times and numbers of burns vary but whose terminal orbits do not. The optimal terminal points will vary from solution to solution because they are free for optimization.

Figure 2.4 displays a family of optimal transfers. Each data point in the figure represents an extremal orbit transfer by its total transfer time and final mass. The transfers are planar and the dynamics do not take drag or oblateness effects into account. Furthermore, their terminal orbits are the same as for the transfer shown in Figure 2.1.

Though this family appears quite disjointed, it is actually quite connected. These connections can be best seen by starting at the leftmost transfer (point (1) in Fig. 2.4) and tracing solutions of increasing transfer time. The solutions from point (1) to point (2) are the original set of two-burn solutions, obtained via homotopy and a TPBVP solver (BOUNDSCO and MBCM).

At point (1) the total burn time equals the transfer time; point (1) is a one-burn solution. Point (2) represents a local optimum in transfer time; the Hamiltonian for point (2) is zero and this satisfies the transversality condition.

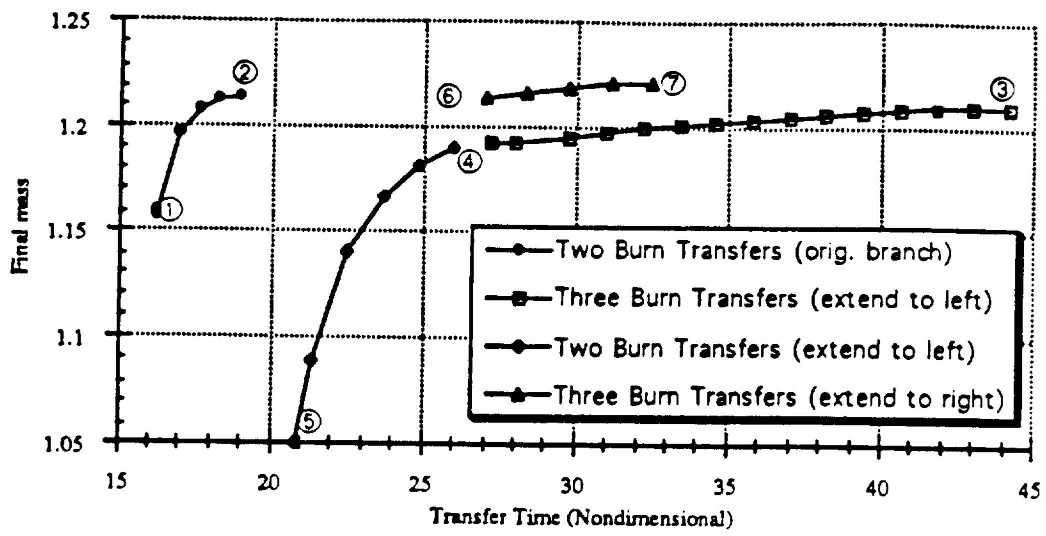

Figure 2.4 Plot of a Family of Optimal Transfers as Final Mass versus Transfer Time

As a result of Theorem II.1, the switching function at point (2) indicates the existence of additional solutions. The situation is shown in Figure 2.5. Because of the slope of H_T and the fact that it is zero at both the initial and final times (from Theorem II.1), the transfer may be extended optimally by the addition of a coast arc at the beginning and/or at the end of the transfer. This may seem trivial; one might observe that coast arcs can always be added; however, this particular situation leads to the addition of *burns*. Lawden's solution[10] to the costates on a coast arc shows that on such an arc with a vanishing Hamiltonian the switching function is periodic. This means that the switching function, once crossing zero, must return to zero. In other words, for an n burn transfer like that represented by Fig. 2.5, the periodicity of the coast arc switching function hints at the existence of two different n+1-burn solutions and an n+2-burn solution; each by different additions of coast arcs.

To optimally extend a transfer with coast arcs such that the switching function will again vanish, it is required that the switching function at a terminal orbit both be equal to zero and have an appropriate sign for its slope: positive at the initial time and/or negative at the final time. This situation can be seen in Figure 2.5 below, for the portion of the switching function labeled "Original Transfer."

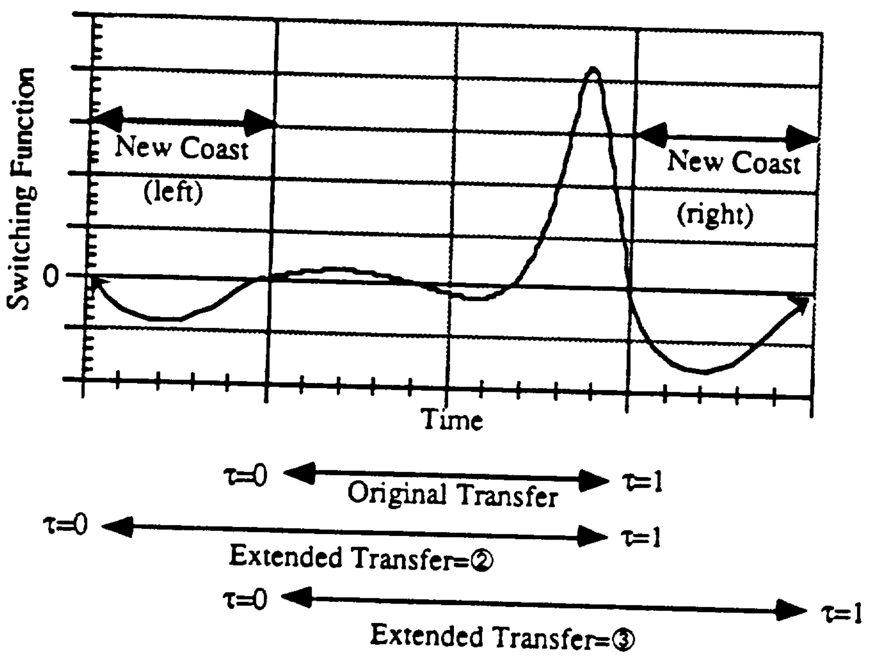

Figure 2.5 Extending the Switching Function to Create More Optimal Transfers; symbols ② and ③ refer to points in Figure 2.4

One may observe that the process does not guarantee a new burn - only a new coast arc. However, using numerical methods, one may discover that the burn can be lengthened.

Adding the coast arc is trivial; lengthening the burn arc is not. The following burn-addition procedure worked well. To add a burn to an *n*-burn solution with optimal transfer time that begins and ends with a burn arc: Append a coast arc to the solution at the chosen time, initial or final, making sure that states and costates are continuous. This is easily done by integrating forward from the final time or backward from the initial time. At both ends of the new coast arc the switching function must be zero. Use this extended transfer as a guess for the numerical routine setup for an n+1-burn problem with a slightly longer transfer time. Finally, use homotopy to obtain an n+1-burn solution with a longer transfer time.

For the guesses constructed in this report, the new coast arc was extended so that the switching became positive for a finite time. Since the thrust was set to T_{max} for this new interval, the boundary conditions were violated and the new arc was a non-optimal burn because the natural boundary condition was violated. However, it was found that this new burn aided in the convergence of iterations.

There are three options for creating the next transfer in the family: extend the transfer to right, extend it to the left, or extend it in both directions. However, because of numerical difficulties, this last option was not favored. First, consider extension to the right. Physically, this corresponds to adding the new burn closer to the final orbit. The resulting transfer is represented by point (6) in Figure 2.4. Starting with point (6), solutions with longer transfer times were easily found but solutions with shorter transfer times were not found at all.

Now consider the second option, extension to the left. Physically, this corresponds to adding a burn near the initial orbit. The resulting transfer is represented by point (3) of branch (3-4-5) in Figure 2.5. Numerical difficulty was discovered in attempting to find a solution with a greater transfer time than point (3); however, solutions with lower transfer times were found constituting branch (3-4-5). Additionally, note that this branch, though a branch of optimal solutions, is unfavorable when compared to branch (6-7) of the family. This example of multiplicity may be viewed as a rearrangement of the burns in the trajectory. It has not been shown analytically, but there is likely a connection to a similar result for non-optimal impulsive trajectories[18].

By the above discussion, points (2) and (3) and (6) are, in fact, the same transfer. The only difference between these transfers is the addition of a coast arc, which makes no difference in the performance associated with the transfer. This means that the branches of the family are connected and these connections are as follows, with the transfer time increasing: (1) to (2) (which is identical to (6)) to (7); or (5) to (4) to (3) (which is identical to (2)).

Figure 2.6 shows the switching function corresponding to the transfer represented by point (7). Compare this to Figure 2.5. The situation is repeating itself; the terminal switching points in Fig. 2.6 are close to zero. Clearly, one may attempt to expand this family of transfers from point (7).

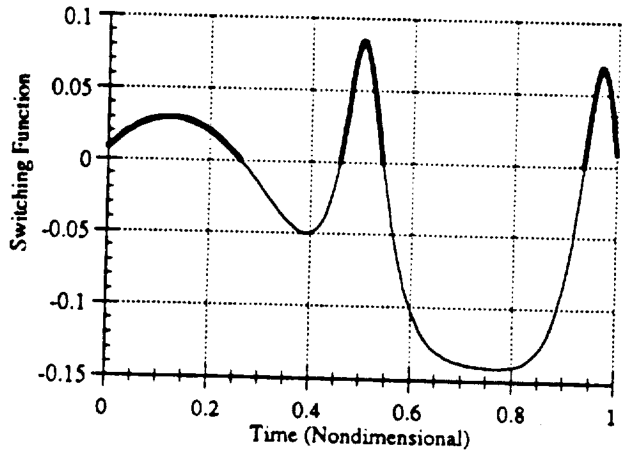

Figure 2.6 Switching Function of Transfer at Point 7 in Figure 2.5

II.3.2 Multiple Solutions in the Family

Evidence of the existence of multiple solutions was found. For a specified problem (including specification of the transfer time and the number of burns) there may exist more than one extremal transfer. Such multiple solutions are represented by any point on branch (3-4) and any point on branch (6-7) which have equal transfer times.

Conditions for multiplicity are not clear, but it is clear that solutions are not necessarily unique. It is also clear that one cannot say that just because the transfer time for one solution is longer than another, the former has a greater final mass; although this is typically an assumption made in the literature.

One cannot help but wonder why the solutions of branch (6-7) are more fuel-conservative than those of branch (3-4). Both branches are extensions of branch (1-2), but the difference is *where the new burn is placed.* When the burn was placed near the initial orbit, far from the attracting body, the branch was unfavorable. When the burn was placed near the final orbit, close to the attracting body, the branch was favorable. A principle often seen in impulsive trajectories seems to carry over in some form to finite burn trajectories; it appears to be better to implement changes in velocity near the attracting body, where changes in velocity will produce large increases in the already large kinetic energy, as opposed to far away from the attracting body, where kinetic energy is lower.

Finally, it is clear that during the burn addition process, one may control the placement of new burns. By tending to place new burns closer to the attracting body, undesirable solutions might be avoided.

The possibility of multiple solutions was recognized by Brusch[40] for one-burn low-thrust transfers originating from a circular orbit. Brusch also provides some excellent analysis concerning this phenomenon. In this research, it was found that multiple solutions exist for multiple-burn low-thrust transfers originating from an elliptical orbit. That the phenomenon may occur for the more general case indicates that there are likely many cases with multiple solutions.

[40]Brusch, R.G. and Vincent, T.L., "Low-Thrust, Minimum-Fuel, Orbital Transfers," *Astronautica Acta*, Vol. 16, pp. 65-74.

II.4. Conclusions

In this section the indirect methods BOUNDSCO and MBCM have demonstrated the ability to solve the optimal orbit transfer problem for small numbers of burns and small numbers of revolutions. Particular solutions have been presented in some detail. These solutions demonstrate some effects of drag and oblateness on the optimal transfer.

A new method for adding burns to time-optimal orbit transfers has been presented. This method is based on a newly observed property of the optimal switching function and a proof has been given for this property. The method has proven its practical utility by generating a family of solutions.

This family of solutions is a set of fixed-time optimal transfers with identical terminal orbits and parameterized by transfer time. Using this family, some new properties of optimal orbit transfers have been seen: multiple-burn transfers are not necessarily unique, transfers with greater transfer time do not necessarily have greater final mass, and local optima do not necessarily occur at transitions between N and $N+1$ burns when using homotopy to increase the transfer time.

Addressing the inclusion of orbit perturbations, neither BOUNDSCO nor MBCM had difficulty obtaining solutions with atmospheric drag or oblateness terms.

SECTION III

NEW METHODS FOR OPTIMIZING ORBIT TRANSFERS

III.1. Introduction

The bang-bang structure of the optimal orbit transfer solution is well-known. This means the optimal transfer is made up of a series of individual interior transfers between a sequence of orbits beginning with the specified initial orbit and ending with the desired final orbit. However, the fact that these transfers are, individually, optimal transfers has not yet been widely exploited. In this section, this notion is expressed concisely in a mathematical sense and shown to be quite useful for numerical methods.

Two methods that originated with this notion are presented. First, the Patched Method is a hybrid method with a greatly reduced number of parameters. In fact, not only are the number of parameters reduced, but they are all free for optimization.

The Patched Method also takes advantage of another simple idea: any interior one-burn transfer taken between two neighboring interior orbits of an N-burn transfer should be easier to solve than the N-burn transfer as a whole. It then makes sense to consider using the orbital elements of each intermediate transfer orbit as free parameters. Given these parameters, the performance (final mass) is computed by solving each individual one-burn problem in succession.

The Patched Method, however, pays for its robustness in speed. Therefore, it seems to be most useful as a way of refining and developing initial guesses for the second method, the Modified Patched Method (MPM). MPM is an indirect method; no variables are directly optimized. It enforces conditions necessary for the transfer to be an extremal solution. MPM assumes a bang-bang structure; however, as in BOUNDSCO, the Patched Method, and many other methods found in the literature, MPM does not enforce satisfaction of Pontryagin's Maximum Principle. For this problem, Pontryagin's Maximum Principle supplies the switching law as Eqs (2.6) and (2.7). These methods only guarantee that the thrust will switch values at the zeros of the switching function, Eq. (2.6); they do not guarantee that the polarity will be consistent with Eq. (2.7). However, this turns out to be an easy condition to check after iterations converge.

A few reasonable and common assumptions are made in both methods. It is assumed that the only forces on the spacecraft are ideal gravity and the thrust from the rocket motor. The number of arcs of maximum thrust is assumed fixed; choosing the number of burns is often desirable and makes the problem easier to solve. The first and last arcs are assumed to be of maximum thrust; however, no generality is lost here under the assumption of ideal gravity. Arcs of intermediate thrust are assumed not to exist in the trajectory because numerical experience indicates that such arcs are rare if they exist at all. It is assumed that no part of the trajectory will be rectilinear; in other words, the angular momentum vector never vanishes. Rectilinear trajectories are unlikely to ever be of interest in an orbit transfer problem and, if they are of interest, the implications of zero angular momentum should motivate the development of specialized software.

III.2. The Patched Method

Usually, when a hybrid method is formulated the assumption is made that the solution to this new problem is always a solution to the original problem. Intuitively, this is often easy to accept. However, it is even more reassuring to prove whatever equivalency exists between the original formulation and that used by the hybrid method.

This subsection describes the architecture of the Patched Method, explaining how it functions. Also, it is shown that necessary conditions from the traditional problem statement are, in fact, equivalent to the necessary conditions which arise from the optimization loop of the Patched Method.

III.2.1. Architecture of the Method

The architecture of the Patched Method is best described as an inner and an outer loop. Given a choice of orbital elements, the inner loop solves each one-burn problem in succession. Each one-burn transfer has its terminal points and transfer time free for optimization. However, the result is a suboptimal transfer; it lacks the optimal choice of intermediate transfer orbits. The choice of transfer orbits is made by the outer loop via unconstrained minimization of the complete trajectory's fuel consumption.

The method that has been chosen for the outer loop is the conjugate gradient method. Since such methods tend to have better performance if they are supplied with an analytical gradient, such a gradient was formulated for this case; the formulation will be presented in this section. The particular FORTRAN code is taken from a common reference[41].

The architecture of this method indicates a useful new paradigm for the orbit transfer problem. One might think of the multiple-burn transfer optimization problem as optimizing the fuel used by choice of the intermediate transfer orbits, expressed as

$$\text{given } \alpha_0, \alpha_N, m_o, c, T; \quad \min_{\alpha_i,\, i=1,N-1} \sum_{i=1}^{N} t_{fi}\left(\alpha_{i-1}, \alpha_i, T, c, m_o - c\sum_{j=1}^{i} t_{f(j-1)}\right) \tag{3.1}$$

[41]Press, W.H., et. al. *Numerical Recipes: the Art of Scientific Computing*, New York: Cambridge University Press, 1989.

where $t_{fo}=0$ and $t_{fi}(\alpha_{i-1},\alpha_i,T,m_i)$ shall be called the *transfer time function* which computes the optimal transfer time for the orbit transfer problem defined by the initial orbital elements α_{i-1}, the final orbital elements α_i, the thrust level T, the initial mass m_i and the fuel consumption rate c. In (3.1), the value for the initial mass of each burn is calculated knowing the transfer times for the burns before, giving an unconstrained minimization problem; alternatively this could have been expressed as a constraint on the minimization.

In this section it will be proven that certain conditions necessary to solve (3.1) are equivalent to certain conditions necessary to solve the orbit transfer fuel-optimization problem, under certain assumptions. It will be seen that the restrictions imposed are few and quite practical; however, it is not claimed that the two problems themselves are equivalent; this may or may not be true. Nevertheless, this paradigm has certain advantages. The problem expressed in (3.1) is a parameter optimization problem. If an expression for the transfer time function were available, this would quite likely be easier to solve than the TPBVP.

Unfortunately, there are no analytical expressions or approximations for the transfer time function. The Patched Method must compute it numerically in the inner loop. The inner loop uses both Direct Collocation with Nonlinear Programming (DCNLP) and multiple-shooting to solve the one-burn transfer. Each time the optimal solution for a one-burn trajectory is required, either method may be used. For the first iteration, the choice is up to the user. If DCNLP is requested, the solution is found for a high tolerance. Once this tolerance is achieved, a multiple-shooting guess is constructed. Multiple-shooting is then used to reduce the error to the desired, lower, tolerance. If multiple-shooting was requested as the initial method and it fails, a DCNLP guess is constructed and DCNLP is attempted. If DCNLP is successful, then multiple-shooting is used again. This structure was chosen because it was found that DCNLP was typically much too slow to use with each outer-loop iteration but multiple-shooting typically could not converge rough guesses. The failure of multiple-shooting typically occurred with the first iteration if the initial guess for the transfer was poor or the failure would occur if the outer loop took too large a step.

III.2.2. Using Direct Method Solutions as Guesses for Indirect Methods

At this point, the question of converting the solution from a direct method to the guess for an indirect method arises (the inverse process is trivial because the solution obtained by an indirect method inherently contains more information). The adjoined performance index for the *j*th of *N* one-burn problems (*j*=1,...,N) is

$$J_j = m_j(t_j) + \nu_{2,j-1}{}^T\left[\psi\left(\mathbf{x}_j(0)\right) - \alpha_{j-1}\right] + \nu_{2j}{}^T\left[\psi\left(\mathbf{x}_j(t_{fj})\right) - \alpha_j\right] \qquad (3.2)$$
$$+ \xi_j{}^T\left[m_j(0) - \beta_j\right] + \int_0^{t_{fj}} \lambda_j{}^T(t)\left[\mathbf{f}\left(\mathbf{x}_j(t), \mathbf{e}_{Tj}(t)\right) - \dot{\mathbf{x}}_j(t)\right]dt$$

where $\mathbf{x}_j(t)$ is the state, $u_j(t)$ is the control, t_{fj} is the free final time (the initial time is fixed at 0), α_{j-1} and α_j are the initial and final boundary parameters, $\psi_1(\mathbf{x})$ and $\psi_2(\mathbf{x})$ are the boundary constraint vector functions, $m_j(t)$ is the spacecraft mass, $\mathbf{f}\left(\mathbf{x}_j(t), \mathbf{e}_{Tj}(t)\right)$ is the state dynamics, and $m_j(t_j)$ is the performance index to be maximized. The parameter β_j is fixed while solving each one-burn; its value is equal to initial mass constraint (m_o) or the final mass of the previous burn:

$$\beta_j = m_{j-1}\left(t_{f(j-1)}\right) \qquad (3.3)$$

The discretized version for the same problem, divided into *M* nodes indexed by *i* and designed for a direct method, follows:

$$\begin{aligned}\bar{J}_j = \bar{m}_{j,M} + \eta_{2j-1}{}^{\mathrm{T}}\left[\zeta_1(\mathbf{y}_{j,1}) - \alpha_{j-1}\right] + \eta_{2j}{}^{\mathrm{T}}\left[\zeta_2(\mathbf{y}_{j,M}) - \alpha_j\right] \\ +\sigma_j{}^{\mathrm{T}}\left[\bar{m}_{j,i} - \beta_j\right] + \sum_{i=1}^{M} \mu_{j,i}{}^{\mathrm{T}}\Delta_i(\mathbf{y}_{j,i},\omega_{j,i})\end{aligned} \tag{3.4}$$

where $\mathbf{y}_i$ is the state, ω_i is the control, $\zeta_1(\mathbf{y})$ and $\zeta_2(\mathbf{y})$ are the boundary constraint functions, $\Delta_i(\mathbf{y}_i,\omega_i)$ are integration constraints,$\bar{m}_{j,i}$ is the spacecraft mass, and $\bar{m}_{j,M}$ is the performance index to be maximized Assignment of β_j, in this case, is similar to Eqn. (3.3) as follows:

$$\beta_j = \bar{m}_{j-1,M} \tag{3.5}$$

Since, for any $1<k<M$, both formulations solve the same problem with $j=k$, one can assume that $J_k = \bar{J}_k$ for any choice of α_k and α_{k+1} with$\bar{m}_{j-1,M} = m_{j-1}\left(t_{f(j-1)}\right)$, then $\frac{\partial J_j}{\partial \alpha_j} = \frac{\partial \bar{J}_j}{\partial \alpha_j}$, $\frac{\partial J_j}{\partial \alpha_{j+1}} = \frac{\partial \bar{J}_j}{\partial \alpha_{j+1}}$, and $\frac{\partial J_j}{\partial m_{j-1}\left(t_{f(j-1)}\right)} = \frac{\partial \bar{J}_j}{\partial \bar{m}_{j-1,M}}$. The implications of this are best seen in the first-order changes for both performance indices:

$$\begin{aligned}\delta J_j = \delta m_j(t_j) \\ +\nu_{2j-1}{}^{\mathrm{T}}\left[\psi_{1\mathbf{x}}(\mathbf{x}_j(0))\delta\mathbf{x}_j(0) - \delta\alpha_{j-1}\right] \\ +\nu_{2j}{}^{\mathrm{T}}\left[\psi_{2\mathbf{x}}(\mathbf{x}_j(t_j))\delta\mathbf{x}_j(t_j) - \delta\alpha_j\right] \\ +\xi_j{}^{\mathrm{T}}\left[\delta m_j(0) - \delta\beta_j\right] \\ +H\left(\mathbf{x}_j(t_j),\mathbf{e}_{Tj}(t_j),\lambda_j(t_j)\right)dt_j \\ +\int_0^{t_j}\Big[H_{\mathbf{x}}\left(\mathbf{x}_j(t),\mathbf{e}_{Tj}(t),\lambda_j(t)\right)\delta\mathbf{x}_j(t) \\ +H_u\left(\mathbf{x}_j(t),\mathbf{e}_{Tj}(t),\lambda_j(t)\right)\delta\mathbf{e}_{Tj}(t) - \lambda_j{}^{\mathrm{T}}\dot{\mathbf{x}}_j(t)\Big]dt\end{aligned} \tag{3.6}$$

$$\begin{aligned}\delta\bar{J}_j = {} & \delta\overline{m}_{j,M} \\ & +\eta_{2j-1}{}^{T}\left[\zeta_{1_y}(\mathbf{y}_{j,1})\delta\mathbf{y}_{j,1} - \delta\alpha_{j-1}\right] \\ & +\eta_{2j}{}^{T}\left[\zeta_{2_y}(\mathbf{y}_{j,M})\delta\mathbf{y}_{j,M} - \delta\alpha_j\right] \\ & +\sigma_j{}^{T}\left[\delta\overline{m}_{j,i} - \delta\beta_j\right] \\ & +\sum_{i=1}^{M}\mu_{j,i}{}^{T}\Delta_{i_{y_{j,i}}}(\mathbf{y}_{j,i},\omega_{j,i})\delta\mathbf{y}_{j,i} + \sum_{i=1}^{M}\mu_{j,i}{}^{T}\Delta_{i_{\omega_{j,i}}}(\mathbf{y}_{j,i},\omega_{j,i})\delta\omega_{j,i}\end{aligned} \tag{3.7}$$

Knowing the solutions for both optimal control problems, one can substitute for the state and control of the local extremals into Eqs. (3.6)-(3.7), respectively. The resulting equations are simply:

$$\delta J_j = -\nu_{2j-1}{}^{T}\delta\alpha_{j-1} - \nu_{2j}{}^{T}\delta\alpha_j - \xi_j{}^{T}\delta\beta_j \tag{3.8}$$

$$\delta\bar{J}_j = -\eta_{2j-1}{}^{T}\delta\alpha_{j-1} - \eta_{2j}{}^{T}\delta\alpha_j - \sigma_j{}^{T}\delta\beta_j \tag{3.9}$$

It is now quite clear that since the gradients were surmised to be approximately equal, then $\nu_{2j-1} \approx \eta_{2j-1}$, $\nu_{2j} \approx \eta_{2j}$, and $\xi_j \approx \sigma_j$.

A simple approach to converting a solution obtained with a direct method into an appropriate guess for an indirect method is now clear. One may use a direct method to compute η_{2j-1}, η_{2j}, and σ_j; then use Eq. (2.8b) to obtain an approximation of the costates at the initial time. Knowing the states and the costates at the initial time, obtaining an approximate time history merely requires the solution of an initial value problem.

III.2.3. Gradient of the Cost Function

For this application, the gradient of the cost is required. The cost for the entire transfer is

$$J_{overall} = \sum_{j=1}^{N} t_{fj} = -\frac{g_o I_{sp}}{T}\left[m_N(t_{fN}) - m_1(0)\right] \tag{3.10}$$

where the mass at the end of the jth burn is a function of α_j, α_{j-1}, and m_{j-1}. This is obviously equivalent expression to (3.1). Omitting some simple steps of calculus and algebra, the gradient of the cost functional $J_{overall}$, may easily be written as

$$\begin{aligned}
\frac{\partial J}{\partial \alpha_i} &= \frac{-g_o I_{sp}}{T}\left[\prod_{j=i+1}^{N-1}\frac{\partial m_{j+1}(t_{f(j+1)})}{\partial m_j(t_j)}\right]\left[\frac{\partial m_{i+1}(t_{f(i+1)})}{\partial \alpha_i} - \frac{\partial m_{i+1}(t_{f(i+1)})}{\partial m_i(t_{fi})}\frac{\partial m_i(t_{fi})}{\partial \alpha_i}\right], i = 1,\ldots,N-2 \\
\frac{\partial J}{\partial \alpha_{N-1}} &= \frac{-g_o I_{sp}}{T}\left[\frac{\partial m_N(t_{fN})}{\partial \alpha_{N-1}} - \frac{\partial m_N(t_{fN})}{\partial m_{N-1}(t_{f(N-1)})}\frac{\partial m_{N-1}(t_{f(N-1)})}{\partial \alpha_{N-1}}\right]
\end{aligned} \tag{3.11}$$

Equations (3.11) are not yet sufficient to implement the Patched Method. Expressions for evaluating the terms in Eqs. (3.11) are required. To begin, note that m_j is the performance index of the jth burn. Referring back to Eq. (3.8), one observes that

$$\frac{\partial J_j}{\partial \alpha_{j-1}} = \frac{\partial m_j(t_{fj})}{\partial \alpha_{j-1}} = -\nu_{2j-1}^{\mathrm{T}} \tag{3.12a}$$

$$\frac{\partial J_j}{\partial \alpha_j} = \frac{\partial m_j(t_{fj})}{\partial \alpha_j} = -\nu_{2j}^{\mathrm{T}} \tag{3.12b}$$

$$\frac{\partial J_j}{\partial \beta_j} = \frac{\partial m_j(t_{fj})}{\partial m_{j-1}(t_{f(j-1)})} = -\xi_j \tag{3.12c}$$

so that Eqs. (3.11) can be restated as

$$\begin{aligned}
\frac{\partial J}{\partial \alpha_i} &= \frac{g_o I_{sp}}{T}\left[\prod_{j=i+1}^{N-1}(-\xi_{j+1})\right]\left[\nu_{2i+1}^{\mathrm{T}} + \xi_{i+1}\nu_{2i}^{\mathrm{T}}\right], i = 1,\ldots,N-2 \\
\frac{\partial J}{\partial \alpha_{N-1}} &= \frac{g_o I_{sp}}{T}\left[\nu_{2N-1}^{\mathrm{T}} + \xi_N \nu_{2(N-1)}^{\mathrm{T}}\right] \quad .
\end{aligned} \tag{3.13}$$

Which, simply, gives the gradient of the overall cost function in terms of the Lagrange multipliers from each respective one-burn problem. It is interesting to note that zeroing this gradient supplies simple relations between the Lagrange multipliers associated with the beginning of one burn to those associated with the termination of the previous burn. It is the "patching" together of optimal burns implied by these relations that inspired the name of the Patched Method.

III.2.4. An Equivalent Set of Necessary Conditions

The following results will prove useful to showing the practicality of the Patched Method conditions and, later, the practicality of the Modified Patched Method conditions:

Lemma III.1: If the matrix $\Gamma \in R^{(n-1)\times n}$ yields $rank(\Gamma) = n-1$ and satisfies $\Gamma\mathbf{f} = 0$, $\mathbf{f} \in R^n$ while $\mathbf{f}$ satisfies $\lambda^T\mathbf{f} = 0$, $\lambda \in R^n$ and $\mathbf{f}^T\mathbf{f} \neq 0$, then λ may be expressed as $\lambda = \Gamma^T\mathrm{v}$ where $\mathrm{v} \in R^{n-1}$.

Proof:

If $rank(\Gamma) = n-1$, $\Gamma\mathbf{f} = \mathbf{0}$, and $\mathbf{f}^T\mathbf{f} \neq 0$, then $\mathbf{f}$ is in the null space of Γ and it is obvious that $rank([\Gamma^T \quad \mathbf{f}]) = n$. This in turn implies that there exists a $\mathrm{v} \in R^{n-1}$ and $\beta \in R$ such that

$$\lambda = [\Gamma^T \quad \mathbf{f}]\begin{bmatrix}\mathrm{v}\\ \beta\end{bmatrix}$$

Now, $\lambda^T\mathbf{f} = 0 \Rightarrow \mathrm{v}^T\Gamma\mathbf{f} + \beta\mathbf{f}^T\mathbf{f} = 0 \Rightarrow \beta\mathbf{f}^T\mathbf{f} = 0 \Rightarrow \beta = 0.$ ■

Lemma III.2: Consider the following system of ordinary differential equations:

(i) $\dfrac{d}{dt}\mathbf{x}(t) = \mathbf{f}(t)$

(ii) $\frac{d}{dt}\lambda(t) = -\left[\frac{\partial}{\partial \mathbf{x}}\mathbf{f}(\mathbf{x}(t))\right]^{\mathrm{T}}\lambda(t)$

and a matrix function $\Gamma(\mathbf{x})$, if $\frac{d}{dt}\Gamma(\mathbf{x}(t)) + \Gamma\frac{\partial}{\partial \mathbf{x}}\mathbf{f}(\mathbf{x}(t)) = \mathbf{0}$, then the vector function $\lambda(t) = \Gamma(\mathbf{x}(t))^{\mathrm{T}}\mathrm{v}$ is a solution to the differential equation (ii).

Proof:

To show that a function is a solution to (ii), it suffices to substitute the function into both sides of (ii) and show that equality holds.

$$L.H.S. = \frac{d}{dt}\left(\Gamma(\mathbf{x}(t))^{\mathrm{T}}\mathrm{v}\right) = \left[\frac{d}{dt}\Gamma(\mathbf{x}(t))\right]^{\mathrm{T}}\mathrm{v}$$
$$R.H.S. = -\left[\frac{\partial}{\partial \mathbf{x}}\mathbf{f}(\mathbf{x}(t))\right]^{\mathrm{T}}\Gamma(\mathbf{x}(t))^{\mathrm{T}}\mathrm{v}$$

The left hand side will equal the right hand side if $\frac{d}{dt}\Gamma(\mathbf{x}(t)) + \Gamma\frac{\partial}{\partial \mathbf{x}}\mathbf{f}(\mathbf{x}(t)) = \mathbf{0}$. ■

The following definitions are precursors to a theorem that will prove the equivalence between necessary conditions for the Patched Method, which will be expressed in the definition of conditions $\{II\}$, and necessary conditions derived from the usual application of optimal control theory, which will be expressed in the definition of conditions $\{I\}$. The specific problem formulation for which such conditions are equivalent will be defined as $\{P\}$.

In what follows, C_i^0 denotes the set of i-dimensional vector functions that are continuous with respect to all arguments, vector and/or scalar, and U denotes the set of piece-wise continuous scalar functions with one scalar argument.

Definition: The optimal control problem $\{P\}$ is of the form:

minimize $J = y(t_f)$ subject to the following constraints:

$\dot{\mathbf{x}}(t) = \mathbf{f}(\mathbf{x}(t)) + \mathbf{g}(y(t), \mathbf{v}(t))u(t)$, $\mathbf{x}(t) \in C_n^0$, $\mathbf{v}(t) \in C_m^0$;
$\dot{y}(t) = cu(t)$, $y(t) \in C_1^0$
$0 \le u(t) \le u_{max}$, $u(t) \in U$;
$\psi(\mathbf{x}(t_o)) - \alpha_o = \mathbf{0}$, $\psi(\mathbf{x}(t_f)) - \alpha_f = \mathbf{0}$, $\psi(\mathbf{x}(t)) \in C_{n-1}^0$;
$y(t_o) = y_o$;
t_f is free for optimization, t_o is fixed

and satisfying the following assumptions:

(i) $\left[\frac{\partial \psi}{\partial \mathbf{x}}(\mathbf{x}(t))\right]\mathbf{f}(\mathbf{x}(t)) = \mathbf{0}$;
(ii) $u(t_i) \neq 0$, $u(t_f) \neq 0$, and the number of arcs with $u = u_{max}$ is N
(iii) $\mathbf{g}(\mathbf{x}(t), y(t), \mathbf{v}(t))$ is not linear in $\mathbf{v}(t)$
(iv) the solution only contains arcs with $u=0$ or $u=u_{max}$;
(v) $rank\left(\frac{\partial \psi}{\partial \mathbf{x}}(\mathbf{x}(t))\right) = n-1$;
(vi) $\left(\frac{d}{dt}\frac{\partial}{\partial \mathbf{x}}\psi(\mathbf{x}(t)) + \frac{\partial}{\partial \mathbf{x}}\psi(\mathbf{x}(t))\frac{\partial}{\partial \mathbf{x}}\mathbf{f}(\mathbf{x}(t))\right) = \mathbf{0}$ when $\dot{\mathbf{x}}(t) = \mathbf{f}(\mathbf{x}(t))$
(vii) $\mathbf{f}^{\mathrm{T}}(\mathbf{x}(t))\mathbf{f}(\mathbf{x}(t)) \neq 0 \ \forall t \in [t_o, t_f]$

Consider the usual optimal control formulation, introduction of the Lagrange multiplier functions $\hat{\lambda}(t)$, the Hamiltonian $H(\mathbf{x}(t), y(t), \mathbf{v}(t), u(t), \hat{\lambda}(t))$ function, and the following partition of $\hat{\lambda}(t)$

$$\hat{\lambda}(t) = \begin{bmatrix} \hat{\lambda}_x(t) \\ \hat{\lambda}_y(t) \end{bmatrix}, \ \hat{\lambda}_x(t) \in C_n^0 \ , \ \hat{\lambda}_y(t) \in C_1^0$$

Definition: For optimal control problem $\{P\}$, the conditions $\{I\}$ are

$$H\left(\mathbf{x}(t), y(t), \mathbf{v}(t), u(t), \hat{\lambda}(t)\right) = \hat{\lambda}_{\mathbf{x}}^{\mathrm{T}}(t)\, \mathbf{f}(\mathbf{x}(t)) + \left[\hat{\lambda}_{\mathbf{x}}^{\mathrm{T}}(t)\, \mathbf{g}(y(t), \mathbf{v}(t)) + c\hat{\lambda}_y(t)\right] u(t) = 0 \tag{3.14}$$

$$\frac{d}{dt}\hat{\lambda}_{\mathbf{x}}(t) = -\left[\frac{\partial}{\partial \mathbf{x}}\mathbf{f}(\mathbf{x}(t))\right]^{\mathrm{T}} \hat{\lambda}_{\mathbf{x}}(t) \tag{3.15}$$

$$\frac{d}{dt}\hat{\lambda}_y(t) = -\hat{\lambda}_{\mathbf{x}}(t)^{\mathrm{T}}\left[\frac{\partial}{\partial y}\mathbf{g}(y(t), \mathbf{v}(t))\right] u(t) \tag{3.16}$$

$$\hat{\lambda}_{\mathbf{x}}(t)^{\mathrm{T}}\left[\frac{\partial}{\partial \mathbf{v}}\mathbf{g}(y(t), \mathbf{v}(t))\right] = 0 \tag{3.17}$$

$$\hat{\lambda}_{\mathbf{x}}(t_f) = \left[\frac{\partial \psi}{\partial \mathbf{x}}(\mathbf{x}(t_f))\right]^{\mathrm{T}} \hat{\mathbf{v}}_f \tag{3.18}$$

$$\hat{\lambda}_{\mathbf{x}}(t_o) = -\left[\frac{\partial \psi}{\partial \mathbf{x}}(\mathbf{x}(t_o))\right]^{\mathrm{T}} \hat{\mathbf{v}}_o \tag{3.19}$$

$$\hat{\lambda}_y(t_f) = 1 \tag{3.20}$$

$$\hat{\lambda}_{\mathbf{x}}(t_{si})^{\mathrm{T}} \mathbf{g}(y(t_{si}), \mathbf{v}(t_{si})) + c\hat{\lambda}_y(t_{si}) = 0,\ i = 1, \ldots 2(N-1) \tag{3.21}$$

These are the transversality condition, Eq. (3.14); the Euler-Lagrange differential equations, Eqs. (3.15)-(3.17); the natural boundary conditions, Eqs. (3.18)-(3.20); and that the switching function vanishes at the switching points, Eq. (3.21). It is also required by conditions $\{I\}$ that the control $u(t)$ switch values across each switching point, in a pattern consistent with assumption (ii).

Definition: For optimal control problem $\{P\}$, the conditions $\{II\}$ are

$$H_i\left(\mathbf{x}(t), y(t), \mathbf{v}(t), u(t), \bar{\lambda}_i(t)\right) = \bar{\lambda}_{\mathbf{x}i}(t)^{\mathrm{T}} \mathbf{f}(\mathbf{x}(t)) + \left[\bar{\lambda}_{\mathbf{x}i}(t)^{\mathrm{T}} \mathbf{g}(y(t), \mathbf{v}(t)) + c\bar{\lambda}_{yi}(t)\right] u(t) = 0 \tag{3.22}$$

$$\frac{d}{dt}\bar{\lambda}_{\mathbf{x}i}(t) = -\left[\frac{\partial}{\partial \mathbf{x}} \mathbf{f}(\mathbf{x}(t))\right]^{\mathrm{T}} \bar{\lambda}_{\mathbf{x}i}(t) \tag{3.23}$$

$$\frac{d}{dt}\bar{\lambda}_{yi}(t) = -\bar{\lambda}_{\mathbf{x}i}(t)^{\mathrm{T}}\left[\frac{\partial}{\partial y} \mathbf{g}(y(t), \mathbf{v}(t))\right] u(t) \tag{3.24}$$

$$u(t) = u_{max} \tag{3.25}$$

$$\bar{\lambda}_{\mathbf{x}i}(t)^{\mathrm{T}}\left[\frac{\partial}{\partial \mathbf{v}} \mathbf{g}(y(t), \mathbf{v}(t))\right] = 0 \tag{3.26}$$

$$\bar{\lambda}_{\mathbf{x}}(t_i) = -\left[\frac{\partial \psi}{\partial \mathbf{x}}(\mathbf{x}(t_i))\right]^{\mathrm{T}} \bar{\mathbf{v}}_{oi} \tag{3.27}$$

$$\bar{\lambda}_{\mathbf{x}}(t_{fi}) = \left[\frac{\partial \psi}{\partial \mathbf{x}}(\mathbf{x}(t_{fi}))\right]^{\mathrm{T}} \bar{\mathbf{v}}_{fi} \tag{3.28}$$

$$\bar{\lambda}_{yi}(t_{fi}) = 1 \tag{3.29}$$

$$\bar{\mathbf{v}}_{o(i+1)} + \bar{\lambda}_{y(i+1)}(t_{i+1})\bar{\mathbf{v}}_{fi} = 0 \tag{3.30}$$

$$\left\{\begin{matrix} \mathbf{x}(t_{i+1}) = \mathbf{x}(t_{fi}) + \int_{t_{fi}}^{t_{i+1}} \mathbf{f}(\mathbf{x}(t))dt \\ y(t) = y(t_{i+1}) = y(t_{fi}) \\ u(t) = 0, \;\; t \in \left[t_{fi}, t_{i+1}\right] \end{matrix}\right\} \tag{3.31}$$

where Eqs. (3.22)-(3.26) are defined for $t \in \left[t_i, t_{fi}\right]$ and the following partition is defined

$$\bar{\lambda}_i(t) = \begin{bmatrix} \bar{\lambda}_{\mathbf{x}i}(t) \\ \bar{\lambda}_{yi}(t) \end{bmatrix}, \; \bar{\lambda}_{\mathbf{x}i}(t) \in C_n^0 \;, \; \bar{\lambda}_{yi}(t) \in C_1^0$$

All conditions in $\{II\}$ are defined for i=1..N except Eqs. (3.30)-(3.31) which are only defined for i=1..N-1. Finally, $t_1 = t_o$ is assigned and the value for t_f is seen to be t_{fN}.

Theorem III.1: If and only if

$$\left\{\mathbf{x}(t), y(t), \mathrm{v}(t), u(t), \hat{\lambda}(t) \middle| \, t \in [t_o, t_f]\right\}, \hat{\mathrm{v}}_o, \hat{\mathrm{v}}_f, t_f, \left\{t_{si} \middle| \, i = 1, \ldots 2(N-1)\right\} \tag{3.32}$$

satisfies $\{I\}$ then

$$\left\{\mathbf{x}(t), y(t), \mathrm{v}(t), u(t) \middle| \, t \in [t_1, t_{fN}]\right\}, \left\{\left(\bar{\lambda}_i(t), \ t \in [t_i, t_{fi}]\right), t_i, t_{fi}, \bar{\mathrm{v}}_{oi}, \bar{\mathrm{v}}_{fi} \middle| \, i = 1, \ldots N\right\} \tag{3.33}$$

satisfies $\{II\}$, assuming that the constraints and assumptions from $\{P\}$ are satisfied.

Proof:

It will be shown, for both the necessary and sufficient parts of the theorem, that if one condition holds, then a construction may be made such that the other is satisfied.

Assume that (3.32) satisfies $\{I\}$. A solution to $\{II\}$ will be constructed from (3.32) going backwards in time. For the last u=u_{max} arc, where $t \in [t_N, t_{fN}]$, define

$$\bar{\mathrm{v}}_{fN} = \hat{\mathrm{v}}_f \tag{3.34}$$

$$t_N = t_{s2(N-1)} \tag{3.35}$$

$$\bar{\lambda}_N(t) = \hat{\lambda}(t), \ t \in [t_N, t_{fN}] \tag{3.36}$$

These definitions allow Eqs. (3.14)-(3.18) and Eq. (3.20) to imply satisfaction of Eqs. (3.22)-(3.26), (3.28), and (3.29) for $t \in [t_N, t_{fN}]$ and i=N. Eq. (3.21) for i=2(N-1) specifies that the switching function is zero at the beginning of this interval, where t=t_N. Therefore, satisfaction of Eq. (3.22) for i=N clearly implies that $\bar{\lambda}_{xN}{}^T(t_N)\, \mathbf{f}(\mathbf{x}(t_N)) = 0$. Considering this result, Lemma III.1 with $\Gamma(\mathbf{x}(t_N)) = \frac{\partial \psi}{\partial \mathbf{x}}(\mathbf{x}(t_N))$ and assumptions (i), (v), and (vii), implies that there exists a $-\bar{v}_{oN} \in R^{n-1}$ such that Eq. (3.27) is satisfied for i=N. This completes the definitions for the final u=u_{max} arc.

Consider the next interval, where $t \in \left[t_{f(N-1)}, t_N\right]$, the definitions will now be extended into this interval. Define $t_{f(N-1)}$=$t_{s(2N-3)}$. The conditions $\{I\}$ specify that $u(t)$=0 for t in this interval. This implies that Eqs. (3.31) with i=N-1 are consistent with the switching structure of $\{I\}$. Define

$$\bar{\lambda}_{xN}(t) = \hat{\lambda}_x(t),\ t \in \left[t_{fN-1}, t_N\right]$$

With this definition and that Eq. (3.27) is satisfied for i=N, Lemma III.2 with $\Gamma(\mathbf{x}(t)) = \frac{\partial \psi}{\partial \mathbf{x}}(\mathbf{x}(t))$ and assumption (vi) implies that the Lagrange multipliers satisfy

$$\bar{\lambda}_x\left(t_{f(N-1)}\right) = \left[\frac{\partial \psi}{\partial \mathbf{x}}\left(\mathbf{x}\left(t_{f(N-1)}\right)\right)\right]^{\mathrm{T}}\left[-\bar{v}_{oN}\right] = \hat{\lambda}_x\left(t_{s(2N-3)}\right)$$

The definition $\bar{v}_{f(N-1)} = -\frac{1}{\hat{\lambda}_y(t_N)}\bar{v}_{oN}$ then implies that Eq. (3.30) for i=N-1 is satisfied. The construction for the last u=0 arc is complete.

Define

$$t_{N-1} = t_{s(2N-4)}$$

$$\bar{\lambda}_{N-1}(t) = \frac{1}{\hat{\lambda}_y(t_N)}\hat{\lambda}(t),\ t \in \left[t_{N-1}, t_{f(N-1)}\right]$$

Note that this definition implies satisfaction of (3.29) for i=N-1 because $\hat{\lambda}_y(t_N) = \hat{\lambda}_y\left(t_{f(N-1)}\right)$. This also makes satisfaction of Eq. (3.30) for i=N-1 imply satisfaction of (3.28) for i=N-1. After establishing these constructions, the arguments for the previous u=u_{max} and u=0 arc may be repeated. With each repeat, the construction is made with scaling by an even earlier value from $\hat{\lambda}_y(t)$ in the following sequence $\hat{\lambda}_y(t_i), i = N, \ldots 2$. Such repetition may be continued until the beginning of the first burn is reached. At this point, the definition

$$\bar{v}_{o1} = \frac{1}{\hat{\lambda}_y(t_2)} \hat{v}_o$$

implies satisfaction of (3.27) with i=1 and completes the proof of the "if" part of the theorem.

Assume that (3.33) satisfies $\{II\}$. The construction of the solution to $\{I\}$ will proceed backwards in time. Consider the last u=u_{max} arc, where $t \in [t_N, t_{fN}]$. Define

$$\hat{v}_f = \bar{v}_{fN}$$

$$t_{s2(N-1)} = t_N$$

$$\hat{\lambda}(t) = \bar{\lambda}_N(t),\ t \in [t_N, t_{fN}]$$

For $t \in [t_N, t_{fN}]$ and i=N, this construction lets Eqs. (3.22)-(3.26) and (3.28) and (3.29) imply satisfaction of Eqs. (3.18) and (3.20) at the final point and Eqs. (3.14)-(3.17) during the interval. Now, it is obvious that satisfaction of Eqs. (3.14) and (3.27) with i=N in this interval under assumption (i) implies that Eq. (3.21) is satisfied for i=2(N-1); in other words $t_{s2(N-1)}$ is a switching point. This completes the construction for the last u=u_{max} arc.

The definitions will now be extended into the interval $[t_{f(N-1)}, t_N]$. With Eqs. (3.31), the conditions $\{II\}$ specify that $u(t)$=0 for t in this interval. Define $t_{s(2N-3)}$=$t_{f(N-1)}$. This implies that Eqs. (3.31) are consistent with this switching structure of $\{I\}$ up to and including this interval. Now define

$$\hat{\lambda}_x(t) = \left[\frac{\partial\psi}{\partial \mathbf{x}}(\mathbf{x}(t))\right]^T \left[-\hat{\mathbf{v}}_{oN}\right]$$

for all t in this interval. Knowing $u(t)$=0 and that Eqs. (3.31) are satisfied in this interval, Lemma III.2 with assumption (vi) and $\Gamma(\mathbf{x}(t)) = \frac{\partial\psi}{\partial \mathbf{x}}(\mathbf{x}(t))$ implies satisfaction of Eq. (3.15) in this interval. Define

$$\hat{\lambda}_y(t) = \bar{\lambda}_{yN}(t_N)$$

for all t in this interval. Knowing $u(t)$=0, this immediately implies satisfaction of Eq. (3.16) in the interval. Finally, since Eq. (3.14) was satisfied in the previous interval, Eqs. (3.15)-(3.16) are satisfied continuously from $t=t_f$ to any point in the current interval, and since the control switched values at a switching point, then Eq. (3.14) is satisfied in this interval. This completes the construction for the last u=0 arc.

Define $t_{s(2N-4)}=t_{N-1}$. Consider the interval $[t_{N-1},t_{f(N-1)}]$. Conditions {II} specify that this is a $u=u_{max}$ interval which, by the definitions, is consistent with the switching structure of {I}. Define

$$\hat{\lambda}_x(t) = \bar{\lambda}_{yN}(t_N)\bar{\lambda}_{x(N-1)}(t)$$

$$\hat{\lambda}_y(t) = \bar{\lambda}_{yN}(t_N)\bar{\lambda}_{y(N-1)}(t)$$

in this interval. Equations (3.22) and (3.28) with i=N-1 imply that $t_{f(N-1)}$ is a switching point. Considering the definitions, Eq. (3.28) with i=N-1 and Eq. (3.30) with i=N-2 obviously imply continuity of the Lagrange multipliers $\hat{\lambda}_x(t)$ across the switching point $t_{f(N-1)}$; continuity of $\hat{\lambda}_y(t)$ across this point is immediately implied by the definition. Therefore, Eqs (3.15) and (3.16) are satisfied across the switching point.

The previous arguments for the final $u=u_{max}$ and $u=0$ arcs may be repeated, implying satisfaction of the conditions in $\{I\}$ for each interval. After repeating the arguments and reaching the beginning of the trajectory, the following definitions will have been made and are presented for the sake of clarity:

$$\hat{\lambda}_x(t) = \left[\prod_{j=i+1}^{N} \bar{\lambda}_{yj}(t_j)\right]\left[\frac{\partial\psi}{\partial\mathbf{x}}(\mathbf{x}(t))\right]^{\mathrm{T}}\left[-\bar{\mathrm{v}}_{oi}\right],\ t \in \left[t_{f(i-1)}, t_i\right],\ i = 2,\ldots N-1$$

$$\hat{\lambda}_y(t) = \left[\prod_{j=i+1}^{N} \bar{\lambda}_{yj}(t_j)\right],\ t \in \left[t_{f(i-1)}, t_i\right],\ i = 2,\ldots N-1$$

$$\hat{\lambda}(t) = \left[\prod_{j=i+1}^{N} \bar{\lambda}_{yj}(t_j)\right]\bar{\lambda}_i(t),\ t \in \left[t_i, t_{fi}\right],\ i = 1,\ldots N-1$$

Finally, for the first $u=u_{max}$ interval, one more definition is required. The definition

$$\hat{\mathrm{v}}_o = \left[\prod_{i=2}^{N} \lambda_{yi}(t_i)\right]\bar{\mathrm{v}}_o$$

forces satisfaction of Eq. (3.27) with $i=1$ to imply satisfaction of Eq. (3.19). ■

The theorem does not assure satisfaction of Pontryagin's Minimum Principle. This principle requires that

$$\begin{aligned} u(t) &= 0 \text{ when } \hat{\lambda}_x(t)^{\mathrm{T}}\mathbf{g}(y(t), \mathrm{v}(t)) + c\hat{\lambda}_y(t) > 0 \\ u(t) &= u_{max} \text{ when } \hat{\lambda}_x(t)^{\mathrm{T}}\mathbf{g}(y(t), \mathrm{v}(t)) + c\hat{\lambda}_y(t) < 0 \end{aligned} \tag{3.37}$$

It should be noted that in the application of the Patched Method to the optimal orbit transfer problem, a second-order condition was taken into account. Lawden's pointer vector theory is a second-order condition and is explicitly specified. Also, note that this condition was determined considering the maximization problem instead of the equivalent minimization problem.

To apply Theorem III.1 to the orbit transfer optimization problem, the assumptions of the theorem must be satisfied. Assumptions (i), (iii), and (vii) are obviously satisfied. There may still be debate over assumption (iv); however, based on numerical experience, orbit transfers that violate (iv) are rare if they exist at all.

Assumption (ii) is made in anticipation of the ideal gravity assumption. In such a case, coasting before the first burn contributes zero cost and coasting after the final burn contributes zero cost. It therefore makes no sense to allow such arcs as part of the trajectory to be calculated. If an initial and/or final coast arc is desired, it may be added to the computed trajectory without affecting optimality.

Rectilinear orbits will be explicitly excluded from candidate orbit transfer trajectories. Such orbits intersect the center of gravitation and are, therefore, rarely of interest for the orbit transfer problem. With this exclusion made, assumptions (v) and (vi) may now be shown true for the orbit transfer optimization problem.

It is desired that if $h = |\mathbf{r} \times \mathbf{v}| \neq 0$, then the vector function

$$\psi(\mathbf{x}) = \psi\left(\begin{bmatrix} \mathbf{r} \\ \mathbf{v} \end{bmatrix}\right) = \begin{bmatrix} \mathbf{I}_{5\times5} & \mathbf{0}_{5\times1} \end{bmatrix} \begin{bmatrix} \mathbf{r} \times \mathbf{v} \\ \mathbf{v} \times (\mathbf{r} \times \mathbf{v}) - \dfrac{\mu}{\sqrt{\mathbf{r}^T\mathbf{r}}}\mathbf{r} \end{bmatrix} \in C_5^0$$

yields $rank\left(\dfrac{\partial\psi(\mathbf{x})}{\partial\mathbf{x}}\right) = 5$. Note that this formulation for $\psi(\mathbf{x})$ calculates the angular momentum and eccentricity vectors, then removes the third component of the eccentricity vector. $\psi(\mathbf{x})$ as defined above yields

$$\frac{\partial\psi(\mathbf{x})}{\partial\mathbf{x}} = \begin{bmatrix}\mathbf{I}_{5\times5} & \mathbf{0}_{5\times1}\end{bmatrix}\begin{bmatrix} [-\mathbf{v}_\times] & [\mathbf{r}_\times] \\ \left[(\mathbf{v}^T\mathbf{v})\mathbf{I} - \mathbf{v}\mathbf{v}^T + \frac{\mu}{(\mathbf{r}^T\mathbf{r})^{3/2}}\left(\mathbf{r}\mathbf{r}^T - (\mathbf{r}^T\mathbf{r})\mathbf{I}\right)\right] & \left[2\mathbf{r}\mathbf{v}^T - (\mathbf{r}^T\mathbf{v})\mathbf{I} - \mathbf{v}\mathbf{r}^T\right]\end{bmatrix}$$

where the subscript "X" denotes the skew symmetric matrix representation of the cross product. The result, $rank\left(\frac{\partial\psi(\mathbf{x}(t))}{\partial\mathbf{x}}\right) = 5$ is desired. The task is simplified by the following simple manipulation

$$\frac{\partial\psi(\mathbf{x}(t))}{\partial\mathbf{x}} = \begin{bmatrix}\mathbf{I}_{5\times5} & \mathbf{0}_{5\times1}\end{bmatrix}\begin{bmatrix}\mathbf{I}_{3\times3} & \mathbf{0}_{3\times3} \\ \mathbf{v}_X & \mathbf{I}_{3\times3}\end{bmatrix}\begin{bmatrix} [-\mathbf{v}_\times] & [\mathbf{r}_\times] \\ \left[\frac{\mu}{(\mathbf{r}^T\mathbf{r})^{3/2}}\mathbf{r}_X\mathbf{r}_X\right] & \left[\mathbf{r}\mathbf{v}^T - \mathbf{v}\mathbf{r}^T\right]\end{bmatrix}$$

which makes use of the identity $\mathbf{a}_X\mathbf{b}_X = \mathbf{b}\mathbf{a}^T - (\mathbf{a}^T\mathbf{b})\mathbf{I}$. This, in combination with

$$rank\left(\begin{bmatrix}\mathbf{I}_{5\times5} & \mathbf{0}_{5\times1}\end{bmatrix}\begin{bmatrix}\mathbf{I}_{3\times3} & \mathbf{0}_{3\times3} \\ \mathbf{v}_X & \mathbf{I}_{3\times3}\end{bmatrix}\right) = 5$$

implies

$$rank\left(\frac{\partial\psi(\mathbf{x}(t))}{\partial\mathbf{x}}\right) = min\left\{5\ ,\ rank\left(\begin{bmatrix} [-\mathbf{v}_\times] & [\mathbf{r}_\times] \\ \left[\frac{\mu}{(\mathbf{r}^T\mathbf{r})^{3/2}}\mathbf{r}_X\mathbf{r}_X\right] & \left[\mathbf{r}\mathbf{v}^T - \mathbf{v}\mathbf{r}^T\right]\end{bmatrix}\right)\right\}$$

It is most convenient to consider, without loss of generality, the following rotation of vectors $\mathbf{r}$ and $\mathbf{v}$ into the X-Y plane via an orthonormal matrix $\mathbf{W}$ defined such that

$$\mathbf{W}\mathbf{r} = \begin{bmatrix}x \\ y \\ 0\end{bmatrix} \text{ and } \mathbf{W}\mathbf{v} = \begin{bmatrix}u \\ v \\ 0\end{bmatrix}$$

It is easy to show that this rotation does not affect $rank\left(\frac{\partial\psi(\mathbf{x}(t))}{\partial\mathbf{x}}\right)$. Substitution reveals that, after rotation,

$$rank\left(\begin{bmatrix} [-\mathbf{v}_\times] & [\mathbf{r}_\times] \\ \left[\frac{\mu}{(\mathbf{r}^T\mathbf{r})^{3/2}}\mathbf{r}_\times\mathbf{r}_\times\right] & [\mathbf{r}\mathbf{v}^T - \mathbf{v}\mathbf{r}^T] \end{bmatrix}\right) = rank\left(\begin{bmatrix} 0 & 0 & -v & 0 & 0 & y \\ 0 & 0 & u & 0 & 0 & -x \\ v & -u & 0 & y & x & 0 \\ -gy^2 & gxy & 0 & 0 & -h & 0 \\ gyx & -gx^2 & 0 & h & 0 & 0 \\ 0 & 0 & 0 & 0 & 0 & 0 \end{bmatrix}\right)$$

where $h=xv-yu$ and $g = \frac{\mu}{(\mathbf{r}^T\mathbf{r})^{3/2}}$. It can be shown that

$$det\left(\begin{bmatrix} 0 & 0 & -v & 0 & y \\ 0 & 0 & u & 0 & -x \\ v & -u & 0 & x & 0 \\ -gy^2 & gxy & 0 & -h & 0 \\ gxy & -gx^2 & 0 & 0 & 0 \end{bmatrix}\right) = -gxh^3$$

$$det\left(\begin{bmatrix} 0 & 0 & -v & 0 & y \\ 0 & 0 & u & 0 & -x \\ v & -u & 0 & y & 0 \\ -gy^2 & gxy & 0 & 0 & 0 \\ gxy & -gx^2 & 0 & h & 0 \end{bmatrix}\right) = gyh^3$$

so that as long as $h \neq 0$, $\frac{\partial\psi(\mathbf{x}(t))}{\partial\mathbf{x}}$ has a nonzero minor of order 5. In other words, as long as the orbit is not rectilinear, $rank\left(\frac{\partial\psi(\mathbf{x}(t))}{\partial\mathbf{x}}\right) = 5$.

Now, for assumption (vi) it must be shown that if the vector function $\mathbf{f}(\mathbf{x})$ is

$$\mathbf{f}\left(\begin{bmatrix}\mathbf{r}\\ \mathbf{v}\end{bmatrix}\right)=\begin{bmatrix}\mathbf{v}\\ -\dfrac{\mu}{\left(\mathbf{r}^T\mathbf{r}\right)^{3/2}}\mathbf{r}\end{bmatrix}$$

and $\psi(\mathbf{x})$ is as already defined, then when $\frac{d}{dt}\mathbf{x}(t)=\mathbf{f}(\mathbf{x}(t))$,

$$\left(\frac{d}{dt}\frac{\partial}{\partial\mathbf{x}}\psi(\mathbf{x}(t))+\frac{\partial}{\partial\mathbf{x}}\psi(\mathbf{x}(t))\frac{\partial}{\partial\mathbf{x}}\mathbf{f}(\mathbf{x}(t))\right)=\mathbf{0}$$

It is easy to show that

$$\frac{\partial}{\partial\mathbf{x}}\mathbf{f}(\mathbf{x})=\begin{bmatrix}[0] & [\mathbf{I}]\\ \left[-\dfrac{\mu}{\left(\mathbf{r}^T\mathbf{r}\right)^{3/2}}\mathbf{I}+3\dfrac{\mu}{\left(\mathbf{r}^T\mathbf{r}\right)^{5/2}}\mathbf{r}\mathbf{r}^T\right] & [0]\end{bmatrix}$$

Note that the time notation has been dropped for convenience. Evaluating $\left[\frac{\partial\psi(\mathbf{x})}{\partial\mathbf{x}}\right]\left[\frac{\partial}{\partial\mathbf{x}}\mathbf{f}(\mathbf{x})\right]$ gives

$$\frac{\partial}{\partial\mathbf{x}}\psi(\mathbf{x})\frac{\partial}{\partial\mathbf{x}}\mathbf{f}(\mathbf{x})=\begin{bmatrix}\mathbf{I}_{5\times5} & \mathbf{0}_{5\times1}\end{bmatrix}\begin{bmatrix}\mathbf{M}_{11} & \mathbf{M}_{12}\\ \mathbf{M}_{21} & \mathbf{M}_{22}\end{bmatrix} \text{ where}$$

$$\mathbf{M}_{11}=-\mathbf{v}_{\times}$$

$$\mathbf{M}_{12}=-\frac{\mu}{\left(\mathbf{r}^T\mathbf{r}\right)^{3/2}}\mathbf{r}_{\times}$$

$$\mathbf{M}_{21}=\left(\mathbf{v}^T\mathbf{v}\right)\mathbf{I}-\mathbf{v}\mathbf{v}^T+\frac{\mu}{\left(\mathbf{r}^T\mathbf{r}\right)^{3/2}}\left(\mathbf{r}\mathbf{r}^T-\left(\mathbf{r}^T\mathbf{r}\right)\mathbf{I}\right)$$

$$\mathbf{M}_{22}=\frac{\mu}{\left(\mathbf{r}^T\mathbf{r}\right)^{3/2}}\left\{-\left(\mathbf{r}^T\mathbf{v}\right)+2\left(\mathbf{r}\mathbf{v}^T\right)+2\left(\mathbf{v}\mathbf{r}^T\right)-\frac{3\left(\mathbf{r}^T\mathbf{v}\right)}{\left(\mathbf{r}^T\mathbf{r}\right)}\left(\mathbf{r}\mathbf{r}^T\right)\right\}$$

Next, the time derivative of each term in $\frac{\partial}{\partial\mathbf{x}}\psi(\mathbf{x})$ can be expressed as:

$$\frac{d}{dt}(\mathbf{v}_x) = -\frac{\mu}{(\mathbf{r}^T\mathbf{r})^{1/2}}\mathbf{r}_x$$

$$\frac{d}{dt}(\mathbf{r}_x) = \mathbf{v}_x$$

$$\frac{d}{dt}(\mathbf{v}^T\mathbf{v}) = -2\frac{\mu}{(\mathbf{r}^T\mathbf{r})^{3/2}}\mathbf{r}\mathbf{v}^T$$

$$\frac{d}{dt}(\mathbf{v}\mathbf{v}^T) = -\frac{\mu}{(\mathbf{r}^T\mathbf{r})^{3/2}}(\mathbf{v}\mathbf{r}^T + \mathbf{r}\mathbf{v}^T)$$

$$\frac{d}{dt}\left(\frac{\mu}{(\mathbf{r}^T\mathbf{r})^{3/2}}\mathbf{r}\mathbf{r}^T\right) = \frac{\mu}{(\mathbf{r}^T\mathbf{r})^{3/2}}(\mathbf{r}\mathbf{v}^T + \mathbf{v}\mathbf{r}^T) - \frac{3\mu}{(\mathbf{r}^T\mathbf{r})^{5/2}}(\mathbf{r}^T\mathbf{v})\mathbf{r}\mathbf{r}^T$$

$$\frac{d}{dt}\left(\frac{\mu}{(\mathbf{r}^T\mathbf{r})^{1/2}}\right) = -\frac{\mu}{(\mathbf{r}^T\mathbf{r})^{3/2}}(\mathbf{r}^T\mathbf{v})$$

$$\frac{d}{dt}(\mathbf{r}\mathbf{v}^T) = \mathbf{v}\mathbf{v}^T - \frac{\mu}{(\mathbf{r}^T\mathbf{r})^{3/2}}(\mathbf{r}\mathbf{r}^T)$$

$$\frac{d}{dt}(\mathbf{v}\mathbf{r}^T) = \frac{d}{dt}(\mathbf{r}\mathbf{v}^T)$$

$$\frac{d}{dt}(\mathbf{r}^T\mathbf{v}) = \mathbf{v}^T\mathbf{v} - \frac{\mu}{(\mathbf{r}^T\mathbf{r})^{1/2}}$$

With these expressions it can easily be shown that

$$\frac{d}{dt}\frac{\partial}{\partial \mathbf{x}}\psi(\mathbf{x}(t)) + \frac{\partial}{\partial \mathbf{x}}\psi(\mathbf{x}(t))\frac{\partial}{\partial \mathbf{x}}\mathbf{f}(\mathbf{x}(t)) = 0$$

This is more than just satisfaction of a simple condition that proves useful to the theorem. In fact, this shows that Eq. (2.12) is the solution of the ODEs for the Lagrange multipliers, Eqs. (2.3a-c), when the Hamiltonian vanishes and ideal gravity is assumed. As reviewed earlier, many previous research efforts have focused on obtaining such solutions, but the form found herein is different from those.

III.2.5. Solution using the Patched Method with Eleven Burns

The plots below represent the current capability of the Patched Method. The eleven-burn solution represented by these plots has a larger number of burns than obtained BOUNDSCO or MBCM, in this study. Few solutions, if any, with this number of burns have been obtained in the literature. However, the Modified Patched Method, introduced in the next subsection, has produced solution with even larger numbers of burns.

Also indicative of the Patched Method, the convergence tolerance for the outer loop was set relatively high, 10^{-3}, to prevent prohibitively long computation times.

For this example, the thrust level is 0.09698, the product $g_o I_{sp}$ is 0.3929, the initial mass is 10. The initial orbit is circular with a radius of 1; the final orbit has an eccentricity of 0.398 and a final semimajor axis of 1.708. With this information the value of T/W_o for this transfer is calculated to be 0.009698, placing it in the low-thrust transfer range.

Figure 3.1 is a plot the transfer orbit elements, *viz*. angular momentum, eccentricity vector x-component, and eccentricity vector y-component, versus transfer orbit number. The shape of the angular momentum and eccentricity x-component curves seem to indicate a second order polynomial fit could be used to reduce the number of variables in the problem. The eccentricity y-component is always small in this transfer; suggesting that it could be assumed zero or, more generally, the same parameterization may be used. The zeroth orbit is the fixed initial orbit and the eleventh orbit is the fixed final orbit.

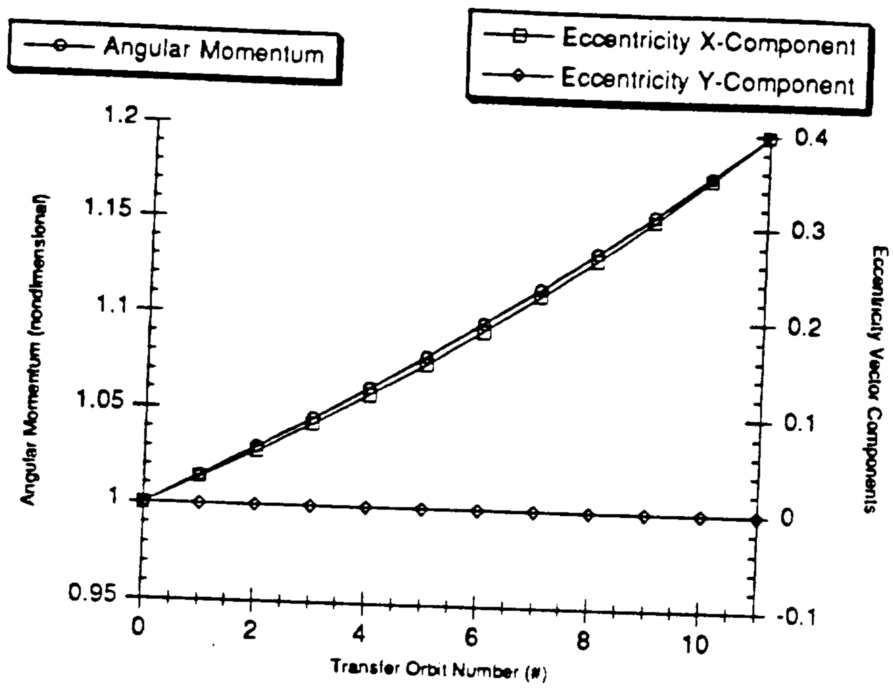

Figure 3.1 Orbital Elements of Each Transfer Orbit of Eleven Burn Solution

Figure 3.2 shows the angular position of the initial orbit exit point and final orbit entry point of each versus the index enumerating which transfer orbit the burn ends at. The symmetry of this plot is somewhat surprising. Even though each transfer orbit has its apse roughly aligned with the x-axis, each pair of angular positions are not reflected about the x-axis. The trend over time is almost exactly opposite between the two positions, but note that the values are not quite the negatives of each other. Also, it is clear that each burn of this transfer are perigee burns; each occurring around perigee.

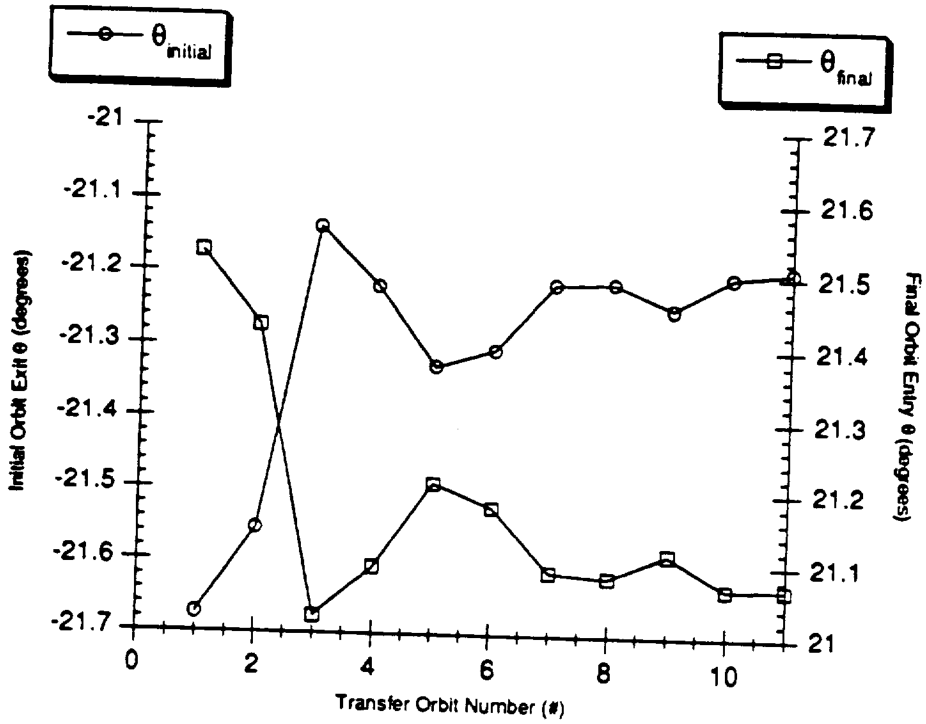

Figure 3.2 Orbit Transfer Terminal Points Indexed by Ending Orbit

Another interesting trend is found in Fig. 3.3, showing the burn length versus the same index as before. The burn length decreases monotonically with each successive burn, but does not decrease linearly. One can, of course, observe a relationship in the trend of burn length and angular positions from Figure 3.2. Both plots have a sharp change at the third burn which holds till the fourth burn and then returns to follow the trend from the first two. The irregular trend for this burn is attributed to the high tolerance given for the convergence criteria.

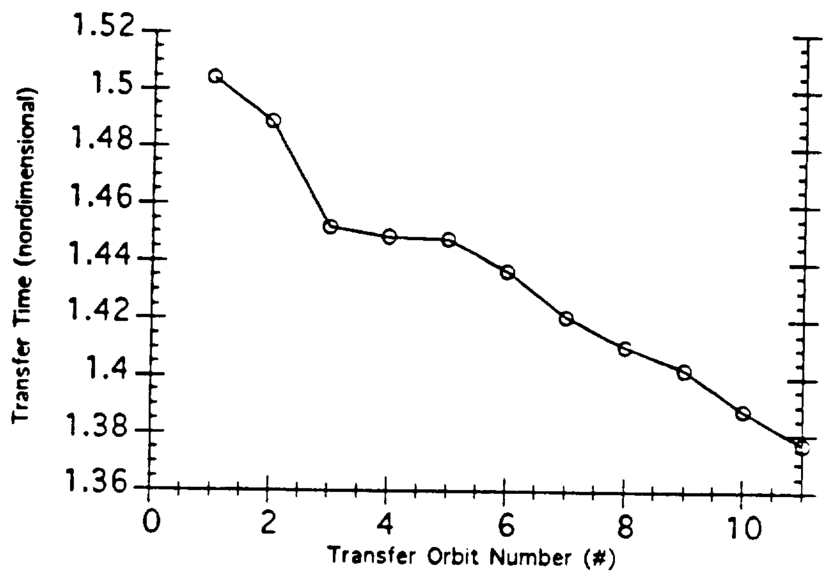

Figure 3.3 Transfer Time Indexed by Ending Orbit for the Eleven Burn Solution

III.3. The Modified Patched Method (MPM)

The Relaxed Patched Method is tailored to the orbit transfer optimization problem through known relations concerning the behavior of states and costates at different points along the trajectory. The concept central to these relations is that each burn of a multiple-burn orbit transfer qualifies as an optimal transfer between its own local terminal orbits. This method uses an algorithm similar to shooting methods.

This method puts forth an algorithm for computing problem constraints given the values of the problem variables. The number of variables and constraints are equal. Also, the method can be used with any multi-dimensional root-finding algorithm. The discussion below describes the variables and computation of the constraints for a two-burn trajectory.

In the following description of the variables and constraints, the vector $\lambda = [\lambda_r^T \quad \lambda_v^T]^T$ is used instead of the more common $[\lambda_r^T \quad \lambda_v^T \quad \lambda_m]^T$ so that λ_m can be discussed separately.

The arc between points #1 and #2 is assumed to be an arc of maximum thrust. Referring to Fig. 3.4, the variables at #1 are the initial true anomaly, θ_1; the first burn length, t_{f1}; and, the vector of constant Lagrange multipliers for the start of the first burn, v_1. The only constraint associated with point #1 is for v_1 to have unity magnitude.

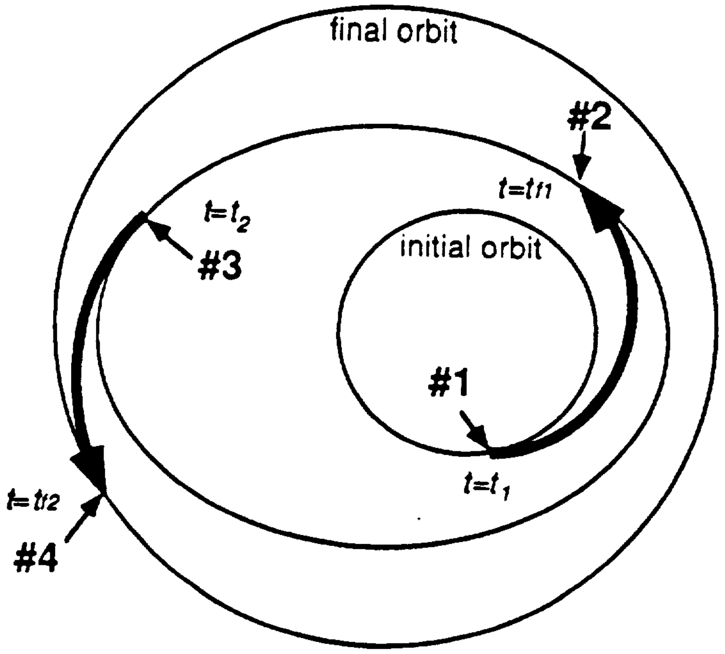

Figure 3.4 Diagram Illustrating the Layout of a Two-Burn Transfer

Knowing the true anomaly, θ, and the rest of the orbital elements, α, state, $\mathbf{x}(t)$ may be calculated with the function $\tilde{\mathbf{x}}(\theta;\alpha)$. Therefore, the Lagrange multipliers, $\lambda(t_1)$, and the state, $\mathbf{x}(t_1)$, at the initial orbit exit point may be computed using

$$\mathbf{x}(t_1) = \tilde{\mathbf{x}}(\theta_1;\alpha_0) \tag{3.38}$$

$$\lambda(t_1) = \left[\frac{\partial\psi}{\partial \mathbf{x}}(\mathbf{x}(t_1))\right]^T \mathrm{v}_1 \tag{3.39}$$

Where $\psi(\mathbf{x})$ is a function that calculates the orbital elements α given the state $\mathbf{x}$. The Lagrange multipliers, $\lambda(t_{f1})$, and final state of the first burn, $\mathbf{x}(t_{f1})$, are calculated by numerical integration of the Euler-Lagrange and state differential equations.

The vector variables α_1 and v_2 are associated with point #2. These are used to evaluate the constraints at point #2 as

$$\psi(\mathbf{x}(t_{f1})) = \alpha_1 \tag{3.40}$$

$$\lambda(t_{f1}) = \left[\frac{\partial\psi}{\partial \mathbf{x}}(\mathbf{x}(t_{f1}))\right]^T \mathrm{v}_2 \tag{3.41}$$

The trajectory between points #2 and #3 is assumed to be an arc of null thrust. The variables θ_2, the initial true anomaly for the second burn, and t_{f2}, the second burn length, are associated with point #3. With these values, the Lagrange multipliers and the state may be calculated, much as before, with

$$\mathbf{x}(t_2) = \hat{\mathbf{x}}(\theta_2;\alpha_1) \tag{3.42}$$

$$\lambda(t_2) = \left[\frac{\partial\psi}{\partial \mathbf{x}}(\mathbf{x}(t_2))\right]^T \mathrm{v}_2 \tag{3.43}$$

Using the integration results from the first burn and Eq. (3.43), the following constraint is evaluated at point #3

$$|\lambda_v(t_{f1})| = |\lambda_v(t_2)| \tag{3.44}$$

The arc between points #3 and #4 is assumed to be of maximum thrust. The variables θ_2, α_1, and ν_2, specified at points #2 and #3 enable the calculation of the Lagrange multipliers, $\lambda(t_{f2})$, and final state, $\mathbf{x}(t_{f2})$, in the same manner as the previous burn - numerically integrating from t_2 to t_{f2} with the initial conditions Eqs. (3.42) and (3.43).

The two-burn trajectory ends at point #4. The constant Lagrange multiplier vector ν_3 is associated with this point. The constraints evaluated at point #4 are

$$\psi(\mathbf{x}(t_{f2})) = \alpha_2 \tag{3.45}$$

$$\lambda(t_{f2}) = \left[\frac{\partial \psi}{\partial \mathbf{x}}(\mathbf{x}(t_{f2}))\right]^{\mathrm{T}} \nu_3 \tag{3.46}$$

These constraints complete the system.

With the discussion of the formulation for a two-burn trajectory concluded, the formulation for a more general problem is clear. For an N-burn trajectory with α_0, α_N, m_o, T, g_o, and I_{sp} specified, the variables are

$$\{\alpha_i | i = 1,\ldots N-1\}, \{\theta_i, t_{fi} | i = 1,\ldots N\}, \{\nu_i | i = 1,\ldots N+1\} \tag{3.47}$$

By use of which, the following quantities are calculated

$$\mathbf{x}(t_i) = \bar{\mathbf{x}}(\theta_i ; \alpha_{i-1}) \; ; \; i = 1,\ldots N \tag{3.48}$$

$$\lambda(t_i) = \left[\frac{\partial \psi}{\partial \mathbf{x}}(\mathbf{x}(t_i))\right]^{\mathrm{T}} \nu_i ; \; i = 1,\ldots N \tag{3.49}$$

$$\left\{\begin{array}{c} \mathbf{x}(t_{fi}) = \mathbf{x}(t_i) + \int_{t_i}^{t_{fi}} \mathbf{f}(\mathbf{x}(t)) + \frac{T}{m(t)}\mathbf{v}(t)dt \qquad (3.50) \\ \lambda(t_{fi}) = \lambda(t_i) + \int_{t_i}^{t_{fi}} \left[-\frac{\partial}{\partial \mathbf{x}}\mathbf{f}(\mathbf{x}(t))\right]^{\mathrm{T}} \lambda(t)dt \qquad (3.51) \\ \text{where } \mathbf{v}(t) = \frac{\lambda_v(t)}{|\lambda_v(t)|} \qquad (3.52) \\ \text{and } m(t) = m_o - \frac{T}{g_o I_{sp}}\left(t - t_{f1} + \sum_{j=1}^{i}(t_{fj} - t_j)\right),\ t \in [t_i, t_{fi}] \qquad (3.53) \end{array}\right\} i = 1,\ldots N$$

The constraints that must be then evaluated and satisfied are

$$|\mathbf{v}_1| = 1 \tag{3.54}$$

$$\psi(\mathbf{x}(t_{fi})) = \alpha_i;\ i = 1,\ldots N \tag{3.55}$$

$$\lambda(t_{fi}) = \left[\frac{\partial \psi}{\partial \mathbf{x}}(\mathbf{x}(t_{fi}))\right]^{\mathrm{T}} \mathbf{v}_{i+1};\ i = 1,\ldots N \tag{3.56}$$

$$|\lambda_v(t_{fi})| = |\lambda_v(t_{i+1})|\ ;\ i = 1,\ldots N-1 \tag{3.57}$$

This gives a total of $2N(M+1)$ variables and the same number of constraints, where M is the number of orbital elements. For nonplanar transfers M=5 but for planar transfers, it is more efficient to rotate the coordinate system so that M=3.

In summary, the Modified Patched Method executes the following procedure for the ith burn, i=1...N, of an N-burn transfer. Given the current iterates θ_i, α_{i-1}, and $\mathbf{v}_i$, (note, however, that α_0 is not an iterate but a specified constant) calculate $\mathbf{x}(t_i)$ and $\lambda(t_i)$ with Eqs (3.48)-(3.49). If i=1, evaluate the scaling constraint, Eq. (3.54). Given t_{fi}, and the calculated initial values $\mathbf{x}(t_i)$, $\lambda(t_i)$, compute $\mathbf{x}(t_{fi})$, $\lambda(t_{fi})$ with Eqs (3.50)-(3.53). Evaluate the burn terminal point constraints, Eqs (3.55)-(3.56). If $i<N$, evaluate the switching function constraint, Eq. (3.57), where $\lambda_v(t_{i+1})$ is calculated with (3.49) knowing $\mathbf{v}_{i+1}$.

When implementing MPM on a computer, the angular variable θ_i should be replaced by the variables l_{1i}, l_{2i} and the constraint $l_{1i}^2 + l_{2i}^2 = 1$. This common substitution removes the periodic redundancy that may confuse a numerical method.

Completion of the iterative process updating the variables in (3.47) to satisfy the conditions in Eqs. (3.54)-(3.56) allows the final condition of the Modified Patched Method to be checked. Briefly, this checks the switching law:

$$\begin{aligned} &\frac{|\lambda_v(t)|}{m(t)} - \frac{\lambda_m(t)}{g_o I_{sp}} > 0 \text{ , } T = T_{max} \\ &\frac{|\lambda_v(t)|}{m(t)} - \frac{\lambda_m(t)}{g_o I_{sp}} < 0 \text{ , } T = 0 \end{aligned} \tag{3.58}$$

This condition is, in fact, borrowed directly from the application of Pontryagin's Maximum Principle. When all conditions are satisfied, it may be claimed that an extremal solution has been obtained.

The relationship between the Patched Method and MPM is primarily in the use of Eqs. (3.49) and (3.56), which perform basically the same function as Eqs. (3.27), (3.28), and (3.30) from the Patched Method. However, MPM also includes a technique apparently first employed by Brown, et. al.[21] which removes one Lagrange multiplier (λ_m) and significantly affects the way the switching conditions are handled. This technique is present here as the use of Equation (3.57).

III.3.1. Equivalency of MPM Conditions and Necessary Conditions

This subsection is concerned with proving the equivalency between necessary conditions and the Modified Patched Method conditions. From the standpoint of showing mathematical equivalence, some combinations of variables and constraints in MPM are unnecessary. Essentially, guessing intermediate orbital elements can be replaced by requiring the state to be continuous between burns.

Definition: For optimal control problem $\{P\}$, the conditions $\{III\}$ are

$$|\nu_1| > 0 \tag{3.59}$$

$$\lambda(t_{fi}) = \left[\frac{\partial\psi}{\partial \mathbf{x}}(\mathbf{x}(t_{fi}))\right]^{\mathrm{T}} \nu_{i+1};\ i = 1,\ldots N \tag{3.60}$$

$$\lambda(t_i) = \left[\frac{\partial\psi}{\partial \mathbf{x}}(\mathbf{x}(t_i))\right]^{\mathrm{T}} \nu_i;\ i = 1,\ldots N \tag{3.61}$$

$$\lambda(t_{fi})^{\mathrm{T}}\mathbf{g}(y(t_{fi}),\mathbf{v}(t_{fi})) = \lambda(t_{i+1})^{\mathrm{T}}\mathbf{g}(y(t_{i+1}),\mathbf{v}(t_{i+1}))\ ;\ i = 1,\ldots N-1 \tag{3.62}$$

$$\left\{\begin{array}{c} \mathbf{x}(t_{fi}) = \mathbf{x}(t_i) + \int_{t_i}^{t_{fi}}\left[\mathbf{f}(\mathbf{x}(t)) + \mathbf{g}(y(t),\mathbf{v}(t))u_{max}\right]dt \\ \lambda(t_{fi}) = \lambda(t_i) + \int_{t_i}^{t_{fi}}\left[-\frac{\partial}{\partial \mathbf{x}}\mathbf{f}(\mathbf{x}(t))\right]^{\mathrm{T}}\lambda(t)dt \\ \text{where } \lambda(t)^{\mathrm{T}}\left[\frac{\partial}{\partial \mathbf{v}}\mathbf{g}(y(t),\mathbf{v}(t))\right] = 0 \\ \text{and } y(t) = y_o + cu_{max}\left(t - t_{f1} + \sum_{j=1}^{i}(t_{fj} - t_j)\right),\ t \in [t_i, t_{fi}] \end{array}\right\} i = 1,\ldots N \tag{3.63}$$

$$\left\{\begin{array}{c} \mathbf{x}(t_{i+1}) = \mathbf{x}(t_{fi}) + \int_{t_{fi}}^{t_{i+1}}\mathbf{f}(\mathbf{x}(t))dt \\ y(t) = y(t_{i+1}) = y(t_{fi}) \\ u(t) = 0,\ t \in [t_{fi}, t_{i+1}] \end{array}\right\} i = 1,\ldots N-1 \tag{3.64}$$

$$\left|\frac{\lambda(t_{fN})^{\mathrm{T}}\mathbf{g}(y(t_{fN}),\mathbf{v}(t_{fN}))}{c}\right| > 0 \tag{3.65}$$

where $t_1 = t_0$ is assigned and the value for t_f is seen to be t_{fN}.

Theorem III.2: If and only if

$$\left\{\mathbf{x}(t), y(t), \mathbf{v}(t), u(t), \hat{\lambda}(t) \middle| t \in [t_o, t_f]\right\}, \hat{\mathbf{v}}_o, \hat{\mathbf{v}}_f, t_f, \left\{t_{s,i} \middle| i = 1, \ldots 2(N-1)\right\} \tag{3.66}$$

satisfies $\{I\}$ then

$$\left\{\mathbf{x}(t), y(t), \mathbf{v}(t), u(t), \lambda(t) \middle| t \in [t_1, t_{fN}]\right\}, \left\{t_i, t_{fi} \middle| i = 1, \ldots N\right\}, \left\{\mathbf{v}_i \middle| i = 1, \ldots N+1\right\} \tag{3.67}$$

satisfies $\{III\}$, assuming that the constraints and assumptions from $\{P\}$ are satisfied.

Proof:

Both sufficiency and necessity will be proven by assuming satisfaction of one set of conditions and then constructing the solution to the other. From here on, assume that the constraints and assumptions from $\{P\}$ are satisfied. The "if" part will be proven after the "only if" part. To prove the "only if" part, it will be useful to follow time in reverse from $t=t_f$ to the initial time, $t=t_o$.

Assume that (3.67) satisfies $\{III\}$. Define a scaling factor $\gamma \in R$,

$$\gamma = \frac{-c}{\lambda(t_{fN})^{T} \mathbf{g}\left(y(t_{fN}), \mathbf{v}(t_{fN})\right)} \tag{3.68}$$

Equation (3.65) ensures that the γ exists as a finite real number. Define $\hat{\mathbf{v}}_f = \gamma \mathbf{v}_{N+1}$, $\hat{\lambda}_x(t_f) = \gamma \lambda(t_{fN})$, and recall that $t_f = t_{fN}$. Note that this construction makes satisfaction of (3.60) with $i=N$ imply satisfaction of (3.18). Now, define $\hat{\lambda}_y(t_f) = 1$ which satisfies (3.20); this makes the switching function in the form of Eq. (3.21) vanish for $t=t_f$.

It is obvious that when assumption (i) holds, Eq. (3.18) is satisfied, and Eq. (3.21) vanishes for $t=t_f$ then Eq. (3.14) is satisfied at $t=t_f$. Now, extend the construction so that $\hat{\lambda}_x(t) = \gamma\lambda(t)$, $t \in [t_N, t_{fN}]$ and Eq. (3.16) is satisfied. Note that this and Eqs. (3.63) imply that all Euler-Lagrange differential equations, Eqs. (3.15)-(3.17), are satisfied in this interval. Therefore, the Hamiltonian is constant in the interval and is hence equal to zero at $t=t_N$. Now, with the Hamiltonian zero, assumption (i) and Eq. (3.61) with $i=N$ implies that the switching function vanishes again at $t=t_N$. Define $t_{s2(N-1)}=t_N$. Since by (3.64) and (3.63), the bang-bang control, $u(t)$, switches from u_{max} to zero at $t=t_N$, the Hamiltonian will be continuous across this switching point and, therefore, zero.

Lemma III.2 with $\Gamma(\mathbf{x}(t))=\frac{\partial\psi}{\partial\mathbf{x}}(\mathbf{x}(t))$ for $t\in\left[t_{fN-1},t_N\right]$, Eq. (3.64), and assumption (vi) implies satisfaction of Eqs. (3.15) and (3.17) in this interval. Extend the construction so that $\hat{\lambda}_y(t)=\hat{\lambda}_y(t_N)=\hat{\lambda}_y\left(t_{fN-1}\right)$ in the interval, thereby satisfying Eq. (3.16). Having this construction, knowing that the switching function vanishes at $t=t_N$, that $u(t)=0$ is assigned in this interval by (3.64), satisfaction of Eq. (3.62) implies that the switching function vanishes at $t=t_{fN-1}$. In order to imply satisfaction of Eq. (3.14) at the end of this interval, it must be recognized that again, the bang-bang control switches values at $t=t_{fN-1}$. Define $t_{s(2N-1)}=t_{fN-1}$.

The arguments in the preceding two paragraphs may be repeated until the initial time, t_o is reached. Recall that $t_1=t_o$. Define $\hat{\mathbf{v}}_o=-\gamma\mathbf{v}_1$ and recall that previous definitions require $\hat{\lambda}_x(t_o)=\gamma\lambda(t_1)$; these definitions imply satisfaction of (3.19). The proof of the "only if" part is complete.

For the "if" part of the theorem, assume that (3.66) satisfies $\{I\}$. Define $\lambda(t)=\hat{\lambda}_x(t)$, $t\in\left[t_o,t_f\right]$ and recall that $t_f=t_{fN}$ and $t_1=t_o$. Define $\mathbf{v}_1=-\hat{\mathbf{v}}_o$ and $\mathbf{v}_1=\hat{\mathbf{v}}_f$. Given assumption (i), it is immediately obvious that all conditions in $\{III\}$ except Eqs. (3.59), (3.62), (3.65), (3.61) with $i\neq1$, and (3.60) with $i\neq N$. Note that (3.61) and (3.60) each apply at a switching point and when $u=u_{max}$. Furthermore, Eq. (3.14) specifies that the Hamiltonian is zero throughout the trajectory. Therefore, by Lemma III.1, Eqs (3.14), (3.21), and assumptions (v) and (vii) there exists a different value ν for each switching point such that Eqs. (3.60) and (3.61) hold; however, Lemma III.1 does not guarantee that the value of ν at one end of the kth u=0 arc (i=k-1 in (3.60)) equals the value of ν at the other end (i=k in (3.61)). But, Lemma III.2 with $\Gamma(\mathbf{x}(t)) = \frac{\partial \psi}{\partial \mathbf{x}}(\mathbf{x}(t))$ and assumption (vi) implies that $\hat{\lambda}_x(t) = \left[\frac{\partial \psi}{\partial \mathbf{x}}(\mathbf{x}(t))\right]^T \nu$ solves (3.15) when u=0. Therefore, the value of ν at one end of a u=0 arc must equal the value of ν at the other end of the u=0 arc.

Eq. (3.65) is implied by the switching function vanishing at t=t_f. Finally, it is obvious that the boundary value problem cannot be solved if $\hat{\lambda}_x(t) = 0$; therefore $|\hat{\nu}_o| > 0$, by assumption (v). That implies satisfaction of Eq (3.59). ■

III.3.2. MPM Example Solutions

The following examples satisfy all the conditions implied by the Euler-Lagrange equations and the Pontryagin Maximum Principle. All quantities have been nondimensionalized.

The first example solution is a 5-burn transfer reproducing a solution presented in a paper by Redding. Both the initial orbit and the final orbit are circular. However, there is an inclination of 28.5° between them. In this presentation of the solution, the initial orbit is equatorial and the final orbit is inclined 28.5°. The initial orbit radius is 1, the final orbit radius is 6.4. The initial nondimensional acceleration is 0.0517 and the nondimensional characteristic velocity is 0.567. Both the transfer computed by Redding and this solution calculated with the Modified Patched Method have final transfer orbits with e=0.723 and an inclination 26.5° away from that of the final orbit. Perigee burn durations for both range from 1.26 to 1.13. Both have a total transfer time of 60. Finally, it is worth noting that the solution presented here was computed without knowing the particulars of Redding's solution.

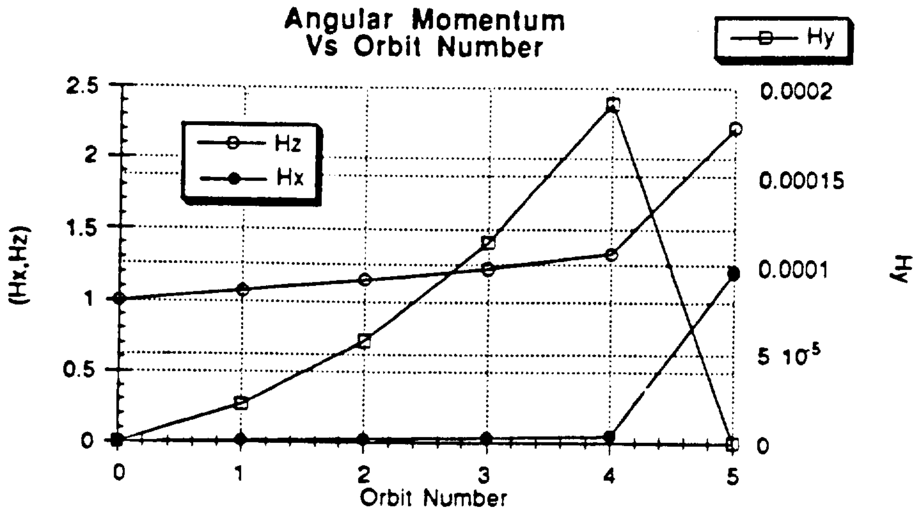

Figure 3.5 Components of the Angular Momentum Vector for each Transfer Orbit vs. Orbit Number of a 5-Burn Transfer with Plane Changes

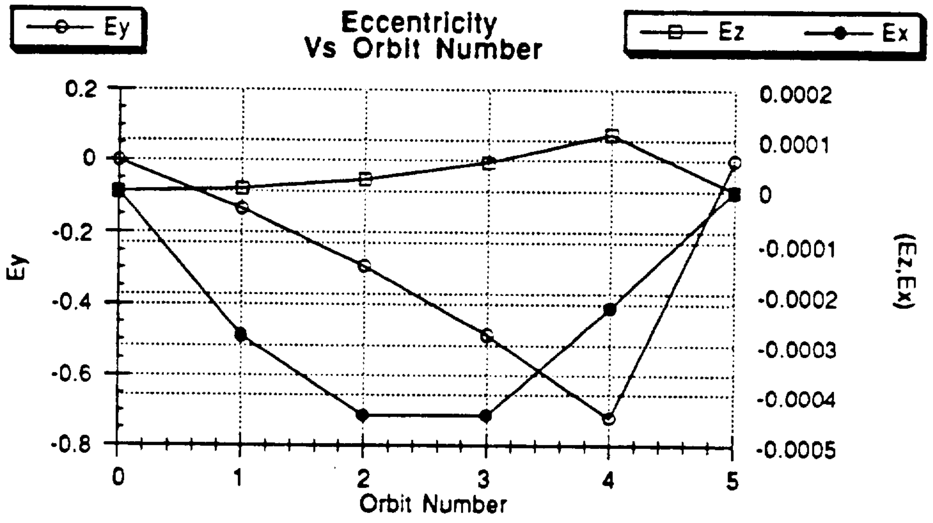

Figure 3.6 Components of the Eccentricity Vector Vs Orbit Number for each Transfer Orbit of a 5-Burn Transfer with Plane Changes

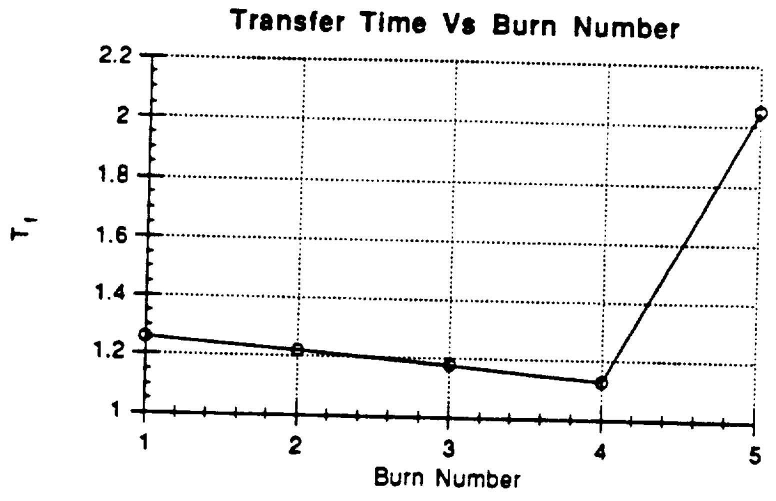

Figure 3.7 Transfer Time Vs Orbit Number for each Burn of a 5-Burn Transfer with Plane Changes

The second example is a 19-burn transfer. The initial nondimensional acceleration produced by the rocket motor (T/m_o) is 0.09698 and the initial nondimensional characteristic velocity ($g_o I_{sp}$) is 0.3929. The initial orbit is circular with a radius of 1, the final orbit has eccentricity of 0.73315 and a semimajor axis of 9.26. The total burn time for this trajectory is 26.84. Figures 3.8 — 3.9 show data in similar form for this transfer as Figures 3.5-3.7 for the previous transfer.

This 19-burn trajectory was extended to a 27-burn trajectory. This process involved the determination of transfers with 20, 22, 23, 24 burns, etc. It was found that adding burns one at a time was usually successful, two at a time slightly less successful, and so on. It was also interesting to see the decreasing improvement of the transfer's performance as plotted in Figure 3.10.

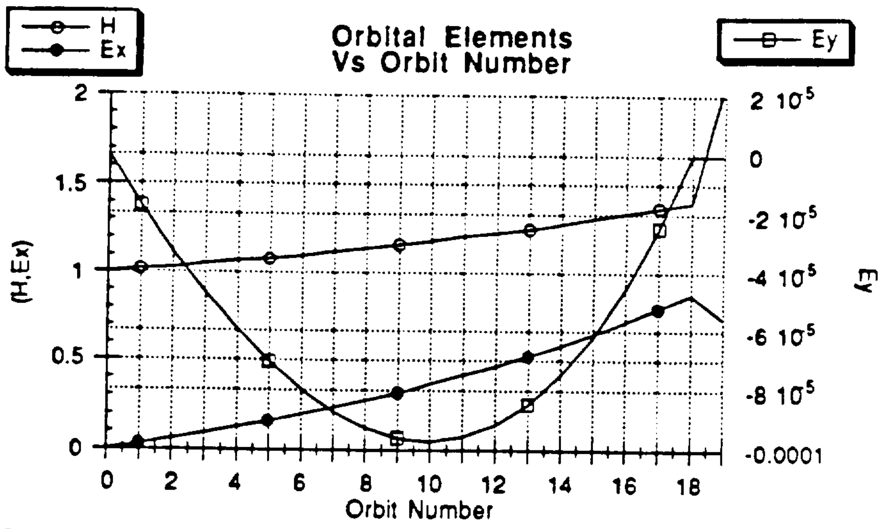

Figure 3.8 Orbital Elements for each Transfer Orbit Vs Orbit Number of a 19-Burn Transfer

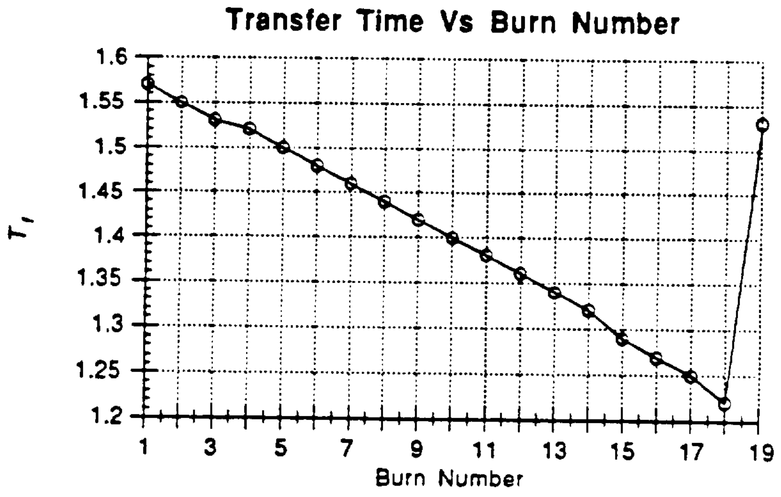

Figure 3.9 Transfer Time vs Orbit Number for each Burn of a 19-Burn Transfer

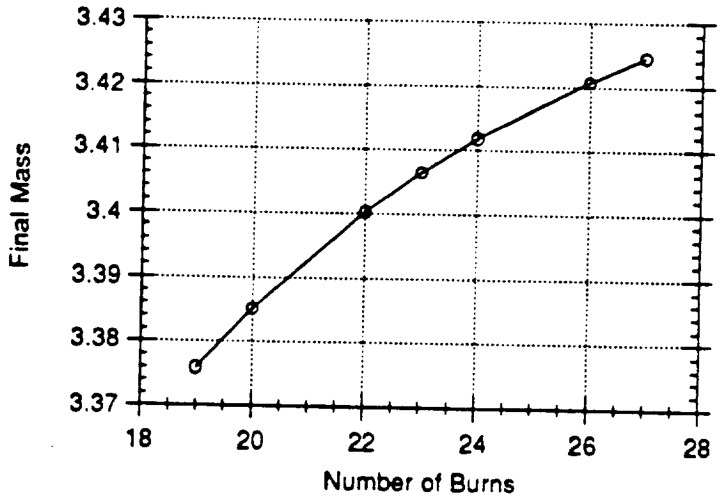

Figure 3.10 Performance Index, Final Mass, of the Extremal Trajectory vs Number of Burns Executed during the Trajectory

The third example is the aforementioned 27-burn trajectory. All parameters are identical between this transfer and the previous except the number of burns. The total burn time for this trajectory is 26.64. This is only a 0.7% decrease in transfer time for 42% more burns.

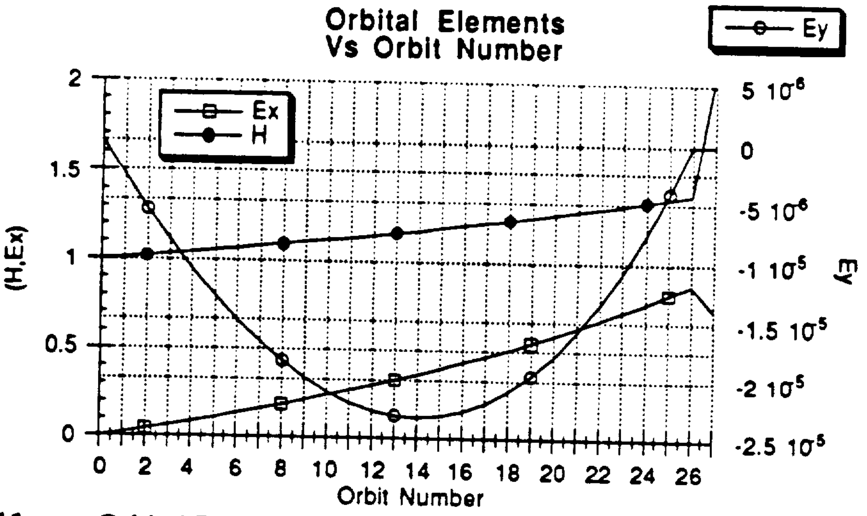

Figure 3.11 Orbital Elements for each Transfer Orbit Vs Orbit Number of a 27 Burn-Transfer

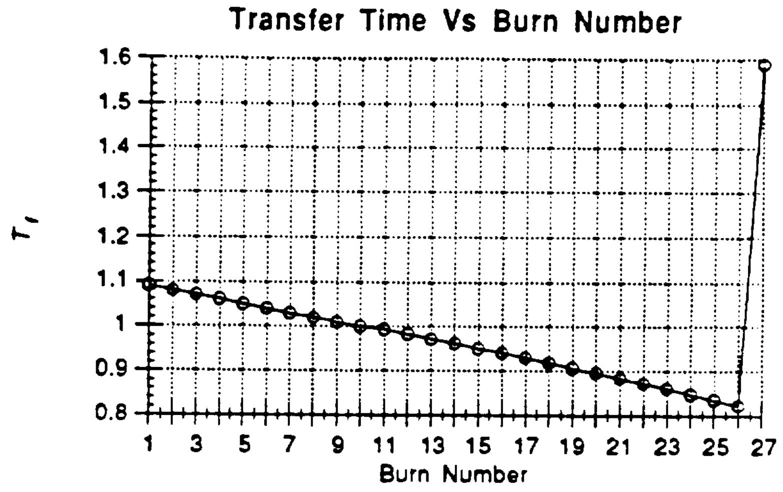

Figure 3.12 Transfer Time vs Orbit Number for each Burn of a 27-Burn Transfer

The fourth transfer is identical to the third except that the final orbit has an inclination of 63.4° This inclination angle was chosen because it is large and represents the inclination of the useful Molniya class of orbits. To obtain the solution, the planar transfer was used as the initial guess and the Modified Patched Method obtained the solution in 6 iterations. The following figures represent the transfer.

Each of these transfers show similar trends. An almost linear variation in the largest components of the angular momentum and eccentricity vectors and for the transfer time when plotted against the orbit or burn number. However, this trend is broken for the last burn. In each transfer, the last burn is an apogee burn and all previous burns are perigee burns. Each perigee burn steadily changes the angular momentum and eccentricity. The apogee burn then makes a last large change that brings the spacecraft to the final orbit. This last burn is also considerably longer than the burn before it. In the 5-burn case, Fig. (3.7) shows that the last burn is much longer than the first burn. In the 19-burn case, Fig. (3.9) shows the last burn almost just as long as the previous burn; in the 27-burn case, Fig. (3.15) indicates that it is considerably longer.

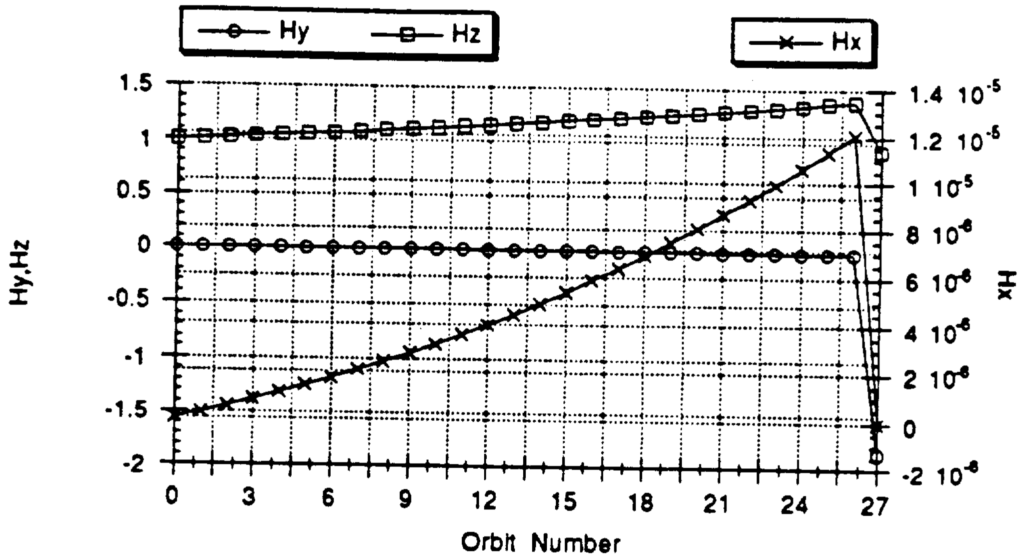

Figure 3.13 Components of the Angular Momentum Vector for each Transfer Orbit vs Orbit Number of a 27-Burn Transfer with a 63.4° Plane Change

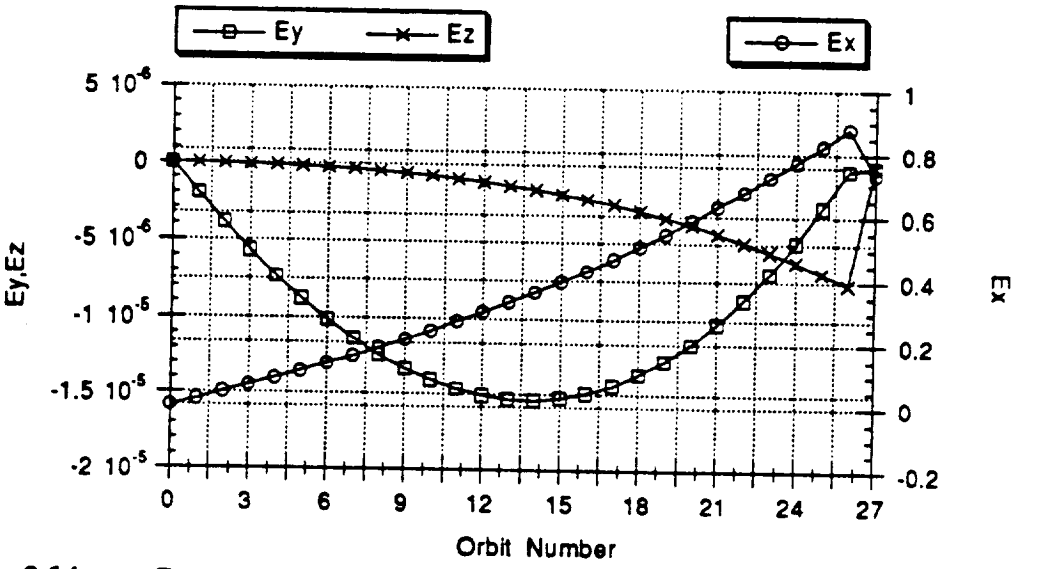

Figure 3.14 Components of the Eccentricity Vector vs Orbit Number for each Transfer Orbit of a 27-Burn Transfer with a 63.4° Plane Change

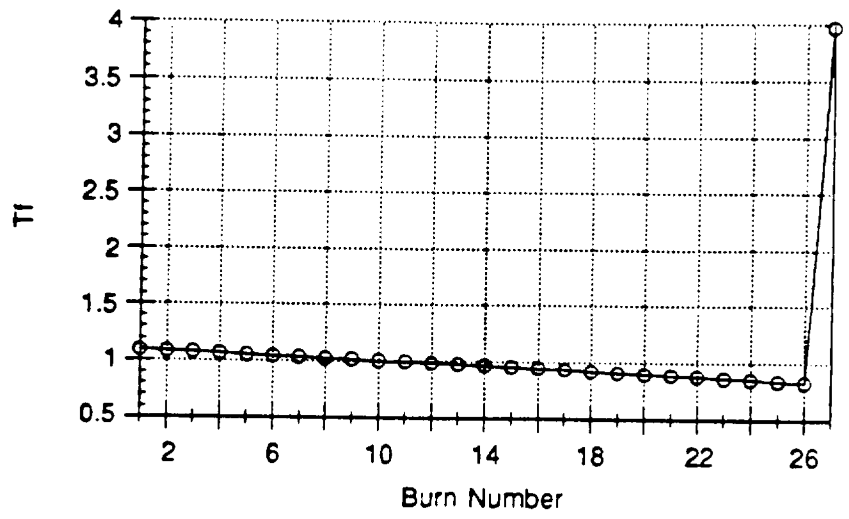

Figure 3.15 Transfer Time vs Orbit Number for each Burn of a 27-Burn Transfer with a 63.4° Plane Change

One feature that seems common to the large number of burns case and the small number of burns case is the use of the distant burn for inclination changes. Referring back to the nonplanar 3-burn transfer shown in Figs. 2.2-2.3, it is clear that the first burn is making most of the inclination change. Also, it is clear from the 27-burn transfer represented in Fig. (3.13) that the h_y component of the angular momentum vector, which indicates the inclination, has very little variation until the final burn takes its value from almost zero to almost -2. This same trend can be seen for the 5-burn transfer represented by Fig. 3.5; where the h_x component indicates inclination for this transfer.

III.4. Inclusion of Perturbation Terms

Neither the Patched Method nor MPM are equipped to produce exact solutions to fuel-optimal orbit transfer problems in the presence of orbit perturbations. Note that including orbit perturbations will cause assumption (i) from $\{P\}$ to be violated.

The tradeoff between making the ideal gravity assumption and obtaining solutions with much larger numbers of burns was deemed acceptable. It is hoped that the techniques used in this tradeoff will find application in future research into the orbit transfer problem including perturbations.

However, BOUNDSCO was able to obtain a solution including orbit perturbations for the 5-burn transfer presented above in Figure 3.5. Perturbations are considered for this trajectory as opposed to the others, because BOUNDSCO iterations did not converge for the others, even after several trials including initial guesses that were slightly perturbed from the exact solution.

Figures 3.16-3.18 shows the changes in orbital elements and transfer time induced by the inclusion of atmospheric drag and oblateness effects. It is clear that the extremal trajectory includes a lengthened second burn which raises the energy of the second transfer orbit, thereby raising its altitude and decreasing the effect of drag. It is not so clear what decides that the longer burn will be the second and not the first. The nodal regression seems to manifest itself as a decreasing H_y component; it is interesting to note that, like inclination changes, the extremal transfer doesn't make the correction until the last burn. Turning attention to the burn lengths, note that the amount by which the first burn is shortened almost exactly counters the amount by which the next burn is lengthened. A similar trend shows itself for the third and fourth burns. The last burn is only slightly shorter, but not enough to indicate whether the total burn time is longer or shorter. In fact the final mass of the ideal gravity transfer was 3.762; for the transfer with perturbations it was 3.760. This is a performance loss of only 0.07%, a surprising result considering that the individual burn times change by as much as 1.6%.

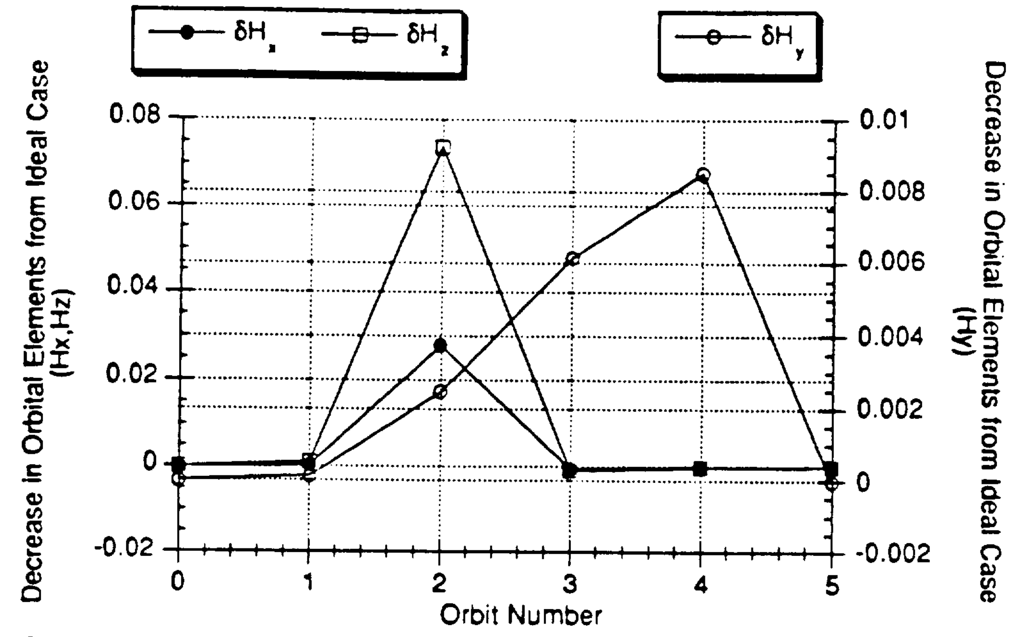

Figure 3.16 Decrease in the Components of the Angular Momentum Vector for the 5-Burn Transfer of Figure 3.5 Considering Orbit Perturbations

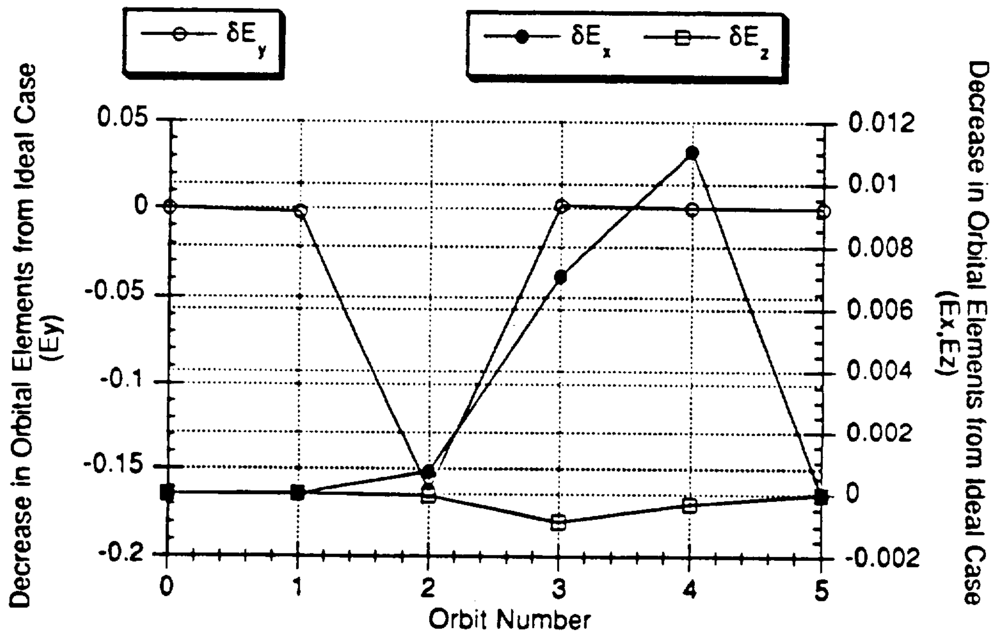

Figure 3.17 Decrease in the Components of the Eccentricity Vector for the 5-Burn Transfer of Figure 3.5 Considering Orbit Perturbations

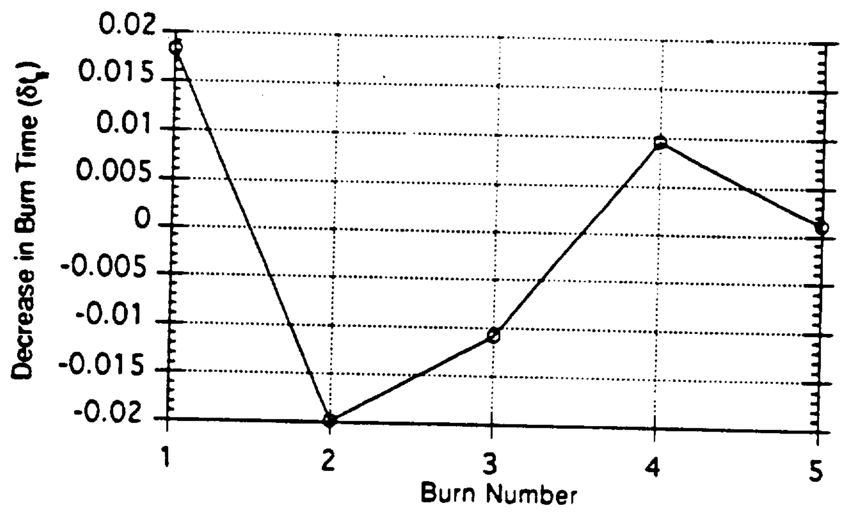

Figure 3.18 Decrease in the Burn Times for the 5-Burn Transfer of Figure 3.5 Considering Orbit Perturbations

III.5 Conclusions

In this section, two new methods for computing multiple-burn orbit transfers are presented. These methods, the Patched Method and the Modified Patched Method, have been developed specifically to fill an apparent gap in computational ability for fuel-optimal transfers with large numbers of burns. For this type of problem, both methods have out-performed BOUNDSCO and MBCM from the previous section.

The conditions upon which each of these methods are based on have been proven equivalent to necessary conditions. However, for both methods it is required that Pontryagin's Maximum Principle be checked after iterations have stopped.

The Patched Method, though slow, was very robust in obtaining solutions. Because of its use of a direct method, it was usually able to obtain the one-burn solutions between each pair of orbits. Also, the optimization of the transfer orbits usually proceeded well in the sense that each iteration would produce a better choice of orbital elements. However, the overall method tended to be quite slow because the cumulative time required to compute the one-burn transfers in succession was quite long and increased with number of burns.

MPM computed solutions beyond the capability of any of the other methods investigated in this report. MPM was much quicker and slightly less robust, as would be expected of a method more akin to multiple-point shooting. Therefore, it is suggested that the Patched Method be used with a very low tolerance to obtain initial guesses for MPM.

Neither the Patched Method nor MPM is designed to handle orbit perturbations. However, the marked improvement in performance found with these configurations should be motivation enough for a future research effort to produce similar configurations that can handle orbit perturbations efficiently.

Also in this section, a new formulation for the solution of the Lagrange multipliers is presented. This formulation is valid over coast arcs where the Hamiltonian vanishes.

SECTION IV

GUIDANCE FOR OPTIMAL ORBIT TRANSFERS

IV.1. Introduction

The guidance scheme examined here is an implicit one which implements neighboring optimal feedback guidance. An implicit guidance system was chosen due to the fact that that type of guidance system often handles disturbances well[42]. Neighboring optimal feedback guidance was chosen because it has the advantage of being a feedback system, as opposed to open-loop guidance and it can be implemented very easily as with a gain-scheduling scheme. There also appears to be a lack of studies in the literature which examine this type of guidance scheme for this problem.

In this formulation, the initial orbit exit point is assumed to be perturbed from the nominal point but the other boundary condition, specifying the final orbit, is assumed unchanged. The goal is to use the controller to bring the trajectory to the final orbit at some point with minimal fuel.

In order for this guidance scheme to be implementable, the neighboring trajectory must exist; the sufficient conditions for a local extremal must be satisfied. The satisfaction of these conditions for the nominal solution will be shown. Following that, the guidance scheme will be investigated, including the use of a time-to-go indexing scheme.

[42]Naidu, D. Subbaram. Aeroassisted Orbital Transfer: Guidance and Control Strategies. New York: Springer-Verlag, 1994.

IV.2. Literature Review

Many researchers have used the first variation to compute extremal solutions to the fuel-optimal orbit transfer problem. However, few, if any, have made use of the conditions related to the second variation of the cost functional in computation. These provide sufficient conditions which, when met, declare an extremal solution as a locally weak optimal solution.

Once the second variation of the cost functional is verified so that it is known whether the sufficient conditions are met, the information obtained can then be used to implement a guidance scheme. Guidance schemes can typically be divided into two categories: implicit and explicit. Implicit guidance systems are characterized by the fact that the vehicle's motion must be precomputed on the ground and then compared to the actual motion. The equations which need to be solved are based upon the difference between these measured and precomputed values. The solutions to these equations are used in the vehicle's steering and velocity control. Explicit guidance systems are generalized by the fact that the vehicle's equations of motion are modeled and solved for by on-board computers during its motion. The solutions for the equations are solved continuously and are used to determine the difference between the vehicle's current motion and its destination. Commands are then generated to alleviate the anticipated error.

Guidance schemes have been presented in various papers.[43] A guidance scheme which is implemented using a linear tangent law is presented by Sinha, Shrivastave, Bhat,

[43]Chuang, C.-H., Goodson, T.D., Ledsinger, L.A., "The Second Variation and Neighboring Optimal Feedback Guidance for Multiple Burn Orbit Transfers," *Proceedings of the 1995 AIAA Conference on Guidance, Navigation, and Control*, Baltimore, Maryland, USA.

and Prabhu.[44] In a paper by Lu[45], a nonlinear guidance law is developed using two different strategies. One strategy uses optimal control theory to generate a new optimal trajectory onboard from the start, while the other uses flight-path-restoring-guidance to bring the trajectory back to the nominal. A guidance scheme that is developed using inverse methods for unthrusted, lift-modulated vehicles along an optimal space curve is presented by Hough.[46] Linearized guidance laws applicable to many different types of space missions are presented by Tempelman.[47] These guidance laws are based on fixed and free final time arrivals. Naidu[42] presents a neighboring optimal guidance scheme applicable to aeroassisted orbital transfers.

IV.3. Preliminary Considerations

Earlier, the optimal orbit transfer problem was given as a maximization problem. To conform to the convention used for the second variation[36] it is transformed to a minimization problem. For the minimization problem, the performance index can be made negative and considered a cost functional

$$J = -m(t_f) \tag{4.1}$$

As the necessary conditions are first-order conditions, they remain unchanged. However, Lawden's pointer vector theory is second-order and requires that the control be such that

$$\mathbf{e}_T = \frac{-\boldsymbol{\lambda}_v}{|\boldsymbol{\lambda}_v|} \tag{4.2}$$

[44]Sinha, S. K., S. K. Shrivastava, M. S. Bhat, and K. S. Prabhu. "Optimal Explicit Guidance for Three-Dimensional Launch Trajectory," *Acta Astronautica*. Vol. 9, 1989, pp. 115-125.

[45]Lu, P., "A General Nonlinear Guidance Law," *Proceedings of the the AIAA Guidance, Navigation, and Control Conference*, Scottsdale, Arizona, 1994.

[46]Hough, M. E., "Explicit Guidance Along an Optimal Space Curve," *Journal of Guidance, Control, and Dynamics*. Vol. 12, 1989, pp. 495-504.

[47]Tempelman, W., "Linear Guidance Laws for Space Missions," *Journal of Guidance, Control, and Dynamics*. Vol. 9, 1986, pp. 495-502.

Furthermore, Pontryagin's Minimum Principle requires that an extremal solution satisfy

$$\begin{aligned} H_S < 0, \quad T = T_{max} \\ H_S > 0, \quad T = 0 \end{aligned} \tag{4.3}$$

where

$$H_S = -\left(\frac{|\lambda_v|}{m} + \frac{\lambda_m}{g_o I_{sp}} \right) \tag{4.4}$$

If an extremal solution to the maximization problem is given as state time history x(t), Lagrange-multiplier time history λ(t), and Lagrange multipliers ν, (associated with boundary conditions) then an extremal solution for the minimization problem with the cost function in Eq. (4.1) can be constructed as x(*t*), (-1)*λ(*t*), and (-1)*ν.

Additionally, it makes more sense in the planar guidance problem to consider the control as an angle *θ*, rather than individual components of a unit vector. This simplifies analysis because the control is now a scalar. Equation (4.2) now gives

$$tan(\theta) = -\frac{\lambda_v}{\lambda_u} \tag{4.5}$$

A practical approach to guidance is suggested by previous results in this report. If a multiple-burn transfer can be thought of as consisting of multiple optimal one-burn transfers, then it should be reasonable to examine a guidance scheme that attempts to match each of the intermediate transfer orbits of the multiple-burn transfer. In other words, use neighboring optimal feedback guidance for one burn at a time.

This is not suggested to be an optimal guidance scheme. By focusing on each burn with neighboring optimal feedback, but not considering the trajectory as a whole, this guidance scheme becomes a sub-optimal guidance scheme.

Each burn can be considered an extremal solution. These extremal solutions are considered to have a fixed initial point and free transfer time but the final point is only constrained in that it must lie on the final orbit. Recall, however, that in computing the multiple-burn transfer the initial point was not fixed; this condition is imposed for practical considerations. If the spacecraft is delivered to the correct orbit, and coasting to the nominal burn-on point has zero cost, then there is no reason to attempt to compute a new burn-on point. This reasoning holds for the beginning of each burn.

IV.4. The Second Variation for One-Burn Problems

Considering the second variation of the augmented cost functional, J, a new optimal control problem can be stated.[36] In this new problem, the state is $\delta\mathbf{x}$, the control δu, and the Lagrange-multipliers are $\delta\lambda$ and $d\mathbf{v}$. The new problem is linear and can be solved using a sweepback method. For the problem considered here, $\mathbf{x}=[\mathbf{r}^T\ \mathbf{v}^T\ m]^T$ and $u=\theta$.

When the final time is free for optimization, the transversality condition must be satisfied by the nominal solution. The notation for this condition is

$$\Omega(\mathbf{x},\mathbf{v},t)\Big|_{t=t_f} = \left(\frac{d\mathrm{G}}{dt}\right)_{t=t_f} = \left(\frac{\partial \mathrm{G}}{\partial \mathbf{x}}\dot{\mathbf{x}}\right)_{t=t_f} = 0 \tag{4.6a}$$

where

$$\mathrm{G}(\mathbf{x},\mathbf{v}) = \phi(\mathbf{x}) + \mathbf{v}^T\psi(\mathbf{x}) \tag{4.6b}$$

In general, neighboring optimal feedback guidance allows consideration of changes in boundary conditions. No such changes are considered, assuming that the destination orbit is fixed. Formulation will be made below for the free final time case.

The change in state and costate can be estimated with a linear time-varying dynamic system. This dynamic system is given below, where it is understood that matrix functions are evaluated with the nominal trajectory.

$$\frac{d}{dt}\delta \mathrm{x} = \mathbf{A}(t)\delta \mathrm{x} - \mathbf{B}(t)\delta\lambda \tag{4.7}$$

$$\frac{d}{dt}\delta\lambda = -\mathbf{C}(t)\delta \mathrm{x} - \mathbf{A}^{\mathrm{T}}(t)\delta\lambda \tag{4.8}$$

where

$$\mathbf{A}(t) = \mathbf{f}_x - \mathbf{f}_u H_{uu}^{-1} H_{ux} \tag{4.9}$$

$$\mathbf{B}(t) = \mathbf{f}_u H_{uu}^{-1} \mathbf{f}_u^{\mathrm{T}} \tag{4.10}$$

$$\mathbf{C}(t) = H_{xx} - H_{xu} H_{uu}^{-1} H_{ux} \tag{4.11}$$

Evaluating Eqs. (4.7)-(4.11) the recurring terms in the differential equations are:

$$\mathbf{f}_x = \begin{bmatrix} 0 & 0 & -\left(\frac{\mu}{r^3}\right) - \frac{3\mu x^2}{r^5} & \frac{3\mu xy}{r^5} & 0 \\ 0 & 0 & \frac{3\mu xy}{r^5} & -\left(\frac{\mu}{r^3}\right) - \frac{3\mu y^2}{r^5} & 0 \\ 1 & 0 & 0 & 0 & 0 \\ 0 & 1 & 0 & 0 & 0 \\ 0 & 0 & -\frac{T}{m}cos(\theta) & -\frac{T}{m}sin(\theta) & 0 \end{bmatrix}^{\mathrm{T}} \tag{4.12}$$

$$\mathbf{f}_\theta = \begin{bmatrix} 0 & 0 & -\frac{T}{m}sin(\theta) & \frac{T}{m}cos(\theta) & 0 \end{bmatrix}^{\mathrm{T}} \tag{4.13}$$

$$H_{xx} = \begin{bmatrix} \mathbf{Q} & 0 \\ 0 & 2\frac{\mathrm{T}}{\mathrm{m}^3}|\lambda_v| \end{bmatrix} \tag{4.14}$$

$$\mathbf{Q} = \frac{3\mu}{r^7}\begin{bmatrix} \left\{(3\lambda_u x + \lambda_v y)r^2 - 5(\lambda_v^{\mathrm{T}}\mathbf{r})x^2\right\} & \left\{(\lambda_u y + \lambda_v x)r^2 - 5(\lambda_v^{\mathrm{T}}\mathbf{r})xy\right\} \\ \left\{(\lambda_u y + \lambda_v x)r^2 - 5(\lambda_v^{\mathrm{T}}\mathbf{r})xy\right\} & \left\{(3\lambda_v y + \lambda_u x)r^2 - 5(\lambda_v^{\mathrm{T}}\mathbf{r})xy\right\} \end{bmatrix} \tag{4.15}$$

$$H_{uu} = \frac{T}{m}|\lambda_v| \tag{4.16}$$

$$H_{ux} = 0 \tag{4.17}$$

note that $\mathbf{r} = [x \quad y]^{\mathrm{T}}$, $\mathrm{v} = [u \quad v]^{\mathrm{T}}$, and $\lambda_v = [\lambda_u \quad \lambda_v]^{\mathrm{T}}$ are taken as the nominal trajectory. Using the sweepback method for nonlinear terminal constraints the form for $\delta\lambda$ and $\delta\psi$ can be written as

$$\delta\lambda(t) = \overline{\mathbf{P}}(t)\delta\mathrm{x}(t) + \overline{\mathbf{S}}(t)d\mathrm{v} \tag{4.18}$$

$$\delta\psi = \overline{\mathbf{S}}^{\mathrm{T}}(t)\delta\mathrm{x}(t) + \overline{\mathbf{V}}(t)d\mathrm{v} \tag{4.19}$$

which allows the solution for $d\mathrm{v}$ to be written as

$$d\mathrm{v} = \overline{\mathbf{V}}^{-1}(t_o)\left[\delta\psi - \overline{\mathbf{S}}^{\mathrm{T}}(t_o)\delta\mathrm{x}(t_o)\right] \tag{4.20}$$

As mentioned above, $\delta\psi=0$ will be considered here. The matrices $\overline{\mathbf{P}}(t)$, $\overline{\mathbf{S}}(t)$, and $\overline{\mathbf{V}}(t)$, are computed using the following relations:

$$\overline{\mathbf{P}}(t) = \mathbf{P}(t) - \frac{\mathbf{m}(t)\mathbf{m}^{\mathrm{T}}(t)}{\alpha(t)} \tag{4.21}$$

$$\overline{\mathbf{S}}(t) = \mathbf{S}(t) - \frac{\mathbf{m}(t)\mathbf{n}^{\mathrm{T}}(t)}{\alpha(t)} \tag{4.22}$$

$$\overline{\mathbf{V}}(t) = \mathbf{V}(t) - \frac{\mathbf{n}(t)\mathbf{n}^{\mathrm{T}}(t)}{\alpha(t)} \tag{4.23}$$

Now the matrices $\mathbf{P}(t)$, $\mathbf{S}(t)$, $\mathbf{V}(t)$, $\mathbf{m}(t)$, $\mathbf{n}(t)$, and the scalar function $\alpha(t)$ are computed from a dynamic system. The boundary condition equations for this system are given by:

$$\mathbf{P}(t_f)=\left[\phi_{\mathbf{xx}}+\left(\nu^{T}\psi_{\mathbf{x}}\right)_{\mathbf{x}}\right]_{t=t_f} \tag{4.24}$$

$$\mathbf{S}(t_f)=\left[\psi_{\mathbf{x}}^{T}\right]_{t=t_f} \tag{4.25}$$

$$\mathbf{V}(t_f)=0 \tag{4.26}$$

where in the development for the orbital transfer these are:

$$\mathbf{P}(t_f)=\begin{bmatrix} a & b & d & e & 0 \\ b & c & f & g & 0 \\ d & f & h & i & 0 \\ e & g & i & j & 0 \\ 0 & 0 & 0 & 0 & 0 \end{bmatrix} \tag{4.27}$$

$$a= \nu_2\mu\left[\frac{x}{r^3}-\frac{3x^3}{r^5}+\frac{2x}{r^3}\right]+\nu_3\mu\left[\frac{y}{r^3}-\frac{3x^2y}{r^5}\right] \tag{4.28a}$$

$$b=\nu_2\mu\left[\frac{y}{r^3}-\frac{3x^2y}{r^5}\right]+\nu_3\mu\left[\frac{x}{r^3}-\frac{3xy^2}{r^5}\right] \tag{4.28b}$$

$$c=\nu_3\mu\left[\frac{y}{r^3}-\frac{3y^3}{r^5}+\frac{2y}{r^3}\right]+\nu_2\mu\left[\frac{x}{r^3}-\frac{3xy^2}{r^5}\right] \tag{4.28c}$$

$$d=-\nu_3 v \tag{4.28d}$$

$$e=\nu_1-\nu_2 u+2\nu_3 v \tag{4.28e}$$

$$f=-\nu_1-\nu_2 v+2\nu_3 u \tag{4.28f}$$

$$g=-\nu_2 u \tag{4.28g}$$

$$h=2\nu_3 y \tag{4.28h}$$

$$i=-\nu_3 x-\nu_2 y \tag{4.28i}$$

$$\mathrm{j}=2\nu_2 x \tag{4.28j}$$

and expression for Eq. (4.25) was previously given as Eq. (2.11).

Following from the assumptions expressed as Eqs. (4.18)-(4.19), the following nonlinear equations for **P**, **S**, and **V** must be integrated backwards. The results will be used to check the sufficient conditions governing a minimizing solution.

$$\dot{\mathbf{P}} = -\mathbf{PA} - \mathbf{A}^T\mathbf{P} + \mathbf{PBP} - \mathbf{C} \tag{4.29}$$

$$\dot{\mathbf{S}} = -\left(\mathbf{A}^T - \mathbf{PB}\right)\mathbf{S} \tag{4.30}$$

$$\dot{\mathbf{V}} = \mathbf{S}^T\mathbf{BS} \tag{4.31}$$

$$\dot{\mathbf{m}} = -\left(\mathbf{A}^T - \mathbf{PB}\right)\mathbf{m} \tag{4.32}$$

$$\dot{\mathbf{n}} = \mathbf{S}^T\mathbf{Bm} \tag{4.33}$$

$$\dot{\alpha} = \mathbf{m}^T\mathbf{Bm} \tag{4.34}$$

with the following boundary conditions applying

$$\mathbf{m}\left(t_f\right) = \left(\frac{d\Omega}{d\mathbf{x}}\right)^T_{t=t_f} \tag{4.35}$$

$$\mathbf{n}\left(t_f\right) = \left(\frac{d\psi}{dt}\right)_{t=t_f} \tag{4.36}$$

$$\alpha\left(t_f\right) = \left(\frac{d\Omega}{dt}\right)_{t=t_f} \tag{4.37}$$

The sufficient conditions for a minimizing solution can now be stated as follows:

convexity condition: $H_{\theta\theta}(t) > 0$ for $t_o \le t \le t_f$ (4.38)

normality condition: $\overline{\mathbf{V}}^{-1}(t)$ exists for $t_o \le t < t_f$ (4.39a)

$\alpha^{-1}(t)$ exists for $t_o \le t < t_f$ (4.39b)

conjugate point condition: $\overline{\mathbf{P}}(t) - \overline{\mathbf{S}}(t)\overline{\mathbf{V}}^{-1}(t)\overline{\mathbf{S}}^T(t)$ finite for $t_o \le t < t_f$ (4.40)

The convexity condition is satisfied for any transfer satisfying Equation (4.5). This can be seen by noting that Eq. (4.16) is positive definite, irrespective of the time history for the Lagrange multipliers.

The eigenvalues of $\bar{V}$ are plotted in Figure 4.1. Figures 4.2-4.4 plot the elements of the conjugate point condition matrix. Figure 4.5 is a plot of $\alpha(t)$. Figure 4.1 shows that $\bar{V}$ is positive definite in the required interval. Figure 4.5 shows that $\alpha(t)$ is negative definite in the required interval. Since the normality condition requires that the inverse of $\bar{V}$ and $\alpha(t)$ exists in the interval, this solution is normal. Figures 4.2-4.4 show that the conjugate point condition is satisfied. The elements are bounded in the required interval and grow asymptotically at the final time; the curves in the figures have been truncated to show their variations prior to this asymptotic growth. Therefore, this solution satisfies the sufficient conditions for minimizing the cost functional with free transfer time.

It seems appropriate to first attempt the guidance scheme for a relatively uncomplicated transfer. Such a transfer was presented in Fig. 2.1 and discussed in subsection [II.2.4]. The transfer is planar; no plane changes occur. The guidance scheme considered here will be simulated for this trajectory.

IV.4.1. Neighboring Optimal Feedback Guidance

Conveniently, construction of a neighboring optimal feedback guidance law uses the same information as that required to check the second variation of the cost functional. As a result, much of the derivation required of guidance law has been stated already. The remaining discussion will describe how to form the feedback control law and adjust the characteristics of the bang-bang control in a feedback law.

The control, $\delta\theta$, for the fixed final time problem can be found using

$$\delta\theta(t) = -H_{uu}^{-1}\left[(f_u^T \bar{P})\delta x + f_u^T \bar{S} d\nu\right] \tag{4.41}$$
$$= -H_{uu}^{-1}\left[f_u^T(-\bar{S}\bar{V}^{-1}\bar{S}^T)\right]\delta x$$

and the change in the final time, dt_f, is:

$$dt_f = -\left[\left(\frac{m^T}{\alpha} - \frac{n^T}{\alpha}\bar{V}^{-1}\bar{S}^T\right)\right]\delta x \tag{4.42}$$

Evaluating dt_f determines when the thrust will be turned off to complete the transfer.

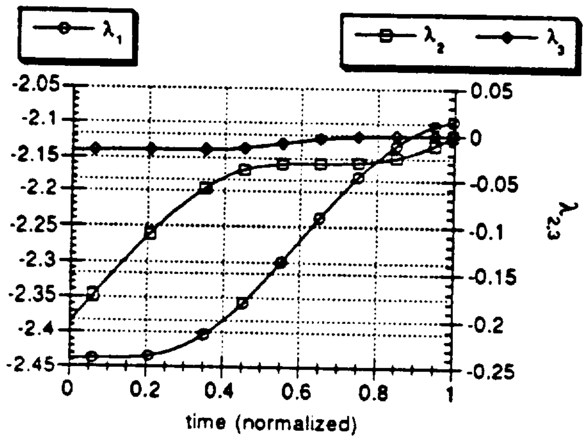

Figure 4.1 Plot of Eigenvalues of $\bar{V}(t)$ for Two-Burn Extremal, Last Burn

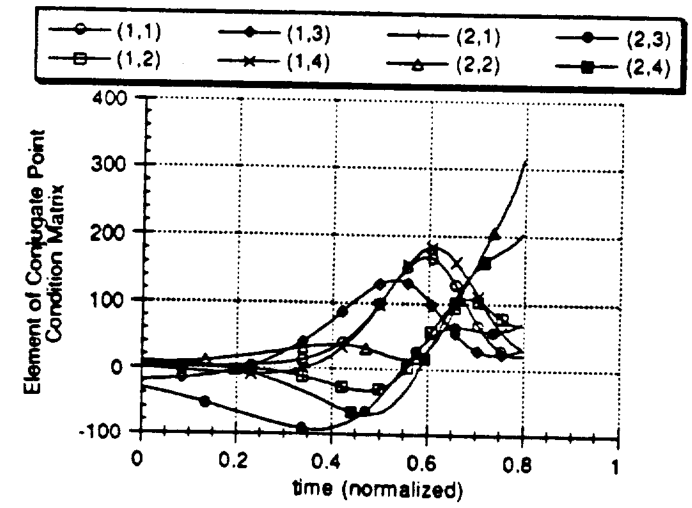

Figure 4.2 Plot of Elements of Conjugate Point Condition Matrix for Two-Burn Extremal, Last Burn

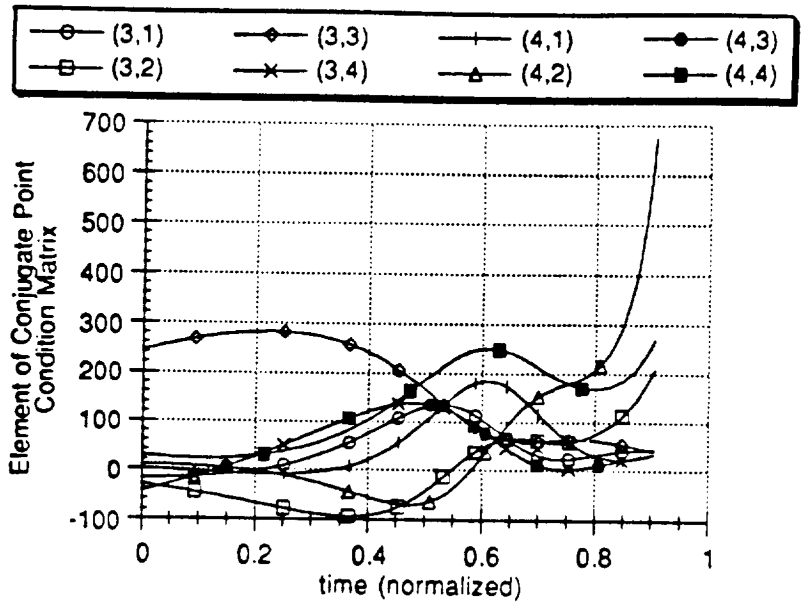

Figure 4.3 Plot of Elements of Conjugate Point Condition Matrix for Two Burn Extremal, Last Burn

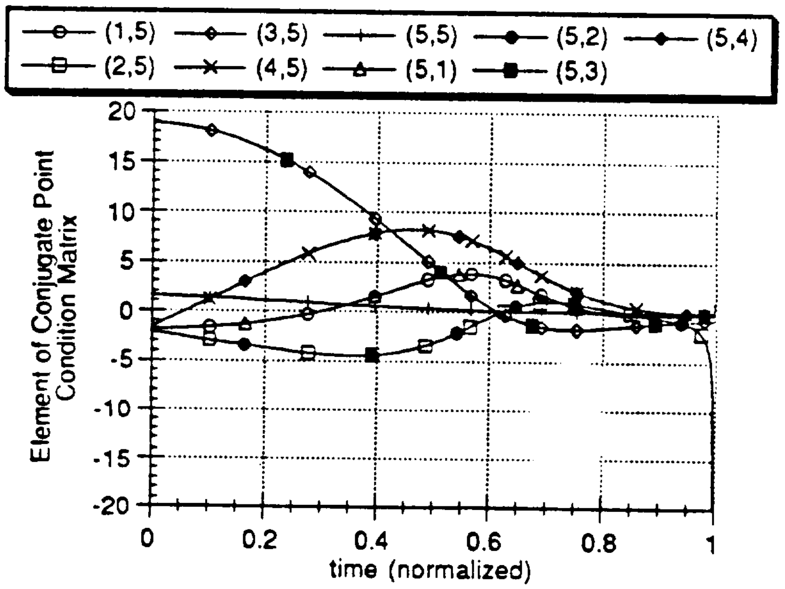

Figure 4.4 Plot of Elements of Conjugate Point Condition Matrix for Two Burn Extremal, Last Burn

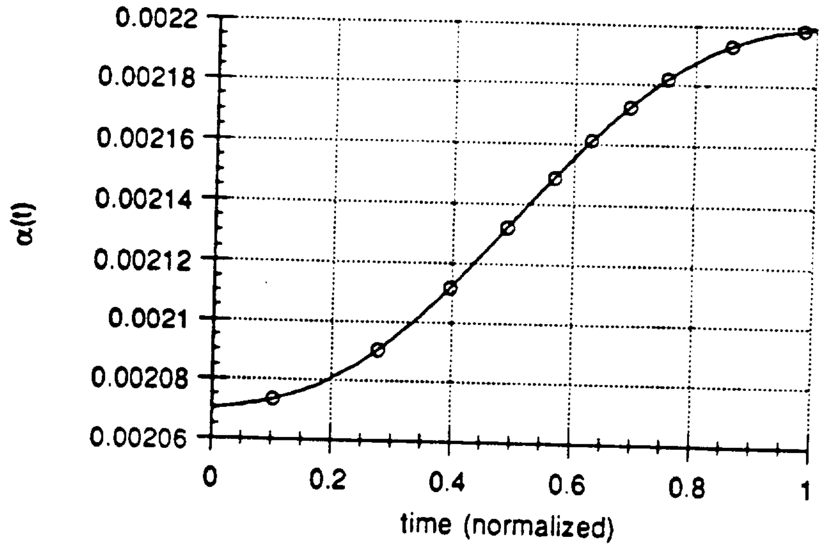

Figure 4.5 Plot of α(t) for Two Burn Extremal, Last Burn

This continuous feedback law has been constructed by estimating *dv* at each instant of time instead of solving for *dv* at the initial time and then using this value for all time

The feedback law depends on **P**, **S**, and **V** as functions of time. A particular advantage of neighboring optimal feedback is that the linearized TPBVP only has to be solved once. Afterwards, sampled values of the feedback gains may be stored. The feedback gains may then be computed for any time by interpolation between stored values. Use of this control should keep the spacecraft on a neighboring optimal solution and deliver it to the required orbit.

The block diagram for the feedback controller needed for neighboring optimal feedback guidance is shown in Figure 4.6.

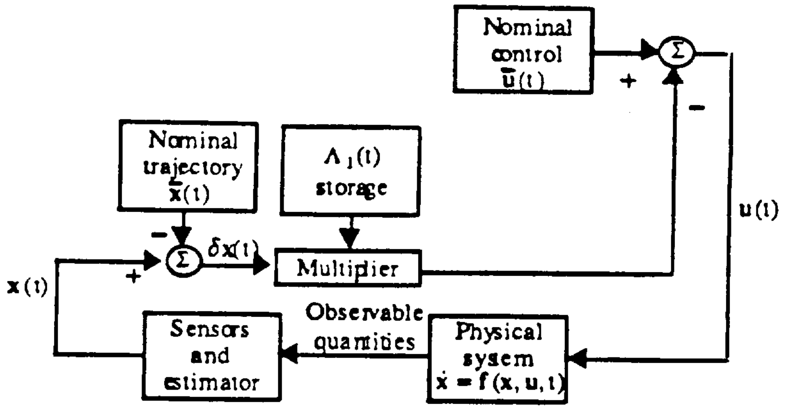

Figure 4.6 Diagram of Neighboring Optimal Feedback Controller Implementation

where $\Lambda_1(t)$ is the feedback gain from Eq. (4.41), computing $\delta\theta$.

IV.4.2. Simulation of the Guidance Algorithm

Justification for a feedback algorithm lies in Fig. 4.7 and Fig. 4.8. It can be noted that there is error in the variation of the states from the neighboring optimal trajectory when guidance is not used, Fig. 4.7, i.e., when the control correction is not used. However, Fig. 4.8 shows that a feedback law is needed because when implementing it, the errors in the variation of the states becomes much less, comparatively, than that using no guidance whatsoever. The neighboring optimal trajectory referenced in Figs. 4.7-4.8 was computed with BOUNDSCO.

IV.4.3. Time-To-Go Implementation

Since this problem is a free final-time problem, the possibility exists that the final-time will increase and the guidance algorithm will "run out of gains"; this is a familiar issue for neighboring optimal feedback guidance. The approach used in this study is based on discretizing the gains by N time nodes $\{t_1,...,t_i,...t_N\}$ where t_N is earlier than the nominal t_f. The gains at the nominal t_f will be infinite and impractical to store. Both the gains for calculating dt_f, via Eq. (4.42), and for $\delta\theta$, via Eq. (4.41), are then calculated at any time by linear interpolation between stored values.

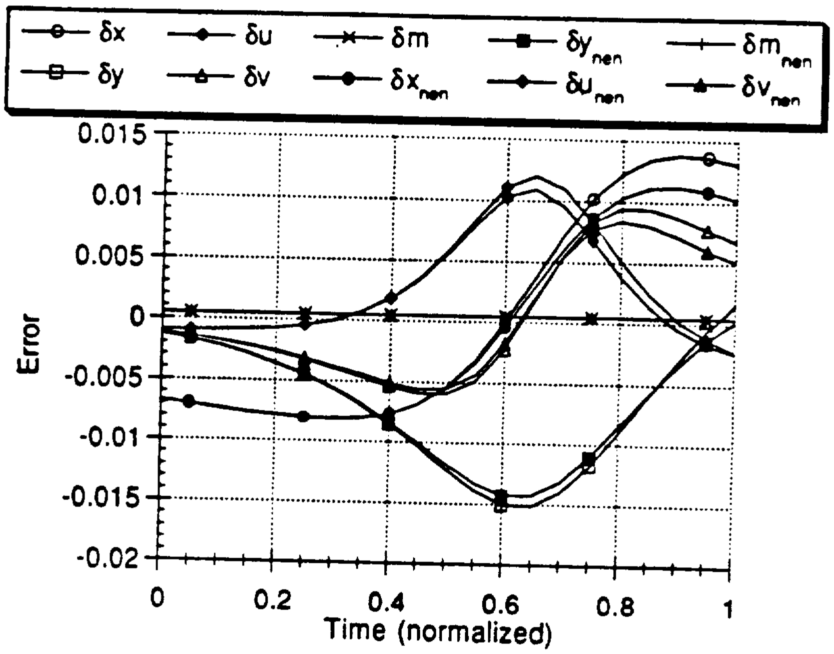

Figure 4.7 Plot of State Variation from the Nominal Trajectory vs. Time for Neighboring Optimal Trajectory ($()_{nen}$) and a Trajectory Without Guidance (no subscript)

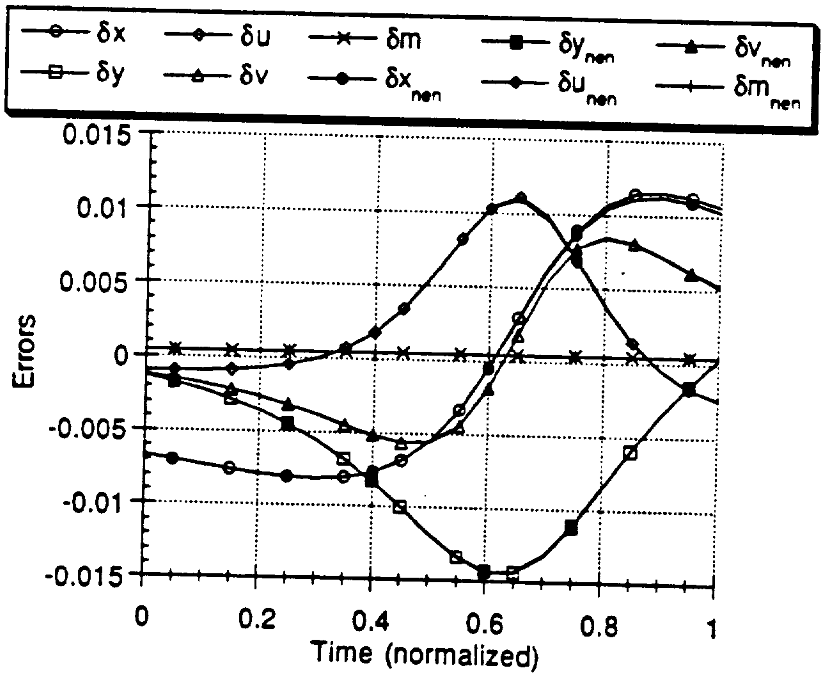

Figure 4.8 Plot of State Variation from the Nominal Trajectory vs. Time for Neighboring Optimal Trajectory ($()_{nen}$) and a Trajectory With Guidance (no subscript)

To consider time-to-go, the guidance must make active use of the dt_f estimation. Since both the nominal and the actual trajectories start at t_1, dt_{f1} can be initially calculated using the gains at that time. The length of the first guidance interval is then found by relating it to the estimated time-to-go.

$$\Delta t_{s1} = \frac{t_f + dt_{f1}}{t_f}(t_2 - t_1) \tag{4.43}$$

Then, at the end of the *i-1*th guidance interval, the gains at t_i are used to calculate dt_{fi}. Using this information, the length of the *i*th guidance interval can be computed as

$$\Delta t_{si} = \frac{t_f + dt_{fi} - \sum_{j=1}^{i-1} \Delta t_{sj}}{t_f - t_i}(t_{i+1} - t_i) \tag{4.44}$$

This continues until Δt_i is computed as zero or a negative number or until *i*=N. When *i*=N, the Nth gain is used for the entire interval Δt_N. When this interval ends, the guidance scheme is finished.

The plots below compare guidance performance with and without this time-to-go formulation. The curves represent the time history of the boundary condition error, i.e. Eqs. (1.12) minus the desired orbital elements, evaluated continuously. Figure 4.9 makes continuous use of the gains but indexes these gains at the current actual time without calculating dt_f. For the perturbation simulated, the transfer time needs to increase and this first scheme must terminate prematurely. Figure 4.10 makes use the discretized gains and time-to-go formulation. This simulation also incorporates a practical saturation limit on the size of the gains. The improvement due to the time-to-go formulation is obvious when comparing these plots. Therefore, this is both a practical and superior implementation of the continuous burn guidance considering the boundary condition error.

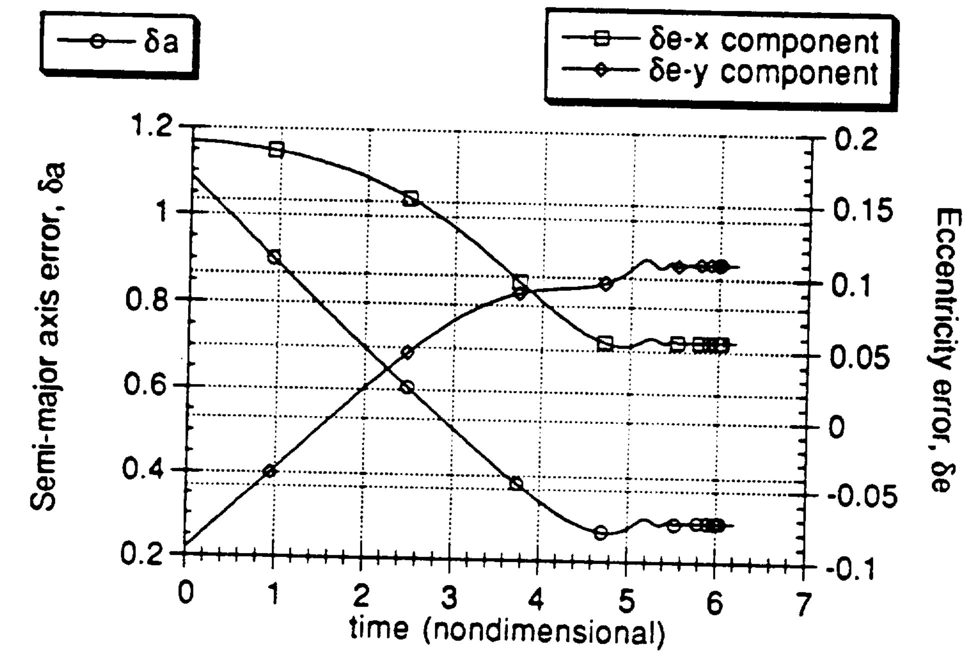

Figure 4.9 Plot of Boundary Condition Error for Continuous Guidance

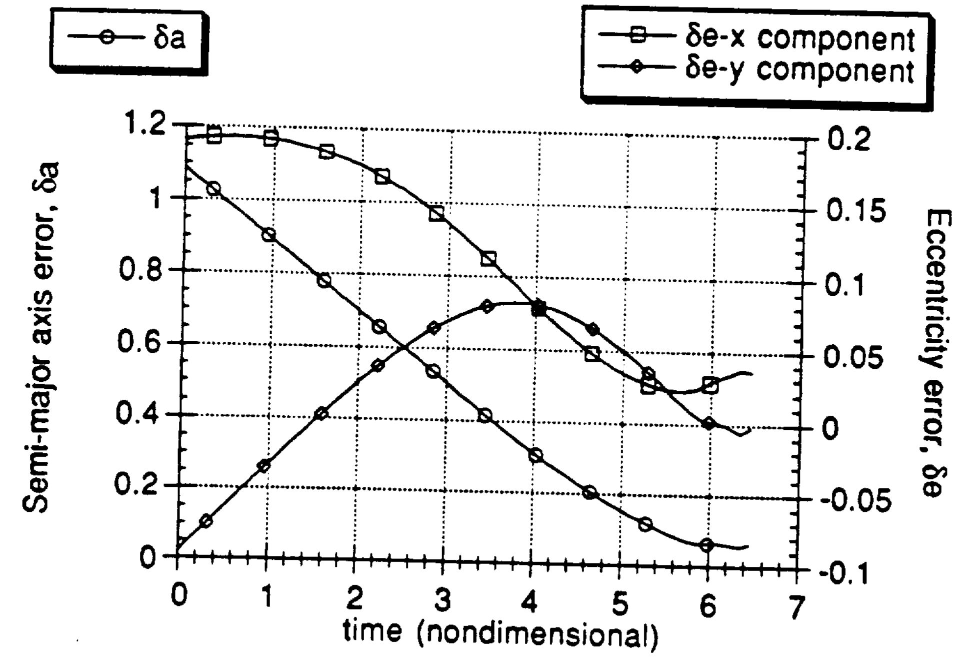

Figure 4.10 Plot of Boundary Condition Error for Discrete Guidance with Time-to-Go

IV.5. Multiple Burn Guidance

The guidance for multiple burns can also be discretized. For the two burn case, discretized guidance using time-to-go is used for the first burn. The guidance algorithm will place the spacecraft on the intermediate transfer orbit via the neighboring optimal trajectory. Since the cost on this coast arc is zero, the spacecraft can coast on this arc until it reaches the point at which the next burn is to start. Once the spacecraft reaches this point, discretized guidance using time-to-go can be used again for the second burn. The boundary conditions for the second burn should than be satisfied by the neighboring path. For multiple burns, this guidance scheme is extended in a straightforward manner.

The guidance scheme detailed above was used to recover the two burn transfer of Fig. 2.1 in the presence of an initial perturbation. Fig. 4.11 shows the boundary condition errors for the first burn given an initial perturbation of 10^{-3} in non-dimensionalized units. The boundary conditions are satisfied rather well for this burn. The resulting boundary condition errors for the second burn are shown in Figure 4.12. The boundary conditions are satisfied very well for this burn.

Figures 4.13 & 4.14 show the boundary condition errors during the second burn for a perturbation of the same magnitude as above in only the x position and the u velocity, respectively. Note that the error in the boundary conditions is slightly greater in Figure 4.14. This suggests that the trajectory is more sensitive to disturbances in the *u* velocity than in the *x* position.

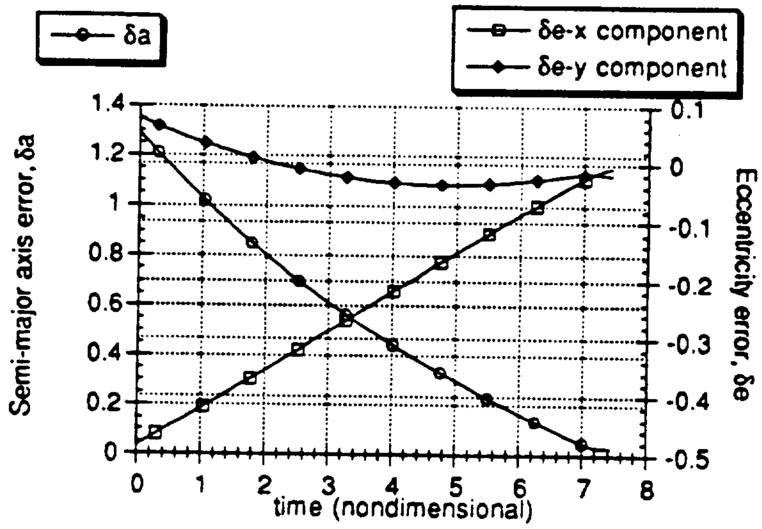

Figure 4.11 Plot of Boundary Condition Error for Discrete Guidance During the First Burn

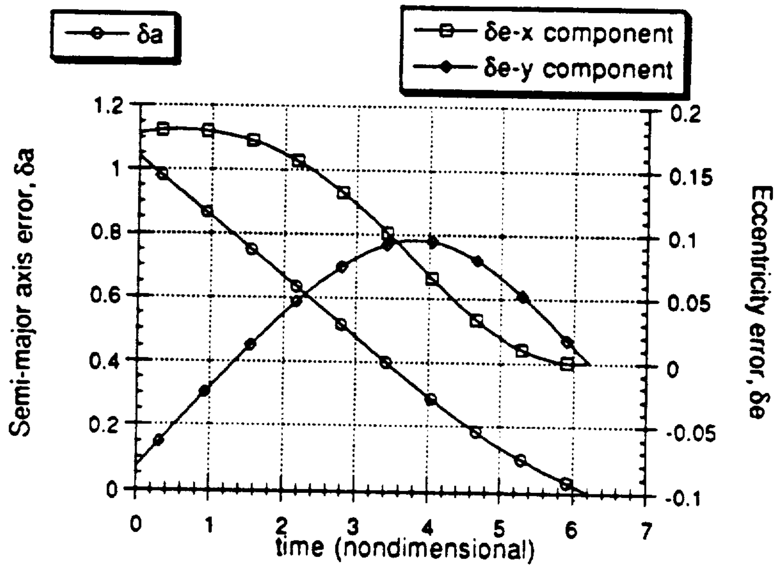

Figure 4.12 Plot of Boundary Condition Error for Discrete Guidance During the Second Burn (Continuation of Fig. 4.11)

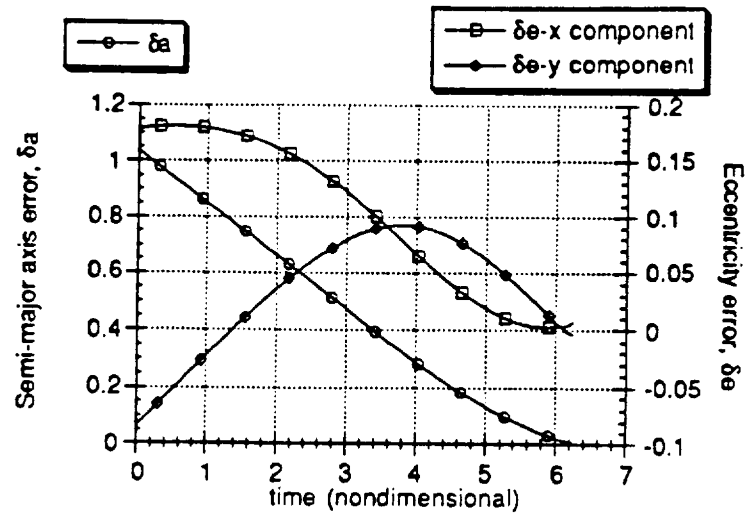

Figure 4.13 Plot of Boundary Condition Error for Discrete Guidance During the Second Burn for error in x at the initial time

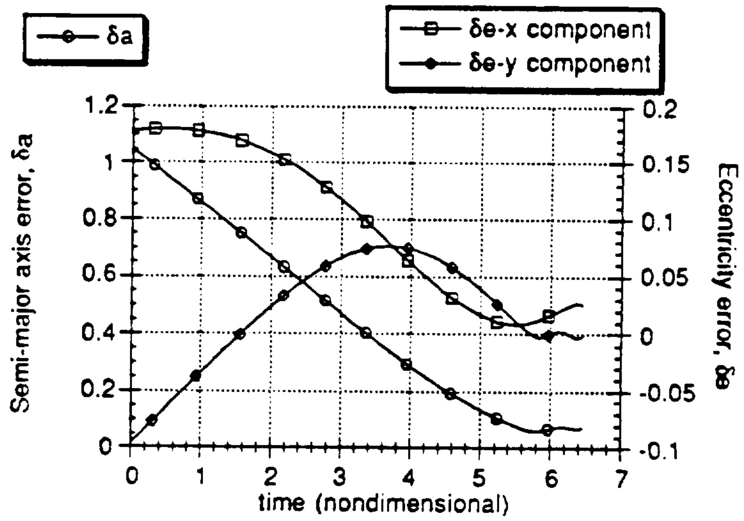

Figure 4.14 Plot of Boundary Condition Error for Discrete Guidance During the Second Burn for error in u

The resulting orbit transfer trajectory is shown in Figure 4.15. This plot corresponds to the boundary condition errors as shown in Figures 4.11 and 4.12.

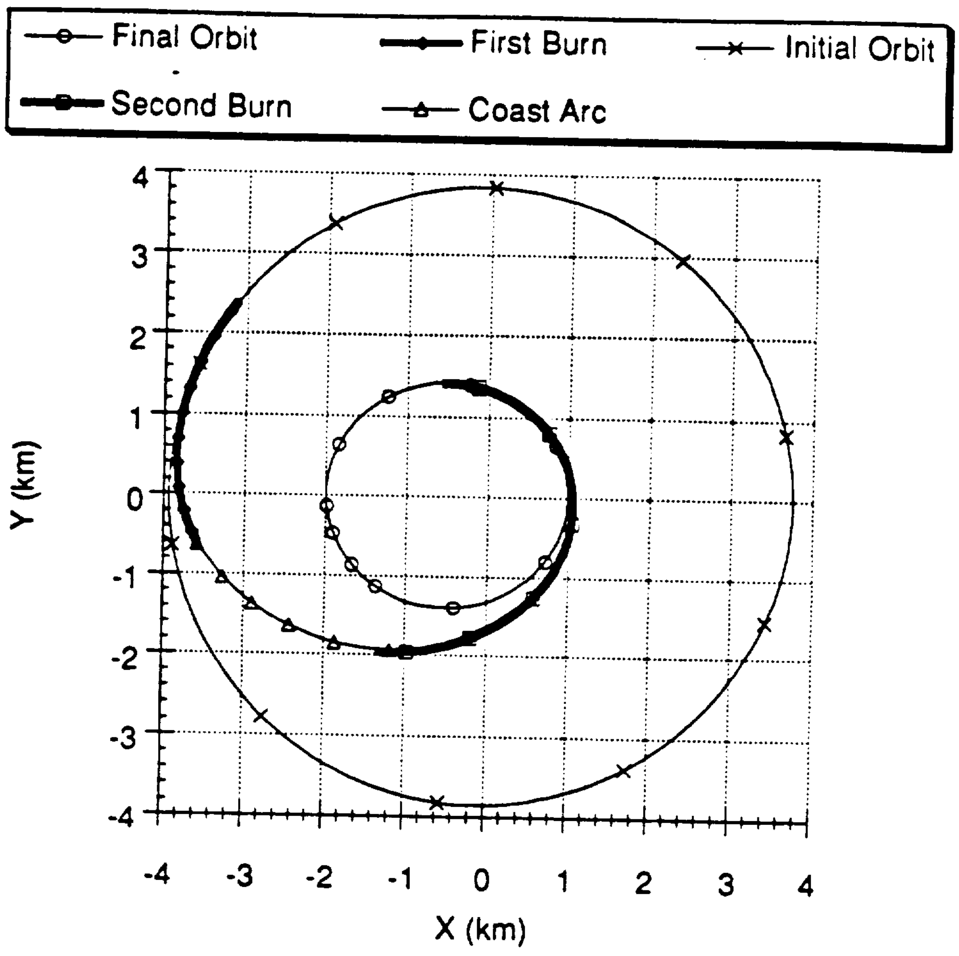

Figure 4.15 Plot of the Two Burn Orbit Transfer (from Fig. 2.1) with Initial Perturbation

IV.6. Conclusions

Extremal one burn trajectories have been shown to be weak locally optimal solutions using sufficient conditions. This does not prove that the multiple-burn transfer from which they were taken is itself a weak locally optimal solution, but it does allow the use of a new suboptimal guidance scheme.

This scheme was shown to reduce the terminal errors for small perturbations of the initial state. To increase the size of allowable perturbations, a time-to-go indexing scheme was simulated. This time-to-go indexing did improve the performance of the guidance scheme.

The suboptimal multiple-burn guidance with time-to-go indexing was simulated ıor a planar transfer. The performance of this guidance scheme did not match expectations. The implication is that the region in which a linear control correction is a valid assumption was quite small. Actually, this is not a surprising conclusion since obtaining the nominal solutions is usually quite a challenge for iterative algorithms that attempt linear corrections for each iteration. If indeed this implication is correct, then a more sophisticated approach for neighboring feedback control is required.

SECTION V

CONCLUSIONS AND RECOMMENDATIONS FOR FURTHER STUDY

V.1. Transfers with Small Numbers of Burns

It has been found that methods already present in the literature are capable of computing fuel-optimal orbit transfers with small numbers of burns. The methods investigated here were multiple-point shooting and modified shooting. However, a common way to attempt to increase the performance of a transfer is to increase the number of burns executed and, unfortunately, these methods are not very robust in that sense.

A new method has been introduced that is very useful for adding burns to fuel-optimal orbit transfers. The method is used in conjunction with homotopy and an iterative technique for computing transfers; the iterative technique must incorporate knowledge of the Lagrange multipliers. The method does require that the initial point, the final point, and the transfer time be free for optimization. It also assumes that the transfer is performed under the influence of ideal gravity. This assumption is required to obtain the switching function property that the method relies on.

It is recommended that this method be further developed such that orbit perturbations are taken into account. Since the switching function property in question no longer applies for this case, the task is challenging. Obviously, a fairly different approach must be taken. It is likely that requiring trajectories to begin and end with coast arcs will be necessary, since cost arcs will no longer be orbits. Perhaps then some conditions may be identified under which the coast arcs could be extended to find optimal locations for the burns to be added.

V.3. Transfers with Large Numbers of Burns

The results of this research point to the Modified Patched Method as a practical way to compute fuel-optimal transfers with large numbers of burns. It does not appear that such a method existed previously in the literature, making MPM and theoretical results behind it the central contributions of this report.

An interesting spin-off of the theoretical development is a new formulation for the integration of the Lagrange multipliers over a time-optimal coast arc for the nonplanar case assuming ideal gravity. The formulation results from satisfaction of Lemma III.2. This particular formulation proved quite useful for MPM and may prove useful in future algorithms and future theoretical developments.

MPM does not allow for orbit perturbations. This restriction was a small price to pay for performance previously unobtained, *viz.* the ability to compute transfers with upwards of 27-burns and large inclination changes. Now that this performance has been obtained for the ideal gravity case, it is suggested that a future research effort should be able to produce a method with similar performance, or better, while taking orbit perturbations into account.

If an attempt is made to adapt MPM for orbit perturbations without recovering any properties lost, then MPM will degenerate into multiple-point shooting. This study has already concluded that multiple-point shooting does not perform well for large numbers of burns; therefore, some recovery of the properties from Theorem III.1 and/or Theorem III.2 must be made. Since the concept central to both the Patched Method and

MPM is the relationship of the optimal orbit transfer problem with the problem expressed by (3.1), it seems reasonable to expect some form of (3.1) to be recovered in the presence of orbit perturbations.

V.2. Multiple-Burn Guidance

A suboptimal multiple-burn guidance scheme was developed through this research and its performance investigated. The scheme may be described as "burn-by-burn" neighboring optimal feedback guidance with a time-to-go indexing scheme for each burn. The performance of this guidance scheme did not match expectations.

Since guidance has much practical importance, it is suggested that future research attempt to develop an improved guidance scheme. It is likely that this would involve techniques to improve neighboring optimal feedback or replacing this with some other one-burn guidance scheme. On the other hand, a future research effort might attempt to find an optimal guidance algorithm for the multiple-burn transfer as a whole. Since there is a strong relationship between the sufficient conditions for optimality and the computation of neighboring optimal feedback gains for the one-burn problem, a similar relationship might be expected for the multiple-burn problem. If an optimal multiple-burn guidance scheme is developed, it will likely lead to the development of sufficient conditions for the optimality of multiple-burn transfers.

Appendix

ORBPACK Users Manual

A Package of FORTRAN Programs to Construct Guesses and Solve Low- and Medium- Thrust Optimal Orbit Transfer Problems

Applied Control Laboratory
Georgia Institute of Technology

Table of Contents

I. Introduction

ORBPACK is a collection of FORTRAN 77 programs for computing optimal orbit transfers. For the most part, these are all indirect methods; they are concerned with solving the Two Point Boundary Value Problem provided by optimal control theory.

None of these routines guarantee a globally optimum solution; only extremal solutions are claimed by convergence of iterations. With the exception of MBCM, solutions obtained with these methods must have their switching law checked. One must be sure that, in the computed solution, the thrust is on when the switching function is positive and the thrust is off when the switching function is negative. Furthermore, these methods assume that no intermediate thrust arcs will be found in the solution.

The charts below summarizes the programs in ORBPACK:

Solvers

Name	Method	Libraries	Suggested Use
BND3D	Multiple Shooting (BNDSCO)	BNDSCO	medium/low thrust; few burns
MBCM3D	Shooting w/ Minimizing Boundary Condition Method	VF02AD	medium/low thrust; few burns
PAT2D	Patched Method	BNDSCO; IMSL	medium/low thrust
MPMM2D, MPMM3D	Modified Patched Method	IMSL; ODEPACK	medium/low thrust; short burns

Accessories

Name	Use	Libraries
GSHOOT	random shooting for one-burn guesses	IMSL; ODEPACK
MPM2D3D	convert MPMM2D files to MPMM3D files	N/A
MP2BND	convert MPMM3D files to BND3D files	ODEPACK
BND2MBCM	convert BND3D files to MBCM files	N/A

All codes as supplied in ORBPACK solve multiple burn orbit transfers with free final time and free initial and final points. BND3D is already configured so to switch between free and fixed final time problems. MBCM3D can easily be reconfigured for such. PAT2D, MPMM2D, and MPMM3D have fixed configurations.

PAT2D, MPMM2D, and MPMM3D are also fixed to solve only problems where ideal gravity is assumed. BND3D and MBCM3D are configured to solve problems that include drag and oblateness effects. Finally, codes with the "2D" suffix are configured to solve planar transfers; the "3D" suffix indicates that the code is configured for nonplanar transfers.

II. Orbit Transfer Problem Definition

II.1. Parameters

All the programs in ORBPACK require the following orbit transfer parameters to be determined:

For the gravitating body:
- the gravitational constant for the central body (μ)

For the rocket motor:
- maximum thrust
- specific impulse (I_{sp})

For the terminal orbits, BND3D and MBCM3D require:
- semimajor axis
- eccentricity
- right ascension (degrees)
- argument of perigee (degrees)
- inclination (degrees)

For the terminal orbits, MPMM2D, MPMM3D, and PAT2D require:
- angular momentum vector (X, Y, Z components)
- eccentricity vector (X, Y components)

Each program also requires a value for Earth's acceleration at sea-level (g_o) in appropriate units; this number is only used in conjunction with the specific impulse to compute the fuel consumption.

BND3D and MBCM3D can account for oblateness and drag effects. For oblateness: R_e is the equatorial radius of the central body and J_2 is a constant describing the mass distribution of the central body; for Earth J_2=1082.61x10^{-6}. For drag: β is a constant from the atmosphere model describing air density variation in the prescribed altitude region, ρ_o is the atmosphere density at the altitude r_o, S is the cross-sectional area of the craft, and C_D is the craft's drag coefficient.

The gravitational potential, including oblateness, is modeled as:

$$U = \frac{\mu m}{r} + \frac{1}{2} J_2 R_e^2 \frac{\mu m}{r^3}\left(1 - 3cos^2(\theta)\right)$$

where r is the magnitude of the position vector **r**. The drag force is modeled as:

$$\mathbf{F}_{drag} = \frac{1}{2}\rho_o e^{-\beta(r-r_o)} S C_D v\mathbf{v}$$

where v is the magnitude of the velocity **v**. Note that this form for the density variation indicates an isothermal region of the atmosphere.

II.2. Scaling

It is very useful for numerical methods to work with numbers that are at or near the same order. This can be accomplished through nondimensionalizations. Such nondimensionalizations for the orbit transfer problem follow:

$$\hat{\mathbf{r}} \equiv \mathbf{r}/r^{\star}$$

$$\hat{m} \equiv m/m^{\star}$$

$$\hat{t} \equiv t/\sqrt{r^{\star 3}/\mu}$$

and they require the following:

$$\hat{\mathbf{v}} \equiv \mathbf{v}/\sqrt{\mu/r^{\star}}$$

$$\hat{t}_f \equiv t_f/\sqrt{r^{\star 3}/\mu}$$

$$\hat{r}_o \equiv r_o/r^{\star}$$

$$\left(\hat{\rho}_o \hat{S}\hat{C}_D\right) \equiv \rho_o S C_D\left(r^{\star}/m^{\star}\right)$$

$$\hat{T} \equiv \left(T/m^{\star}\right)/\left(\mu/r^{\star 2}\right)$$

$$\hat{\beta} \equiv \beta r^{\star}$$

$$\left(\hat{g}_o \hat{I}_{sp}\right) \equiv g_o I_{sp}\sqrt{r^{\star}/\mu}$$

$$\hat{R}_e \equiv R_e/r^{\star}$$

Note that these nondimensionalizations result in dynamics with μ=1. The choices of $r^{\star}$ and $m^{\star}$ are completely arbitrary. A choice for $m^{\star}$ might be one such that the initial nondimensionalized mass is 1 or 10. A choice for $r^{\star}$ might be the radius of the planet or a number such that the initial semimajor axis, radius of perigee , or an "average" radius is 1.

III. Making Guesses for the Optimal Transfer

There are many different ways that one could conceive of to make guesses. The routines for making guesses, listed below, have been provided.

The tutorials in Chapter VIII demonstrate how to make guesses with these methods.

III.1. *GSHOOT* Random Guess (Single Burn Only)

The subroutine GSHOOT will randomly make guesses for the one-burn orbit transfer problem in two dimensions. Input for GSHOOT is a text file. Its output consists of two text files which represent data for direct and indirect methods.

How to use *GSHOOT*

GSHOOT requires a file, named "GINPUT," for input. A typical "GINPUT" file follows:

```
MU     = 1.00
GO     = 1.00
ISP    = 0.5673
THRUST = 0.5166
MO     = 10.0000
AO     = 1.00000
EO     = 0.000
WO     = 0.000
AF     = 1.285
EF     = 0.219
WF     = 0.000
TMAX   = 0.000
NGS    = 100
NIX    = 3
```

where MU (μ) is the gravitational constant, GO (g_o) is the gravitational acceleration of the earth at sea level, ISP (I_{sp}) is the motor's specific impulse, and Thrust is the motor's thrust level. MO (m_o) is the initial mass for the transfer. The next parameters specify the terminal orbits: AO (a_o) is the initial orbit's semimajor axis, EO (e_o) the initial orbit's eccentricity, and WO (ω_o) is the initial orbit's argument of perigee; AF (a_f), EF (e_f), and (ω_f) are the corresponding parameters for the final orbit. TMAX is the maximum burn time; if it is set to zero, then TMAX is assigned by GSHOOT to the amount of time required for the mass to vanish. NGS is how many guesses to make; half of these will be almost tangential thrusting with random initial true anomaly and the other half will have random initial direction and random initial true anomaly. For a detailed description of the file format, see Appendix A.

GSHOOT will create output files "DIRECT.DAT" and "INDIRECT.DAT" which can be used to construct a multiple burn guess in the PATCH2D file format. Both of these files have identical headers:

```
T      = .
GO     = .
ISP    = .
AO     = .
EXO    = .
EYO    = .
AF     = .
EXF    = .
EYF    = .
```

These output files contain the necessary information

If this output file represents a guess for any but the last burn, delete the last three of these lines (AF, EXF, EYF) when constructing the multiple-burn guess file. However, if this guess is for the last burn, keep the last three lines and delete lines six through eight (AO, EXO, EYO). If the guess is any but the first burn, then delete the first three lines (T, GO, ISP).

How *GSHOOT* works

GSHOOT makes a random guess by choosing the constant Lagrange multipliers (v) as a random vector with unity magnitude. Since all the Lagrange multipliers may be scaled by an arbitrary constant, there is no loss of generality. The state vector is computed knowing the initial orbital elements and randomly choosing the initial true anomaly. Next, the vectors λ_r and λ_v are calculated for the initial time, using the following equation:

$$\begin{bmatrix} \lambda_r(t_o) \\ \lambda_v(t_o) \end{bmatrix} = \left[\frac{\partial \psi}{\partial \mathbf{x}}(\mathbf{x}(t_o)) \right]^T \mathbf{v} \qquad (3.1)$$

The initial value for λ_m is found by specifying that the switching function is zero at the initial time:

$$\lambda_m(t_o) = (g_o I_{sp}) \frac{|\lambda_v(t_o)|}{m(t_o)} \qquad (3.2)$$

That the switching function is zero at the initial time is known to be true for the free transfer time and free terminal points problem. With the initial state and costate known, the initial value problem is integrated forward in time until either the desired final semimajor axis (AD) is reached, the current radius becomes small, the spacecraft enters a parabolic orbit, or the mass becomes small.

For guesses that are almost tangential, λ_v is chosen to be (+/-) **v** and λ_r is chosen to be (+/-) $(\mu/r^3)\mathbf{r}$. The positive sign usually produces orbit raising and the negative sign orbit lowering. Note that this initial guess for the costates zeros the Hamiltonian when the switching function is zero. Therefore, the v_i's can be found by solving the least-squares problem of Eq. (3.1).

GSHOOT will try as many guesses as the user requests. The guess that best meets the required boundary conditions will be output.

III.2. PAT2D Sub-Optimal Transfer Guess (Multiple Burn Only)

PAT2D creates sub-optimal trajectories in the sense that the choice of intermediate transfer orbits has been fixed and each burn is an optimal one-burn orbit transfer. PAT2D iterates upon the choice of intermediate transfer orbits until it finds a choice that gives a local maximum in final mass The PAT2D program is described in detail in Chapter V.

Using PAT2D to Compute Guesses

PAT2D requires two files for input. The first file, "PATCH2D.TOLS," sets accuracy levels and limits the number of iterations (for more information on this file, see Chapter V). The second file, "PATCH2D.GUESS," supplies the guess information for both the choice of intermediate transfer orbits and the trajectories of the burn arcs between them. This latter file must be in the PAT2D format (for more information, see Appendix A and Chapter V).

The guess information from GSHOOT, or some other source, must be put into the PAT2D format. When run, the first thing that PAT2D will do is solve the one-burn problems defined by the intermediate transfer orbits. Often, the output from this step alone is a sufficiently good solution guess . This output is contained in the file "PATCH2D.INITIAL."

On the other hand, it is not uncommon for that output to be an insufficient guess. In this case, one approach is to allow PAT2D to iterate. At some point during the iteration, the user may take the file "PATCH2D.BEST" and use it as an initial solution guess. Alternatively, the user may set a rather loose stopping criterion for PAT2D and wait until this criterion is met. In this approach, the file "PATCH2D.SOL" will be the solution guess.

IV. The Modified Patched Method (MPMM2D, MPMM3D)

The subroutine MPM2D (MPM3D) is a realization of the Modified Patched Method in two (three) dimensions. The file "MPMM2D.f" (MPMM3D.f) contains an implementation of MPM2D (MPM3D) using IMSL's NEQNF to solve the nonlinear equations, its FORTRAN program name is MPMM2D (MPMM3D).

IV.1. Using MPMM2D to Compute Solutions

MPMM2D (MPMM3D) requires only one input file, which must follow the PAT2D (PAT3D) format (see Appendix A). This data file must be named "MPM2D.GUESS" ("MPM3D.GUESS")

The code "MPM2D3D.f" will convert an "MPM2D.GUESS" file into a "MPM3D.GUESS" file. In this code, no other input is required except "MPM2D.GUESS"

Data File (Input)

In "MPM2D.GUESS," ("MPM3D.GUESS") the tolerance setting (TOL) is the root-finding tolerance. The tolerance used in numerical integration is one-thousandth of this number. No information in the header is ignored.

For MPMM2D (MPMM3D), the option SEL may only be chosen as 1 or 2. These options indicate the data for the burn is given in the format for an indirect method. MPMM2D (MPMM3D) will treat both SEL=1 and SEL=2 identically.

MPMM2D (MPMM3D) only uses specific items from the PAT2D file format. The lines below are representative of the data for one burn in the PAT2D format. The underlined "#" symbols indicate which number items are important to MPM2D calculations.

MPMM2D

```
a    = #
ex   = #
ey   = #
NODE =  3
SEL  =  1
index,x,y,u,v,m,lx,ly,lu,lv,lm,tf,g1,g2,g3,g4,g5,g6
  1, #, #, #, #, #, #, #, #, #, #, #, #, #, #, #, #, #.
  2, #, #, #, #, #, #, #, #, #, #, #, #, #, #, #, #, #,
  3, #, #, #, #, #, #, #, #, #, #, #, #, #, #, #, #, #,
  4, #, #, #, #, #, #, #, #, #, #, #, #, #, #, #, #, #,
```

MPMM3D

```
hx   = #
hy   = #
hz   = #
ex   = #
ey   = #
NODE =  3
SEL  =  1
INDEX,X,Y,Z,U,V,W,M,LX,LY,LZ,LU,LV,LW,LM,TF,G1,G2,G3,G4,G5,G6,G7,G8,G9,G10
  1, #, #, #, #, #, #, #, #, #, #, #, #, #, #, #, #, #, #, #, #, #, #,
  2, #, #, #, #, #, #, #, #, #, #, #, #, #, #, #, #, #, #, #, #, #, #, #, #, #
  3, #, #, #, #, #, #, #, #, #, #, #, #, #, #, #, #, #, #, #, #, #, #, #, #, #
  4, #, #, #, #, #, #, #, #, #, #, #, #, #, #, #, #, #, #, #, #, #, #, #, #, #.
```

The important number items are "a," "ex," and "ey" with "x," "y," "m," "tf," "g4," "g5," and "g6" on the first line only. All other numbers are read by the program but not used. The "x" and "y" coordinates are used only to compute the true anomaly angle that the burn begins at. The only mass value remembered is the initial mass value. The mass costate is used to scale the constant Lagrange multipliers "g4," "g5," and "g6" in a manner consistent with patching the burns together; otherwise, it is not used.

MPM2D Iteration Info to Screen

Listed below is sample screen output from "MPMM2D.F"

```
 Cur. Norm      It#    Best Norm (at) #    Short Time    Bn#   Bst Wrst El.   El#
------------   -----  ------------ -----  ------------  -----  ------------  -----
0.45051E+00       1   0.45051E+00      1  0.11289E+01       4  0.30952E+00     18
0.45051E+00      45   0.45051E+00     15  0.11289E+01       4  0.30952E+00     18
0.63552E-02      90   0.63550E-02     89  0.10551E+01       4  0.28471E-02     14
0.48575E-02     135   0.48575E-02    105  0.10606E+01       4  0.24346E-02     14
---------
Required # Function Evals = 172
------------------------------
 Total Burn Time = 6.514028424486
 Final Mass = 4.066434637841
 Shortest Burn Length = 1.128883878329
 Shortest Burn is #4
 ------------------------------
```

The first block of text is the *iteration table*. The column "Cur. Norm" shows the current 2-norm of the constraint errors in the absolute sense. The iteration, or number of times called, at which this value was computed is listed in column "It#." The lowest norm of constraint errors yet computed, next to the iteration number it was computed at is given under the "Best Norm (at) #" column. The length of the shortest burn at the current iteration is under "Short Time" and the burn with this length is indicated under the "Bn#" column. Finally, the largest absolute value of a constraint component for the best norm is listed under "Bst Wrst El." with "El#" listing which constraint component this is.

MPM3D Iteration Info to Screen

The iteration table from MPM3D is slightly different. It has the following header:

```
 CUR. NORM      IT#    BEST NORM (AT) #    WRST C. EL.   EL#   BST WRST EL.  EL#
------------   -----  ------------ -----  ------------  -----  ------------  -----
```

where "WRST C. EL." indicates the worst element of the current iteration constraint error vector.

For MPMM2D and MPMM3D, below the iteration table is the number of function calls required to reach an error level indicated by the tolerance. After this, some statistics of the solution are given. The "Total Burn Time" is the total amount of time the motor is on. The "Final Mass" is the mass of the spacecraft at the end of the transfer. The "Shortest Burn Length" is length in time of the quickest burn. Finally, the burn number for this quickest, or shortest, burn is listed.

Data File Output

The subroutine MPM2D (MPM3D), if desired, creates an output file that gives the status of iterations. The file is named "MPM2D.ISTAT" ("MPM3D.ISTAT"). This file is useful for computer systems that operate under a queuing system because such a system often does not show output to the screen until after execution is completed. However, such queuing systems usually allow files that are created and closed to appear in the users directory. Therefore, during execution under a queuing system, the user may list the contents of "MPM2D.ISTAT" ("MPM3D.ISTAT") and see current iteration information. The content of "MPM2D.ISTAT" ("MPM3D.ISTAT") is three lines long: the first two lines are the table headings from the iteration table, the third line is the current entry in the iteration table.

Both the main routine MPMM2D (MPMM3D) and MPM2D (MPM3D) contribute to a file named "MPM2D.REPORT" ("MPM3D.REPORT"). The first lines in this file gives feedback from MPMM2D (MPMM3D) while reading "MPM2D.GUESS" ("MPM3D.GUESS") so that any errors in that file may be easily identified.

The first eleven lines give the header parameters. At the beginning of each line, the text from "MPM2D.GUESS" ("MPM3D.GUESS") is given, then the number read from that line, and finally, in parentheses, the name of the variable which MPMM2D (MPMM3D) has assigned this number to. This same pattern is continued as MPMM2D (MPMM3D) reads the orbital elements of the transfer orbits.

The twelfth line and lines below are printed as each line of the input are read. Following this is a listing of the values of each variable used by MPM2D (MPM3D) for the first iteration; then a listing of the constraint values when given these variables.

Next is the iteration table as printed to the screen. Following this, a total number of calls to MPM2D (MPM3D). Then a listing of variables and constraint evaluations for the solution. Finally, at the bottom of the file is the solution summary statistics just as printed to the screen.

The other file created by MPMM2D (MPMM3D) is "MPM2D.SOL" ("MPM3D.SOL"), the solution file. This file contains the solution to the orbit transfer problem in the PAT2D (PAT3D) format.

IV.2. The Structure of the MPMM2D (MPMM3D) Code

The structure of the MPMM2D (MPMM3D) program is generalized in the following diagram, not intended as a formal flow chart:

MPMM2D/MPMM3D Diagram

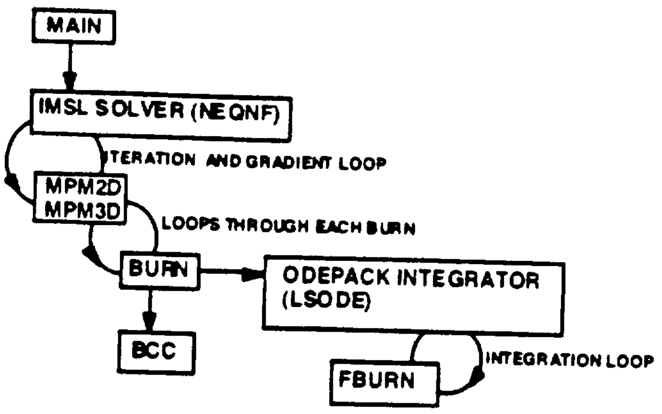

The main routine, calls the multidimensional nonlinear equation solver, IMSL's NEQNF, with the guess from "MPM2D.GUESS" ("MPM3D.GUESS") The solver calls MPM2D (MPM3D) iteratively to solve the problem and to numerically compute partial derivatives. This recurrent use of MPM2D (MPM3D) is illustrated in the diagram by a loop with an arrow on it, connecting the two blocks.

MPM2D (MPM3D) evaluates the MPM conditions given the variables. For each burn in the orbit transfer problem, variables are sent to BURN. This subroutine integrates each burn arc by calling LSODE and evaluates boundary conditions for that burn by calling BCC (BCC). The derivatives for integration, required for LSODE, are supplied by FBURN. FBURN is called repeatedly by LSODE during solution of each burn's initial value problem.

V. The Patched Method in Two Dimensions (PAT2D)

The subroutine FUNC is a realization of the Patched Method in two dimensions. The file "PAT2D.f" contains an implementation of FUNC with the conjugate gradient method. The conjugate gradient algorithm was taken from "Numerical Recipes" and is only slightly modified from what is presented there.

V.1. Using PAT2D to Compute Sub-Optimal/Extremal Solutions

PAT2D requires two input files for execution. These files specify iteration parameters ("PATCH2D.TOLS") and the initial solution guess ("PATCH2D.GUESS"). The "PATCH2D.GUESS" file must be in the PAT2D format (see Appendix A). The format for "PATCH2D.TOLS" is much simpler and demonstrated in the example below:

```
FTOL = 1.00000000000000000000E-08
LTOL = 1.00000000000000000000E-07
GTOL = 1.00000000000000000000E-03
TOL2 = 1.00000000000000000000E-05
ITMX = 200
MFUN = 200
MITN = 1000
ITMB = 15
```

The FORMAT edit descriptors for the first four lines, containing REAL values, are (1X,A6,D27.20) and likewise for the last four lines, containing INTEGER values, (1X,A6,I6). The value for FTOL specifies the function value stopping criterion, when the change in total burn time after a line search is less than FTOL the iteration stops. The value for LTOL is the line search tolerance. GTOL specifies how small the 2-norm of the gradient should be fore stopping. TOL2 is the tolerance for DCNLP one-burn solutions. ITMX is the maximum number of allowed conjugate gradient iterations. MFUN limits function calls and MITN limits the overall iteration count for DCNLP. ITNB limits the number of multiple-shooting iterations performed by BOUNDSCO.

V.2. How PAT2D Works

The diagram below shows the general structure of the code in the file "PAT2D.f."

PAT2D Diagram

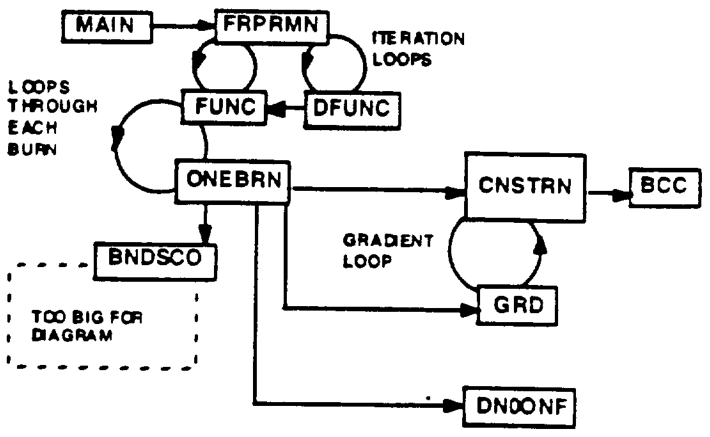

The subroutine FUNC is the heart of PAT2D. This is the function that, given the choice of intermediate orbital elements, calculates the total burn time for the transfer. FRPRMN is the conjugate gradient routine, from "Numerical Recipes," that iteratively calls FUNC and DFUNC (gradient routine) to find the optimal choice of intermediate transfer orbits.

PAT2D has a two-loop structure; there is an inner loop (FUNC/ONEBRN) and an outer loop (FRPRMN). The outer loop successively changes the transfer orbits until a minimum is found in the total burn time (maximum of final mass). The inner loop solves the one burn trajectories between each transfer orbit. Solving this trajectories yields the burn time s for each intermediate transfer. These burn times are summed, giving the output of FUNC.

Note that each successful outer loop iteration produces a suboptimal transfer. This transfer satisfies all the conditions on the state but is not an extremal transfer.

The main routine loads the solution guess and calls FUNC once, before FRPRMN does. This is done because there is no assurance that the trajectory guesses in the PATCH2D.GUESS file will successfully produce a suboptimal solution. The output from this first call is named "PATCH2D.INITIAL" and is often a good guess for MPMM2D. However, if this is a poor guess, then a good strategy is to allow PAT2D several iterations to produce a transfer closer to the solution.

The inner loop iterations are a little complicated. This is the result of an attempt to make them robust. It is also designed so that each successful inner loop iteration produces a solution to the Two Point Boundary Value Problem (TPBVP) with BOUNDSCO, a multiple-point shooting algorithm (MS). However, it is widely known that direct methods often have a large region of convergence than indirect methods. Therefore, Direct Collocation with Nonlinear Programming (DCNLP) has also been implemented.

The following diagram shows how the ONEBRN subroutine interprets the user's selection as to what is the appropriate first action, use MS or DCNLP first?

ONEBRN Flow Chart part 1 (abridged)

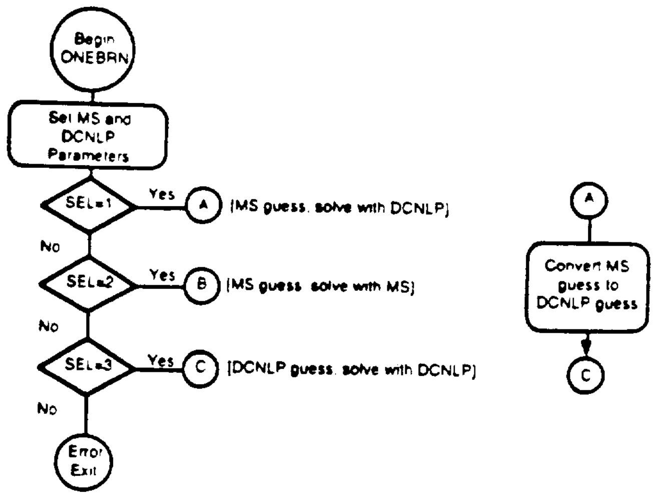
Begin ONEBRN
Set MS and DCNLP Parameters
SEL=1
Yes
A
(MS guess, solve with DCNLP)
No
SEL=2
Yes
B
(MS guess, solve with MS)
No
SEL=3
Yes
C
(DCNLP guess, solve with DCNLP)
No
Error Exit
A
Convert MS guess to DCNLP guess
C

Note that a MS guess can be given for DCNLP in this structure. A DCNLP guess cannot be given for MS because a DCNLP *solution* is required in the conversion process from DCNLP information to MS information.

The next diagrams shows how MS (BNDSCO) and DCNLP (IMSL's DN0ONF) are incorporated:

ONEBRN Flow Chart part 2 (abridged)

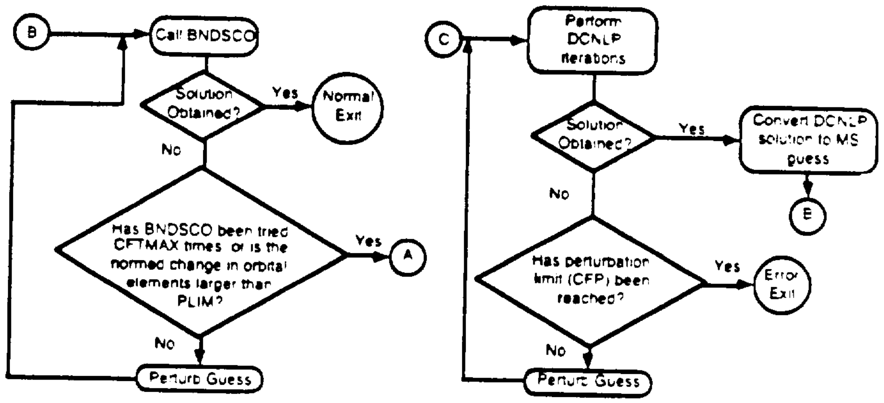
B
Call BNDSCO
Solution Obtained?
Yes
Normal Exit
No
Has BNDSCO been tried CFTMAX times or is the normed change in orbital elements larger than PLIM?
Yes
A
No
Perturb Guess
C
Perform DCNLP iterations
Solution Obtained?
Yes
Convert DCNLP solution to MS guess
E
No
Has perturbation limit (CFP) been reached?
Yes
Error Exit
No
Perturb Guess

Attempts with either method have a similar structure. If a failure in iterations occurs, the guess is perturbed and the method attempted again. After each failure, the perturbation size is increased. If MS fails too many times, control is handed over to DCNLP. However, if DCNLP fails too many times there is no backup and an error exit occurs.

After ONEBRN succeeds in computing a MS solution, the SEL parameter is set to 2 for that burn.

Output files:

- "PATCH2D.HIST" (iteration data)
- "PATCH2D.INITIAL" (first suboptimal sol) first optimal solution obtained, in patch2d format
- "PATCH2D.SOL" contains the extremal solution obtained to tolerance
- "PATCH2D.BURN" (iteration status) prints iteration status; file is useful when program is being run under a queuing system and screen output is withheld. Printed after a burn is solved.
- "PATCH2D.COST" (iteration status); file is useful when program is being run under a queuing sys and screen output is withheld. Printed after a complete transfer is solved.
- "PATCH2D.CURRENT" contains current suboptimal trajectory, unless it is the best.
- "PATCH2D.BEST" contains best suboptimal trajectory to date
- "PATCH2D.PERT" gives information as to the progress of solving the current burn.
- "FRPRMN.OUT" output from conjugate gradient routine, FRPRMN
- "FRPRMN.ITERATES" current output from FRPRMN, for info when using a queuing system

VI. The Multiple Shooting Approach (BND3D)

The BND3D program implements the modified multiple-point (MS) algorithm of BOUNDSCO (**Boundary** value problem solver with **S**witching **Co**nditions). BOUNDSCO makes use of Newton's method, a Broyden update, and Deuflhard's relaxation strategy. One should refer to the BOUNDSCO manual[1] for detailed information on BOUNDSCO. Note that BOUNDSCO does not make use of an analytical gradient.

BND3D also has a homotopy loop around BNDSCO. A homotopy variable U is defined such that, as the loop repeats, U will change from 1 to UMIN (The choice of UMIN is set by the user, but usually is chosen as 0). Certain parameters for the orbit transfer problem definition are included in the homotopy loop and vary as the value of U changes. A tutorial using homotopy is included in the Tutorials section.

The code MP2BND will convert MPMM3D input files into BND3D input files.

VI.1. Using BND3D to Compute Solutions

BND3D requires two input files: "BND3D.SCRIPT" which contains instructions and parameters, and another file (named by user) which contains the solution guess.

The format of the file "BND3D.SCRIPT" depends on how BND3D is to be used. This format is best described line-by-line. The character in the first column of each line is ignored.

The four different layouts of the "BND3D.SCRIPT" file are described below:

Normal Execution: Free Final Time, No Homotopy

- *Line 1*: (1X,A28) On this line, the name of the file containing the solution guess is specified. No more than 28 characters are allowed.
- *Line 2*: (1X,I6) Here, a "1" indicates that boundary condition errors should be displayed to the screen, in addition to the normal BNDSCO iteration output; a "0" indicates otherwise. Usually, one would place a "0" here; this output is usually only useful in finding errors in the input file.
- *Line 3*: (1X,I6) A "1" on this lines chooses the free final time option.
- *Line 4*: (1X,I6) A "0" deselects the homotopy option.
- *Line 5*: (1X,I6) A "1" on this line tells BNDSCO to insert nodes for the switching times in the output; a "0" says not to.

[1]Oberle, H.J, Grimm, W., "BNDSCO: A Program for the Numerical Solution of Optimal Control Problems," English Translation of DFVLR-Mitt. 85-05.

- *Line 6*: (A,D12.5) The value on this line sets the BNDSCO parameter FCMIN. FCMIN is the lower limit of the relaxation factor.
- *Line 7*: (A,D12.5) The value on this line sets the BNDSCO iteration tolerance.
- *Line 8*: (1X,I4) The maximum number of iterations.
- *Line 9*: (1X,A28) The name for the file containing the solution
- *Line 10*: (1X,I6) A "1" on this line requests detailed solution information ("BND3D.EXTRA" and the file named on the next line). A "0" indicates otherwise.
- *Line 11*: (1X,A28) The file name for additional information (if a "1" on the previous line).

Fixed Final Time; No Homotopy

- *Line 1*: (1X,A28) On this line, the name of the file containing the solution guess is specified. No more than 28 characters are allowed.
- *Line 2*: (1X,I6) Here, a "1" indicates that boundary condition errors should be displayed to the screen, in addition to the normal BNDSCO iteration output; a "0" indicates otherwise. Usually, one would place a "0" here; this output is usually only useful in finding errors in the input file.
- *Line 3*: (1X,I6) A "0" on this lines chooses the fixed final time option.
- *Line 4*: (A,D12.5) The value for the final time.
- *Line 5*: (1X,I6) A "0" deselects the homotopy option.
- *Line 6*: (1X,I6) A "1" on this line tells BNDSCO to insert nodes for the switching times in the output; a "0" says not to.
- *Line 7*: (A,D12.5) The value on this line sets the BNDSCO parameter FCMIN. FCMIN is the lower limit of the relaxation factor.
- *Line 8*: (A,D12.5) The value on this line sets the BNDSCO iteration tolerance.
- *Line 9*: (1X,I4) The maximum number of iterations.
- *Line 10*: (1X,A28) The name for the file containing the solution
- *Line 11*: (1X,I6) A "1" on this line requests detailed solution information ("BND3D.EXTRA" and the file named on the next line). A "0" indicates otherwise.
- *Line 12*: (1X,A28) The file name for additional information (if a "1" on the previous line).

Free Final Time, Homotopy Activated

- *Line 1*: (1X,A28) On this line, the name of the file containing the solution guess is specified. No more than 28 characters are allowed.
- *Line 2*: (1X,I6) Here, a "1" indicates that boundary condition errors should be displayed to the screen, in addition to the normal BNDSCO iteration output; a "0" indicates otherwise. Usually, one would place a "0" here; this output is usually only useful in finding errors in the input file.
- *Line 3*: (1X,I6) A "1" on this lines chooses the free final time option.

- *Line 4*: (1X,I6) A "1" selects the homotopy option.
- *Line 5*: (1X,I6) the suggested number of homotopy loops to perform
- *Line 6*: (*) Enter UMIN, the value of the homotopy variable to stop at. The homotopy variable, U, starts at 1 and ends at UMIN. Enter "0.0" here to attempt to achieve the values below.
- *Line 7*: (*) Enter the desired maximum thrust level
- *Line 8*: (*) Enter the desired specific impulse
- *Line 9*: (*) Enter the desired final orbit semimajor axis
- *Line 10*: (*) Enter the desired final orbit eccentricity
- *Line 11*: (*) Enter the desired final orbit argument of perigee
- *Line 12*: (*) Enter the desired initial orbit semimajor axis
- *Line 13*: (*) Enter the desired initial orbit eccentricity
- *Line 14*: (*) Enter the desired initial orbit argument of perigee
- *Line 15*: (*) Enter the desired initial orbit argument inclination
- *Line 16*: (1X,I6) A "1" on this line tells BNDSCO to insert nodes for the switching times in the output; a "0" says not to.
- *Line 17*: (A,D12.5) The value on this line sets the BNDSCO parameter FCMIN. FCMIN is the lower limit of the relaxation factor.
- *Line 18*: (A,D12.5) The value on this line sets the BNDSCO iteration tolerance.
- *Line 19*: (1X,I4) The maximum number of iterations.
- *Line 20*: (1X,A28) The name for the file containing the solution
- *Line 21*: (1X,I6) A "1" on this line requests detailed solution information ("BND3D.EXTRA" and the file named on the next line). A "0" indicates otherwise.
- *Line 22*: (1X,A28) The file name for additional information (if a "1" on the previous line).

Fixed Final Time, Homotopy Activated (in this case, the fixed final time is also achieved through the homotopy loop)

- *Line 1*: (1X,A28) On this line, the name of the file containing the solution guess is specified. No more than 28 characters are allowed.
- *Line 2*: (1X,I6) Here, a "1" indicates that boundary condition errors should be displayed to the screen, in addition to the normal BNDSCO iteration output; a "0" indicates otherwise. Usually, one would place a "0" here; this output is usually only useful in finding errors in the input file.
- *Line 3*: (1X,I6) A "0" on this lines chooses the fixed final time option.
- *Line 4*: (A,D12.5) The value for the final time.
- *Line 5*: (1X,I6) A "1" selects the homotopy option.
- *Line 6*: (1X,I6) the suggested number of homotopy loops to perform
- *Line 7*: (*) Enter UMIN, the value of the homotopy variable to stop at. The homotopy variable, U, starts at 1 and ends at UMIN. Enter "0.0" here to attempt to achieve the values below.
- *Line 8*: (*) Enter the desired maximum thrust level
- *Line 9*: (*) Enter the desired specific impulse
- *Line 10*: (*) Enter the desired final orbit semimajor axis

- *Line 11*: (*) Enter the desired final orbit eccentricity
- *Line 12*: (*) Enter the desired final orbit argument of perigee
- *Line 13*: (*) Enter the desired initial orbit semimajor axis
- *Line 14*: (*) Enter the desired initial orbit eccentricity
- *Line 15*: (*) Enter the desired initial orbit argument of perigee
- *Line 16*: (*) Enter the desired initial orbit argument inclination
- *Line 17*: (1X,I6) A "1" on this line tells BNDSCO to insert nodes for the switching times in the output; a "0" says not to.
- *Line 18*: (A,D12.5) The value on this line sets the BNDSCO parameter FCMIN. FCMIN is the lower limit of the relaxation factor.
- *Line 19*: (A,D12.5) The value on this line sets the BNDSCO iteration tolerance.
- *Line 20*: (1X,I4) The maximum number of iterations.
- *Line 21*: (1X,A28) The name for the file containing the solution
- *Line 22*: (1X,I6) A "1" on this line requests detailed solution information ("BND3D.EXTRA" and the file named on the next line). A "0" indicates otherwise.
- *Line 23*: (1X,A28) The file name for additional information (if a "1" on the previous line).

VI.2. The BND3D Guess File Format

The BND3D Guess file (named in "BND3D.SCRIPT") has a specific format. The first twenty lines specify orbit transfer parameters of type DOUBLE PRECISION and have FORMAT edit descriptors (1X,A9,F30.15). These parameters are as follows and in this order:

MU	gravitational constant of the central body (1.0 for no dimensions)
REQ	equatorial radius of the central body
J2	constant describing the mass distribution of the central body; for Earth J_2=1082.61x10^{-6}
GO	acceleration at sea-level
BETA	constant from the atmosphere model describing air density variation in the prescribed altitude region
RO	r_o, +REQ
ROU	atmosphere density at the altitude r_o,
S	cross-sectional area of the craft
CD	drag coefficient
ISP	specific impulse
THRUST	maximum thrust
AI	initial semimajor axis
EI	initial eccentricity
OMEGAI	initial argument of perigee (degrees)
RAI	initial right ascension (degrees)
I-I	initial inclination (degrees)
AF	final semimajor axis
EF	final eccentricity
OMEGAF	final argument of perigee (degrees)
RAF	final right ascension (degrees)
I-F	final inclination (degrees)

The 21st line (1X,I5) gives the number of intervals (# nodes - 1). The next line is a dummy string line (1X,A) that, on output, is used to provide a header for the data in the following lines (useful in plotting results).
The next (# nodes) lines gives the BND3D state at each node with edit descriptors (1X,F30.15,25(A2,F30.15)). The BND3D state is as follows:

```
 0  1  2  3  4  5  6  7   8    9    10   11   12   13   14   15
(T, X, Y, Z, U, V, W, M, L-X, L-Y, L-Z, L-U, L-V, L-W, L-M, TF,

 ( FINAL ORBIT    ) ( INITIAL ORBIT  )
 16  17  18  19  20  21  22  23  24  25
 G1, G2, G3, G4, G5, G6, G7, G8, G9, G10)

   <X,Y,Z> IS POSITION                 <L-X,L-Y,L-Z> IS LAMBDA-R
   <U,V,W> IS VELOCITY                 <L-U,L-V,L-W> IS LAMBDA-V
   M IS MASS
   L-M IS LAMBDA-M
   T IS THE NORMALIZED TIME [0,1]
```

Where TF is the final time and G# are components of the constant Lagrange multipliers (ν); G1-G5 being ν for the final boundary conditions and G6-G10 being ν for the initial boundary conditions.

The nodes are entered in the reverse order, starting with the final node and ending with the initial node.

Following the node information is a line (1X,I5) for the number of switching points. It is suggested to use an even number of switching points - this indicates to BNDSCO that the first and last intervals are burn arcs.

The next lines (1X,F30.15), one for each switching point, give the switching times in normalized time [0,1]. No lines after these are read.

VI.3. How BND3D Works

BND3D supplies the necessary routines (F and CON) to BNDSCO. "F" supplies the derivatives of the state and "CON" evaluates the boundary conditions. The routine "BCC" computes repeated formulas, "LSG" loads the solution guess, "SAVSOL" saves solution data in the same format as the guess data. The routine "DIFSYB" performs numerical integration.

The flow diagram below indicates the interdependence of the BND3D subroutines.

BND3D Flow Diagram

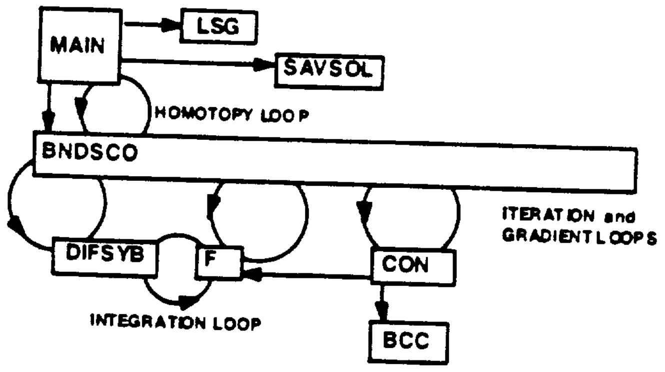

VII. The Minimizing Boundary Condition Method (MBCM3D)

The Minimizing Boundary Condition Method (MBCM) is a relaxed simple shooting algorithm. Instead of using a multidimensional nonlinear equation solver for the two point boundary value problem (TPBVP), it transforms the TPBVP into a nonlinear programming (NLP) problem.

As included in ORBPACK, MBCM3D uses the square of the Hamiltonian as the NLP cost function. All other boundary conditions are taken as NLP constraints.

VII.1. Using MBCM3D to Compute Solutions

MBCM3D requires one input file, MBCM3D.GUESS. This file has a very specific format. The first 47 lines of this file have the FORMAT edit descriptors (1X,A9,E30.15). They describe, in the following order:

MU	gravitational constant of the central body (1.0 for no dimensions)
REQ	equatorial radius of the central body
J2	constant describing the mass distribution of the central body; for Earth J_2=1082.61x10^{-6}
GO	acceleration at sea-level
BETA	constant from the atmosphere model describing air density variation in the prescribed altitude region
RO	r_o, +REQ
ROU	atmosphere density at the altitude r_o,
S	cross-sectional area of the craft
CD	drag coefficient
ISP	specific impulse
THRUST	maximum thrust
AI	initial semimajor axis
EI	initial eccentricity
OMEGAI	initial argument of perigee (degrees)
RAI	initial right ascension (degrees)
I-I	initial inclination (degrees)
AF	final semimajor axis
EF	final eccentricity
OMEGAF	final argument of perigee (degrees)
RAF	final right ascension (degrees)
I-F	final inclination (degrees)
[the next 14 lines give the initial state]	
TF	transfer time
[the next 10 lines give G1-G10]	
ACC	solution tolerance

Where G# are components of the constant Lagrange multipliers (v); G1-G5 being v for the final boundary conditions and G6-G10 being v for the initial boundary conditions.

The last line of "MBCM3D.GUESS" (1X,A9,I10) gives the maximum number of iterations.

The code "BND2MBCM.f" will convert a BND3D guess file named "BND3D.GUESS" into a MBCM3D guess file ("MBCM3D.GUESS").

VII.2. How MBCM3D Works

MBCM3D uses VF02AD to solve the NLP problem. VF02AD uses reverse communication: the main routine calls OF to compute NLP cost and constraints given input; then GRD to compute gradients; then calls VF02AD to compute the new iterates. The main routine then uses these new iterates as input for OF and repeats the loop until VF02AD signals convergence.

OF evaluates the TPBVP as a NLP. The shooting problem is integrated with RK, a Runge-Kutta integration routine. Integration of the shooting problem is interrupted often to check the sign of the switching function. If a sign change is detected, the integration interval is adjusted until the exact switching point is located. During this process, OF keeps track of the sign of the switching function and appropriately adheres to the optimal switching law. This should ensure that the switching law is followed, however, it is always prudent to check the switching law after a solution is claimed.

The flow diagram below indicates the interdependence of the MBCM3D subroutines.

MBCM3D Flow Diagram

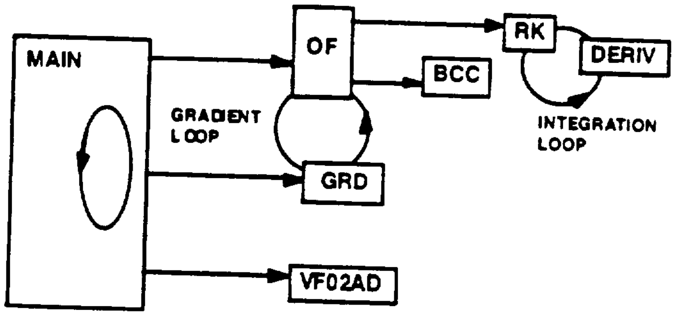

VIII. Tutorials

The following tutorials demonstrate some aspects of using ORBPACK that the user may commonly encounter.

VII.1. Planar Five Burn Transfer

This tutorial demonstrates the use of the supplied code in solving a planar transfer from a circular LEO to circular GEO. The initial radius is 6600 km, the final radius is 42241 km. The initial rocket motor thrust is 9.918 kN; its I_{sp} is 450 seconds. The initial mass is 20980 kg. A five burn solution is desired.

After nondimensionalization, these parameters are: initial mass=10, thrust=0.5166, go=1, Isp=0.5673, initial radius=1, final radius=6.4.

Based on the characteristics of these types of transfers, the following guess for the transfer orbits may seem reasonable:

a	e
1.285	0.2189
1.570	0.3584
1.856	0.4550
3.707	0.7262

All their apses are aligned and the final transfer orbit is similar to the Hohmann transfer orbit.

Use GSHOOT to Construct a Guess

The trajectory for each burn will now be guessed using GSHOOT. The "INDIRECT.DAT" files produced by GSHOOT will then be concatenated together to form an "MPM2D.guess" file. The first burn input file for GSHOOT ("GINPUT") is supplied as "Tutorials/2D 5burn/GSHOOT/burn 1/GINPUT" and listed below:

```
Mu     = 1.00
Go     = 1.00
Isp    = 0.5673
Thrust = 0.5166
Mo     = 10.0000
ac     = 1.00000
ec     = 0.000
wc     = 0.000
ad     = 1.285
ed     = 0.219
wd     = 0.000
TMAX   = 0.000
NGS    = 100
NIX    = 3
```

GSHOOT reports:

```
Best constant Lagrange multipliers (initial)
  C... 0.15245E+00  0.98820E+00  0.14581E-01
Best initial true anomaly
   vo= 0.53047E+01
Best transfer time
   tf= 0.19312E+01
Best relative errors (h,ex,ey,Hs)
  G... 0.18817E-08 -0.49820E-01  0.15555E-02  0.27599E-02
```

The resulting file has been supplied as "Tutorials/2D 5burn/GSHOOT/burn 1/INDIRECT.DAT" The second burn "GINPUT" is ["Tutorials/2D 5burn/GSHOOT/burn 2/"]:

```
Mu     = 1.00
Go     = 1.00
Isp    = 0.5673
Thrust = 0.5166
Mo     = 10.0000
ao     = 1.285
ec     = 0.219
wo     = 0.000
ad     = 1.570
ed     = 0.3584
wd     = 0.000
TMAX   = 0.000
NGS    = 100
NIX    = 3
```

GSHOOT reports:

```
Best constant Lagrange multipliers (initial)
  C... 0.70359E+00  0.17901E+00 -0.24402E-14
Best initial true anomaly
   vo= 0.56451E+01
Best transfer time
   tf= 0.11458E-01
Best relative errors (h,ex,ey,Hs)
  G... 0.10846E-07 -0.82845E-02 -0.16307E-02  0.32135E-03
```

The resulting file has been supplied as "Tutorials/2D 5burn/GSHOOT/burn 2/INDIRECT.DAT" The third burn "" is ["Tutorials/2D 5burn/GSHOOT/burn 3/"]:

```
Mu     = 1.00
Go     = 1.00
Isp    = 0.5673
Thrust = 0.5166
Mo     = 10.0000
a0     = 1.570
e0     = 0.3584
w0     = 0.000
ad     = 1.856
ed     = 0.4550
wd     = 0.000
TMAX   = 0.000
NGS    = 100
NIX    = 3
```

GSHOOT reports:

```
Best constant Lagrange multipliers (initial)
  C... 0.54451E+00  0.26192E+00 -0.10330E-14
Best initial true anomaly
   vo= 0.60064E+01
Best transfer time
   tf= 0.79429E+00
Best relative errors (h,ex,ey,Hs)
  G... 0.92974E-08  0.48454E-02  0.13288E-01 -0.35436E-02
```

The resulting file has been supplied as "Tutorials/2D 5burn/GSHOOT/burn3/" The fourth burn "" ["Tutorials/2D 5burn/GSHOOT/burn 4/"]:

```
mu     = 1.00
Go     = 1.00
Isp    = 0.5673
Thrust = 0.5166
Mo     = 10.0000
ao     = 1.856
eo     = 0.4550
wo     = 0.000
ad     = 3.707
ed     = 0.7262
wd     = 0.000
TMAX   = 0.000
NGS    = 100
NIX    = 3
```

GSHOOT reports:

```
Best constant Lagrange multipliers (initial)
  C... 0.44612E+00  0.30915E+00  0.35928E-14
Best initial true anomaly
   vo= 0.53782E+01
Best transfer time
   tf= 0.18265E+01
Best relative errors (h,ex,ey,Hs)
  G... 0.58828E-08 -0.39904E-01  0.17988E-01 -0.36813E-02
```

The resulting file has been supplied as "Tutorials/2D 5burn/GSHOOT/burn 4/" The fifth burn "" ["Tutorials/2D 5burn/GSHOOT/burn 5/"]:

```
mu      = 1.00
Go      = 1.00
Isp     = 0.5673
Thrust  = 0.5166
Mo      = 10.0000
ac      = 3.707
ec      = 0.7262
wc      = 0.000
ad      = 6.400
ed      = 0.0000
wd      = 0.000
TMAX    = 0.000
NGS     = 100
NIX     = 3
```

GSHOOT reports:

```
Best constant Lagrange multipliers (initial)
  C... 0.28015E+00 -0.71802E+00 -0.63715E+00
Best initial true anomaly
   vo= 0.30096E+01
Best transfer time
   tf= 0.32219E+01
Best relative errors (h,ex,ey,Hs)
  G... 0.26077E-11 -0.93204E-02 -0.25981E-01  0.53808E-01
```

The GSHOOT output has been supplied as "Tutorials/2D 5burn/GSHOOT/burn 5/"

The files easily concatenate. The resulting file has been supplied as "Tutorials/2D 5burn/GSHOOT/MPM2D.guess"

Attempt Computation of Solution with MPMM2D

At this point, we have a solution guess for the entire trajectory in the PATCH2D format. One option for obtaining the solution is to run MPMM2D with this input. However, one may get a iteration history like this:

<u>MPMM2D Output</u>

```
  Cur. Norm      It#    Best Norm (at) #    Short Time     Bn#   Bst Wrst El.   El#
------------ ----- ------------ -----  ------------ -----  ------------ -----
 0.68735E+01     1   0.68735E+01     1   0.79429E+00     3   0.34045E+01    43
 0.68735E+01    45   0.68735E+01    45   0.79429E+00     3   0.34045E+01    43
 0.68735E+01    90   0.68735E+01    45   0.79429E+00     3   0.34045E+01    43
BCC: Possible conflict in orbit choice
     A=-2.617712643152
     E=2.335666952254
     W=2.556150238017
     (LOCATION #1)
BCC: Possible conflict in orbit choice
     A=-2.617712643152
     E=2.335666952254
     W=2.556150238017
     (LOCATION #1)
BURN  WARNING. BCC CLAIMS AN ERROR
      IN THE INITIAL POINT CALCULATION
      W1=5.684341886080808E-14
      W2=1.858576979153
      W3=0.7387094236308
      (LOCATION #1)
BCC: Possible conflict in orbit choice
     A=4.117497825609
     E=1.458915419989
     W=-0.5075814176646
     (LOCATION #1)
     INCONSISTENT:
     A*(1e0-E**2).LT.0E0
STOP  (called by BCC )
CP: 20.155s,  Wallclock: 29.935s,  33.7% of 2-CPU Machine
HWM mem: 213617, HWM stack: 26810, Stack overflows: 0
```

Note that the current norm error started at 6.3735; though such a large error does not always induce failure of MPMM2D, it may.

If MPMM2D Fails, Use PATCH2D

In such a situation, the more robust PATCH2D is useful. Since the file format is identical, this is very convenient. PATCH2D does require one additional input file, for its inner loop tolerances. The file is called "PATCH2D.tols" and for this tutorial, it has been supplied as "Tutorials/2D 5burn/PATCH2D/PATCH2D.tols" and listed below:

```
FTOL = 1.000000000000000000000E-08
LTOL = 1.000000000000000000000E-07
GTOL = 1.000000000000000000000E-03
TOL2 = 1.000000000000000000000E-05
```

We have chosen a rather strict tolerance for "function improvement" convergence, a slightly less strict tolerance for "line search" convergence, a very loose tolerance for "gradient norm" convergence, and a rather loose convergence tolerance for DCNLP iterations.

It needs to be said that the drawback to PATCH2D is its speed. For this tutorial, PATCH2D was run. After renaming "MPM2D.GUESS" to "PATCH2D.GUESS" and running PATCH2D, we see the following iterations:

```
   Function TOL (FTOL) = 1.E-6
   Gradient TOL (GTOL) = 1.E-3
Line Search TOL (LTOL) = 1.E-7
Max # iterates (ITMAX) = 200

IT#  Cost Func     Improvement   Gradient      Criterion     Line  #eval
---- ------------ ------------ ------------ ------------ ---- ------
   0  0.66455E+01  0.00000E+00  0.47211E+02
   1  0.66455E+01  0.00000E+00  0.47211E+02  0.86837E-01   7    12
   2  0.66021E+01 -0.43418E-01  0.14439E+02  0.21908E-01   6    22
   3  0.65911E+01 -0.54372E-01  0.56984E+01  0.52307E-02   4    32
   4  0.65885E+01 -0.56988E-01  0.12130E+02  0.10740E-01   5    41
   5  0.65831E+01 -0.62358E-01  0.82250E+01  0.55562E-01   4    53
   6  0.65554E+01 -0.90139E-01  0.18580E+02  0.13395E-01   5    63
   7  0.65487E+01 -0.96836E-01  0.11992E+02  0.12299E-01   4    72
   8  0.65425E+01 -0.10299E+00  0.39034E+01  0.17844E-02   5    82
   9  0.65416E+01 -0.10388E+00  0.75207E+01  0.88954E-02   5    92
  10  0.65372E+01 -0.10833E+00  0.71069E+01  0.85286E-02   3   101
  11  0.65329E+01 -0.11259E+00  0.80968E+01  0.21341E-02   5   111
  12  0.65318E+01 -0.11366E+00  0.32664E+01  0.13259E-02   6   121
  13  0.65312E+01 -0.11432E+00  0.13498E+01  0.50050E-04   6   131
  14  0.65311E+01 -0.11435E+00  0.55807E+00  0.31056E-04   5   140
  15  0.65311E+01 -0.11436E+00  0.33032E+00  0.16464E-04   3   149
  16  0.65311E+01 -0.11437E+00  0.76877E+00  0.18621E-03   3   159
  17  0.65310E+01 -0.11446E+00  0.11374E+01  0.24299E-03   3   168
  18  0.65309E+01 -0.11458E+00  0.19365E+01  0.14953E-03   4   177
  19  0.65308E+01 -0.11466E+00  0.83243E+00  0.10038E-03   4   186
  20  0.65308E+01 -0.11471E+00  0.54440E+00  0.11258E-04   4   195
  21  0.65308E+01 -0.11471E+00  0.43573E+00  0.76724E-04   5   206
  22  0.65307E+01 -0.11475E+00  0.80416E+00  0.10644E-03   3   215
  23  0.65307E+01 -0.11481E+00  0.15569E+01  0.13474E-03   4   224
  24  0.65306E+01 -0.11487E+00  0.43370E+00  0.33032E-04   3   233
  25  0.65306E+01 -0.11489E+00  0.70424E+00  0.24930E-04   4   242
  26  0.65306E+01 -0.11490E+00  0.58308E+00  0.20997E-03   4   253
  27  0.65305E+01 -0.11501E+00  0.14167E+01  0.27205E-03   4   262
  28  0.65303E+01 -0.11514E+00  0.30933E+01  0.10666E-01   6   277
  29  0.65250E+01 -0.12046E+00  0.75971E+01  0.83111E-02   7   289
  30  0.65209E+01 -0.12463E+00  0.21314E+01  0.34787E-03   5   299
  31  0.65207E+01 -0.12481E+00  0.18041E+01  0.23515E-03   6   309
```

The PATCH2D code had been left to run overnight, about 12 hrs. It did not satisfy any convergence criterion by the 31st iteration, execution was terminated. The output file "PATCH2D.BEST" has been put into in the "Tutorial" folder as "Tutorials/2D 5burn/PATCH2D/PATCH2D.BEST"

Use PATCH2D Output for MPMM2D

Now, this file was renamed to "MPM2D.GUESS" and used for input to "MPMM2D." The iterations are listed below:

```
  CUR. NORM     IT#   BEST NORM (AT) #     SHORT TIME    BN#  BST WRST EL.  EL#
------------ ----- ------------ -----  ------------ ----- ------------ -----
0.40240E+00     1  0.40240E+00     1   0.67665E+00    3   0.31525E+00    34
0.40240E+00    45  0.40240E+00    41   0.67665E+00    3   0.31525E+00    34
0.35362E-02    90  0.35361E-02    72   0.10959E+01    3   0.19249E-02    36
0.24411E-06   135  0.35880E-10   121   0.11288E+01    4   0.30568E-10    26
0.65414E-07   180  0.30394E-10   174   0.11288E+01    4   0.24713E-10    26
0.29068E-10   225  0.29068E-10   225   0.11288E+01    4   0.23206E-10    26
0.72452E-07   270  0.29068E-10   225   0.11288E+01    4   0.23206E-10    26
0.11927E-06   315  0.26968E-10   276   0.11288E+01    4   0.21352E-10    26
0.47058E-07   360  0.22244E-10   331   0.11288E+01    4   0.16456E-10    26
0.28231E-08   405  0.20320E-10   380   0.11288E+01    4   0.15220E-10    26
0.23782E-06   450  0.15318E-10   441   0.11288E+01    4   0.10650E-10    26
0.14141E-10   495  0.13615E-10   493   0.11288E+01    4   0.99760E-11    26
0.11785E-08   540  0.13615E-10   493   0.11288E+01    4   0.99760E-11    26
0.40513E-06   585  0.13339E-10   544   0.11288E+01    4   0.92868E-11    26
0.47061E-07   630  0.11624E-10   599   0.11288E+01    4   0.76525E-11    26
0.78723E-07   675  0.98522E-11   654   0.11288E+01    4   0.60751E-11    26

*** FATAL     ERROR 3 from NEQNF.  The iteration has not made good progress.
***           The user may try a new initial guess.
```

Obviously, the solution was found; however, a shortcoming in the NEQNF solver did not allow it to claim convergence. This seems to be common among nonlinear equation solvers. An easy fix is to perturb the guess slightly. In this case, the eccentricity of the first transfer orbit was perturbed from

```
| ex    = 0.14423753690672836260E+00
```

to

```
| ex    = 0.16433753690672836260E+00
```

For this new guess, in the "Tutorial" folder as "Tutorials/2D 5burn/MPM2D.GUESS," the MPMM2D iterations are:

```
  CUR. NORM     IT#   BEST NORM (AT) #    SHORT TIME    BN#  BST WRST EL.   EL#
------------ ----- ------------ -----  ------------  ----- ------------  -----
 0.40418E+00     1  0.40418E+00     1  0.67665E+00      3  0.31525E+00     34
 0.40418E+00    45  0.40418E+00    41  0.67665E+00      3  0.31525E+00     34
 0.30687E-01    90  0.30687E-01    56  0.10688E+01      3  0.14737E-01     26
 0.46830E-07   135  0.21092E-10   122  0.11288E+01      4  0.13635E-10     35
 0.60908E-07   180  0.18042E-10   172  0.11288E+01      4  0.14477E-10     22
 0.30214E-06   225  0.17836E-10   220  0.11288E+01      4  0.14065E-10     22
---------
REQUIRED # FUNCTION EVALS = 268
-------------------------------
 TOTAL BURN TIME = 6.513750674051
 FINAL MASS = 4.068387805015
 SHORTEST BURN LENGTH = 1.128831615888
 SHORTEST BURN IS #4
-------------------------------
SOLUTION SAVED
```

The solution file is given in the "Tutorial" folder as "Tutorials/2D 5burn/MPM2D.SOL".

VII.2. Convert MPMM3D File to BND3D File, Run BND3D

This tutorial demonstrates how to use MP2BND to convert a MPMM3D file to a BND3D file.

The file "Tutorials/MPM to BND3D/MPM3D.GUESS" is a solution to an orbit transfer problem, as claimed by MPMM3D. The particular problem it solves is not relevant, but it will be clarified anyway. The header of this file follows:

```
TOL  = 0.10000000000000000000E-08
MU   = 0.10000000000000000000E+01
T    = 0.51658300000000068053E+00
Go   = 0.10000000000000000000E+01
Isp  = 0.56730999999999909278E+00
hxo  = 0.47715876030000003993E+00
hyo  = 0.00000000000000000000E+00
hzo  = 0.87881711269999840397E+00
exo  = 0.00000000000000000000E+00
eyo  = 0.00000000000000000000E+00
hxf  = 0.00000000000000000000E+00
hyf  = 0.00000000000000000000E+00
hzf  = 0.25298517739999937248E+01
exf  = 0.00000000000000000000E+00
eyf  = 0.00000000000000000000E+00
NORB =  5
```

The orbit transfer is, therefore, from LEO to GEO and circle to circle in 6 burns. Now, suppose we want to further investigate this problem with the more general BND3D code, so that oblateness and drag effects can be modeled.

Run MP2BND

The main task here is to simply run MP2BND. This code will create the file "BND3D.GUESS" which has been supplied as "Tutorials/MPM to BND3D/BND3D.GUESS."

Run BND3D to check It is prudent at this point to use BND3D to check MPMM3D's results. In this tutorial, the following "BND3D.SCRIPT" file was used:

```
BND3D.GUESS
0
1
0
0
1d-4
1d-10
100
BND3D.SOL
1
BND3D.REINT
```

which is supplied as "Tutorials/MPM to BND3D/BND3D.SCRIPT." This says the input file is "BND3D.GUESS," don't show B.C. errors to the screen, solve with free final time, don't include switching points as nodes in the output, FCMIN=1D-4, TOL=1D-10, use no more than 100 iterations, save solution as "BND3D.SOL," provide additional info and save this info in "BND3D.REINT." The output BND3D produces to the screen is listed below:

```
B.C.S ? 0
FREE FINAL TIME  1
HOMOTOPY: 0
MU=       1.000000000000000000
REQ=      0.0000000000000000000E+00
J2=       0.0000000000000000000E+00
GO=       1.000000000000000000
BETA=     0.0000000000000000000E+00
RO=       0.0000000000000000000E+00
FOU=      0.0000000000000000000E+00
S=        0.0000000000000000000E+00
CD=       0.0000000000000000000E+00
ISP=      0.5673099999999998962
THRUST=   0.5165830000000001014
AI=       1.0000000000010538792
EI=       0.0000000000000000000E+00
OMEGAI=   0.0000000000000000000E+00
RAI=      89.99999999997066880
I-I=      28.50000000009010819
AF=       6.400149998410910026
EF=       0.0000000000000000000E+00
OMEGAF=   0.0000000000000000000E+00
RAF=      0.0000000000000000000E+00
I-F=      0.0000000000000000000E+00

NOTE: ANGLES MUST BE IN DEGREES
M= 44
*N= 25



******************************************************************************
**************************************

  INITIAL DATA



  N=25      M=44      MS=10
  PRESCRIBED RELATIVE PRECISION   .10D-09
  MAXIMUM PERMITTED NUMBER OF ITERATIONS100



******************************************************************************
**************************************
  IT   ABS.ERR.   LEVEL1   LEVEL2   LEVEL3   RELAX. NEW   COND(M)   NORM M
```

```
 0   .14D-07   .11D-07   .11D-07   .76D-08          0   .38D+08   .93D+02
     .14D-07   .11D-07   .11D-07   .76D-08   .000
 1   .14D-07   .67D-07   .67D-07   .14D-07          1   .36D+06   .89D+02
     .14D-07   .67D-07   .67D-07   .14D-07   .001
 2   .14D-07   .67D-07   .67D-07   .14D-07          2   .36D+08   .89D+02
     .14D-07   .66D-07   .66D-07   .13D-07   .008
 3   .14D-07   .66D-07   .66D-07   .13D-07          3   .36D+08   .89D+02
     .11D-07   .51D-07   .51D-07   .10D-07   .121
 4 - .11D-07   .51D-07   .51D-07   .10D-07          4   .36D+08   .89D+02
     .34D-15   .44D-15   .72D-12   .43D-10  1.000
 5   .34D-15   .44D-15   .73D-12   .44D-10          5   .36D+08   .89D+02
     .26D-15   .31D-15   .28D-14   .58D-12  1.000
 6   .26D-15   .31D-15   .33D-14   .43D-12          6   .20D+09   .89D+02
     .73D-15   .21D-14   .32D-14   .77D-11  1.000
 7   .73D-15   .21D-14   .21D-14   .73D-13          0   .37D+08   .89D+02
     .43D-15   .12D-14   .12D-14   .42D-13   .236
 8   .43D-15   .12D-14   .13D-14   .50D-13          1   .47D+09   .89D+02
     .47D-16   .18D-16   .24D-16   .76D-14  1.000
 9   .47D-16   .18D-16   .19D-16   .12D-14          2   .22D+09   .89D+02
     .22D-18   .81D-18   .11D-17   .14D-15  1.000
10   .22D-18   .81D-18   .11D-17   .16D-15          3   .20D+09   .89D+02
     .75D-20   .38D-19   .14D-18   .25D-16  1.000
11   .75D-20   .38D-19   .83D-19   .15D-16          4   .47D+08   .89D+02
     .32D-21   .66D-21   .55D-20   .87D-17  1.000
12   .32D-21   .66D-21   .35D-20   .33D-17          5   .45D+08   .89D+02
     .16D-21   .55D-21   .56D-20   .61D-17  1.000
13   .16D-21   .55D-21   .79D-20   .35D-16          0   .37D+08   .89D+02
     .48D-22   .17D-21   .26D-19   .10D-16   .449
14   .48D-22   .17D-21   .26D-19   .10D-16          0   .37D+08   .89D+02
     .36D-25   .58D-24   .50D-19   .22D-17  1.000
15   .36D-25   .58D-24   .51D-19   .23D-17          0   .37D+08   .89D+02
     .36D-25   .10D-24   .66D-21   .18D-17  1.000
16   .36D-25   .10D-24   .66D-21   .98D-18          1   .42D+08   .89D+02
     .18D-25   .20D-24   .36D-19   .19D-17  1.000
     .29D-25   .28D-24   .40D-19   .56D-17   .403
     .22D-25   .27D-24   .35D-19   .52D-17   .080
     .38D-25   .26D-24   .23D-19   .11D-17   .007
     .28D-25   .50D-25   .93D-20   .68D-18   .001
17   .28D-25   .50D-25   .58D-20   .17D-17          0   .37D+08   .89D+02
     .36D-25   .70D-24   .18D-19   .96D-18   .001
18   .36D-25   .70D-24   .17D-19   .95D-18          0   .37D+08   .89D+02
     .28D-25   .95D-25   .96D-21   .33D-18   .103
19   .28D-25   .95D-25   .27D-20   .16D-18          1   .75D+07   .89D+02
*************************************************************************
**************************************



    SOLUTION OBTAINED AFTER 20     ITERATION STEPS

    SOLUTION DATA


    SWITCHING POINTS





*************************************************************************
**************************************
NAME OF FILE FOR SOLUTION DATA: ->BND3D.SOL                    <-
```

It eventually computes the solution to its own criterion, however, it is clear that BND3D has verified the MPMM3D solution.

Useful Information in BND3D.EXTRA

The information provided by BND3D.EXTRA is arguable essential. This file contains data for the switching function and Hamiltonian as functions of time. The plot below is a graphical representation of what BND3D.EXTRA provides

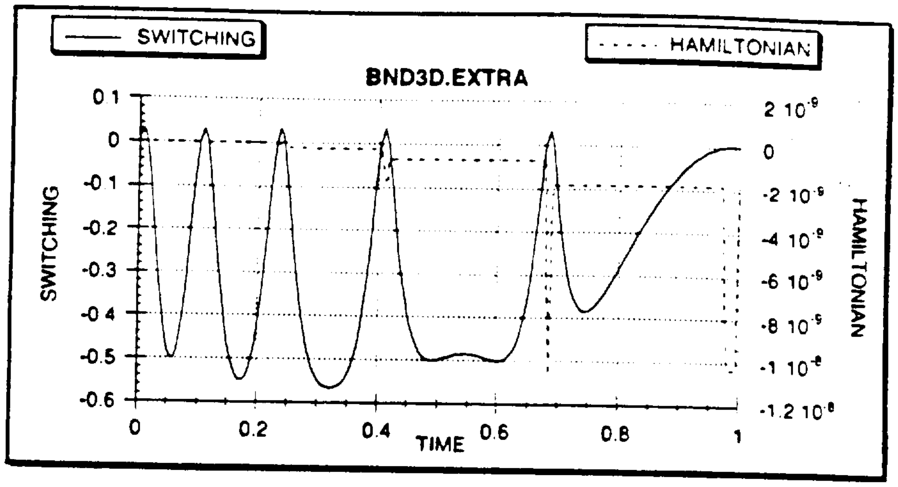

The Hamiltonian is almost zero, and very close to the tolerance. The jumps in the Hamiltonian at the switching points is a common numerical phenomenon. Also very important, note that this verifies the assumed switching structure: thrust on at the beginning, precisely ten switching points, and thrust on at the end. Finally, note the hump between the fourth and fifth burns, noting the location of such humps is often useful in deciding the location of an additional burn

Useful Information in BND3D.REINT

The file "BND3D.REINT" also supplies useful data in the form of a detailed trajectory. The complete state and costate is included. The plot below, a projection of the trajectory onto the x-y plane, was created using the raw data in the "BND3D.REINT" file.

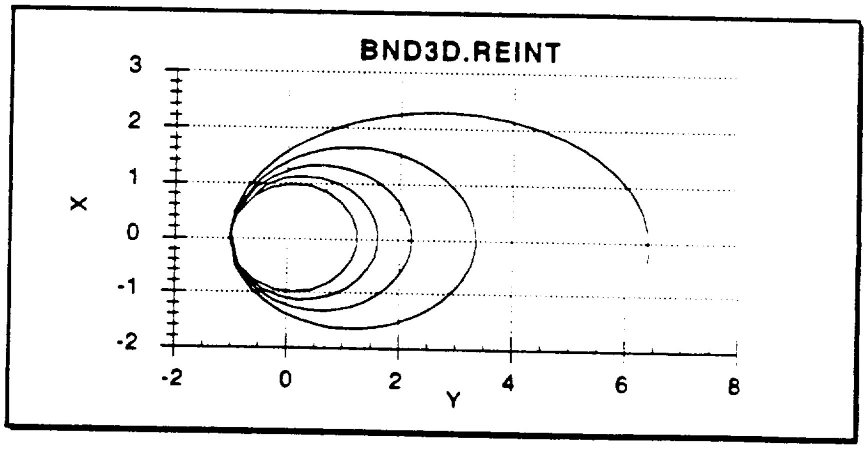

Note that this plot is rotated 90° for clarity.

VII.3. Run BND3D with Homotopy

This tutorial begins with the solution file from the "Convert MPMM3D File to BND3D File, Run BND3D;" tutorial.

Suppose we try and accomplish this change in one step, by altering the "BND3D.GUESS" file. The script ("BND3D.SCRIPT") is, simply:

```
BND3D.GUESS
0
1
0
0
1d-4
1d-10
100
BND3D.SOL
1
BND3D.REINT
```

Here is the BND3D output to the screen:

```
B.C.S ? 0
FREE FINAL TIME: 1
HOMOTOPY: 0
MU=      1.0000000000000000
REQ=     0.00000000000000000000E+00
J2=      0.00000000000000000000E+00
GO=      1.0000000000000000
BETA=    0 00000000000000000000E+00
RO=      0.00000000000000000000E+00
ROU=     0.00000000000000000000E+00
S=       0.00000000000000000000E+00
CD=      0.00000000000000000000E+00
ISP=     0.5673099999999998982
THRUST=  0.5165830000000001014
AI=      1.0000000000010538792
EI=      0.00000000000000000000E+00
OMEGAI=  0.00000000000000000000E+00
RAI=     89.9999999997066880
I-I=     28.5000000009010819
AF=      6.6001499984109l043
EF=      0.00000000000000000000E+00
OMEGAF=  0.00000000000000000000E+00
RAF=     0.00000000000000000000E+00
I-F=     0.00000000000000000000E+00

NOTE: ANGLES MUST BE IN DEGREES
M= 44
*N= 25




 ****************************************************************************
****************************************


   INITIAL DATA



   N=25       M=44      MS=10
   PRESCRIBED RELATIVE PRECISION   .10D-09
   MAXIMUM PERMITTED NUMBER OF ITERATIONS100





 ****************************************************************************
****************************************
 IT    ABS.ERR.   LEVEL1     LEVEL2     LEVEL3     RELAX. NEW   COND(M)     NORM(M)
  0    .15D-02    .15D-02    .22D-01    .11D+03
       .15D-02    .15D-02    .22D-01    .11D+03    .000    0    .39D+08     .93D-02
  1    .15D-02    .15D-02    .19D-01    .10D+03
       .15D-02    .15D-02    .19D-01    .10D+03    .003    0    .37D+08     .89D+02
  2    .15D-02    .15D-02    .48D-01    .11D+03            1    .67D+08     .89D+02
       .16D-02    .18D-02    .22D+00    .13D+03    .026
       .15D-02    .15D-02    .49D-01    .11D+03    .005
  3    .15D-02    .15D-02    .37D+00    .11D+03
       .15D-02    .15D-02    .41D+00    .11D+03    .017    0    .37D+08     .89D+02
  4    .15D-02    .15D-02    .90D+01    .46D+03
       .15D-02    .15D-02    .88D+01    .45D+03    .011    0    .36D+08     .89D+02
  5    .15D-02    .15D-02    .13D+02    .62D+03
       .21D-02    .26D-02    .18D+02    .82D+03    .056    0    .37D+08     .89D-02
       .14D-02    .15D-02    .13D+02    .61D+03    .013
  6    .14D-02    .15D-02    .18D+02    .81D+03            0    .37D+08     .89D-02
```

```
        .26D-02    .36D-02    .28D+02    .12D+04    .073
        .14D-02    .15D-02    .17D+02    .79D+03    .015
   7    .14D-02    .15D-02    .23D+02    .10D+04               0     .37D-08    .89D-02
        .31D-02    .44D-02    .40D+02    .17D+04    .092
        .14D-02    .14D-02    .22D+02    .10D+04    .019
   8    .14D-02    .15D-02    .28D+02    .13D+04               0     .36D-08    .89D-02
        .67D-02    .15D-01    .90D+02    .40D+04    .144
        .13D-02    .15D-02    .27D+02    .12D+04    .023
   9    .13D-02    .15D-02    .36D+02    .16D+04               0     .38D-08    .89D-02
        .50D-02    .11D-01    .84D+02    .36D+04    .155
        .13D-02    .15D-02    .34D+02    .15D+04    .031
  10    .13D-02    .15D-02    .48D+02    .21D+04               0     .40D-08    .89D-02
        .14D-01    .30D-01    .22D+01    .70D+04    .135
  11    .14D-01    .30D-01    .30D+03    .14D+05               0     .29D-08    .91D-02
        .34D-01    .76D-01    .61D+03    .27D+05    .038
        .14D-01    .30D-01    .30D+03    .14D+05    .004
(many lines omitted for brevity)
  62    .15D+00    .15D+01    .29D+01    .24D+03               0     .62D-06    .95D-02
        .14D+00    .15D+01    .26D+01    .20D+03    .089
  63    .14D+00    .15D+01    .26D+01    .17D+03               1     .58D-06    .95D-02
        .52D+01    .26D+02    .10D+04    .23D+06   1.000
        .14D+00    .14D+01    .24D+01    .15D+03    .062
  64    .14D+00    .14D+01    .23D+01    .28D+03               0     .68D-06    .95D-02
        .16D+00    .16D+01    .23D+01    .19D+03    .139
  65    .16D+00    .16D+01    .25D+01    .23D+03               0     .73D-06    .96D-02
        .11D+02    .30D+02    .10D+03    .50D+05   1.000
        .15D+00    .15D+01    .22D+01    .18D+03    .101
  66    .15D+00    .15D+01    .24D+01    .18D+03               1     .92D-06    .96D-02
        .96D+01    .25D+02    .47D+03    .58D+05   1.000
        .17D+00    .15D+01    .22D+01    .14D+03    .091
```

Execution was terminated early because BND3D was clearly stuck. In this type of situation, where BND3D has difficulty, it is often useful to resort to homotopy.

BND3D has a homotopy loop and is utilized, for this tutorial, with the following script (supplied as "BND3D HOMOTOPY/BND3D.SCRIPT"):

```
BND3D.GUESS
0
1
1
10
0D0
0.516583D0
0.5673D0
6.6D0
0D0
0D0
1D0
0D0
0D0
28.5D0
0
1d-4
1d-7
100
BND3D.SOL
1
BND3D.REINT
```

To make convergence easier, the tolerance was reduced to 10^{-7}. Ten homotopy steps have been suggested and the final semimajor axis is requested to be 6.6.

The output to the screen is very long for a homotopy run, and is omitted from the tutorial, however, it may be found in the file "BND3D HOMOTOPY/screen output." One the other hand, the

"BND3D HOMOTOPY/BND3D.REPORT" file indicates how the homotopy progressed:

```
   IJ,          KP,          U,              DU
     0 ,           25 ,  .9000000D+00 ,  -.1000000D+00 ,
     1 ,           22 ,  .8000000D+00 ,  -.1000000D+00 ,
     2 ,           25 ,  .7000000D+00 ,  -.1000000D+00 ,
     3 ,           30 ,  .6000000D+00 ,  -.1000000D+00 ,
     4 ,           19 ,  .5000000D+00 ,  -.1000000D+00 ,
     5 ,           19 ,  .4000000D+00 ,  -.1000000D+00 ,
     6 ,           26 ,  .3000000D+00 ,  -.1000000D+00 ,
     7 ,           19 ,  .2000000D+00 ,  -.1000000D+00 ,
     8 ,           28 ,  .1000000D+00 ,  -.1000000D+00 ,
     9 ,           -4 ,  .1387779D-15 ,  -.1000000D+00 ,
    10 ,           17 ,  .7500000D-01 ,  -.2500000D-01 ,
    11 ,           14 ,  .5000000D-01 ,  -.2500000D-01 ,
    12 ,           23 ,  .2500000D-01 ,  -.2500000D-01 ,
    13 ,           17 ,  .1457168D-15 ,  -.2500000D-01 ,
```

This indicates that even though ten steps were suggest, thirteen were required. Iterations failed for the ninth step. BND3D then adjusted the step size (DU) to one-quarter and continued until completion.

VII.4. Using MBCM3D

The following sample input file has been supplied for MBCM3D ("Tutorials/MBCM3D/MBCM3D.GUESS"):

```
Mu=      ,         1.000000000000000
Req=     ,         0.000000000000000
J2=      ,         0.000000000000000
Go=      ,         0.009800000000000
Beta=    ,         0.000000000000000
Ro=      ,         0.000000000000000
Rou=     ,         0.000000000000000
S=       ,         0.000000000000000
Cd=      ,         0.000000000000000
Isp=     ,       134.000000000000000
Thrust=  ,         0.030000000000000
Ai=      ,         3.847305000000000
ei=      ,         0.023777042000000
omegai=  ,         0.000000000000000
RAi=     ,         0.000000000000000
i-i=     ,         0.000000000000000
Af=      ,         1.500000000000000
ef=      ,         0.333333333333333
omegaf=  ,         0.000000000000000
RAf=     ,         0.000000000000000
i-f=     ,         0.000000000000000
X =      ,        -3.117680190873156
Y =      ,         2.375007893528269
Z =      ,         0.000000000000000
U =      ,        -0.309133504323169
V =      ,        -0.393443660534349
W =      ,         0.000000000000000
M =      ,         1.527000000000000
Lam-X=   ,         0.084150649480784
Lam-Y=   ,        -0.070063915070165
Lam-Z=   ,         0.000000000000000
Lam-U=   ,         0.531758699754281
Lam-V=   ,         0.737783173534899
Lam-W=   ,         0.000000000000000
Lam-M=   ,         0.782111317020586
TF =     ,        19.053149861397220
G1 =     ,         0.000000000000000
G2 =     ,         0.000000000000000
G3 =     ,        -0.656087795635957
G4 =     ,        -0.235988651457670
G5 =     ,        -0.000453092937198
G6 =     ,         0.000000000000000
G7 =     ,         0.000000000000000
G8 =     ,         0.205432772910901
G9 =     ,        -0.028605410141037
G10=     ,         0.006351966699377
ACC=     ,         0.000001001000000
ITM=     , 100
```

```
note. all angles are in degrees
```

The MBCM3D iterations, output to the screen (see file "Tutorials/MBCM3D/screen.output") follow:

```
     ITERATIONS =      1       CALLS OF VF02AD =      1

 X = -0.31176801908732E+01  0.23750078935283E+01  0.00000000000000E+00
     -0.30913350432317E+00 -0.39344366053435E+00  0.00000000000000E+00
      0.15270000000000E+01  0.84150649480784E-01 -0.70063915070165E-01
      0.00000000000000E+00  0.53175869975428E+00  0.73778317353490E+00
      0.00000000000000E+00  0.78211131702059E+00  0.19053149861397E-02
      0.00000000000000E+00  0.00000000000000E+00 -0.65608779563596E+00
     -0.23598865145767E+00 -0.45309293719800E-03  0.00000000000000E+00
      0.00000000000000E+00  0.20543277291090E+00 -0.28605410141037E-01
      0.63519666993770E-02

 F =  0.86334494474323E-07

 C =  0.00000000000000E+00  0.00000000000000E+00 -0.32815853320329E-02
      0.31803978123701E-02  0.18764580733063E-02 -0.29380971909791E-02
      0.43751691898031E-02  0.00000000000000E+00 -0.11115986860401E-01
      0.84402672955175E-03  0.00000000000000E+00 -0.16025476832695E-01
      0.00000000000000E+00  0.00000000000000E+00 -0.74267229734915E-
      0.22530999940806E-03  0.17313153969645E-03  0.00000000000000E-
     -0.22740869749960E-04 -0.21177393630278E-04  0.00000000000000E-
     -0.57569533495894E-05 -0.90623565540682E-05  0.00000000000000E+00

    ITERATIONS =      2      CALLS OF VF02AD =      2

 X = -0.31036502209544E+01  0.23928642144980E+01  0.25568446553099E-19
     -0.31138383425003E+00 -0.39175321263787E+00 -0.42523362633419E-20
      0.15270000000000E+01  0.83765314195680E-01 -0.70567482291251E-01
     -0.80198094106340E-20  0.53596562155236E+00  0.73445589093886E+00
     -0.46481533630015E-20  0.78203818243917E+00  0.19053764914975E-02
     -0.30128171897082E-19  0.12232039786695E-19 -0.65665258011739E+00
     -0.23620859757290E+00 -0.20569805044466E-03 -0.37425954093387E-20
      0.24944301628696E-20  0.20554053313719E+00 -0.28419672604799E-01
      0.64656688122166E-02

 F =  0.24910107180511E-11

 C = -0.58042583485467E-20 -0.30084192465134E-20  0.11276888358675E-02
     -0.86883230043178E-03  0.62779935362639E-03  0.50608043077460E-03
     -0.77566526491424E-03  0.88247087359436E-22  0.13660792767354E-02
     -0.65654083391520E-03 -0.15493696704000E-19  0.49871708071692E-03
     -0.15874219322676E-21 -0.21159365306815E-19  0.63892089315232E-04
     -0.38505109061338E-04  0.29911257119097E-04  0.00000000000000E+00
      0.38208767713602E-06 -0.85325721599361E-07  0.10191807071110E-19
      0.24236870608263E-05  0.30674883788606E-05  0.69050718954859E-20

                                [lines omitted]

    ITERATIONS =      5      CALLS OF VF02AD =      5

 X = -0.31113166253579E+01  0.23830894092665E+01  0.69908109877120E-20
     -0.31009703414240E+00 -0.39273127003103E+00 -0.20284578276292E-20
      0.15270000000000E+01  0.83949089044448E-01 -0.70300590739595E-01
     -0.55823767494574E-20  0.53348632289741E+00  0.73634049255129E+00
     -0.79958433860932E-20  0.78211132986574E+00  0.19073788066349E-02
     -0.75789120825379E-20 -0.15695206359468E-20 -0.65608762138191E+00
     -0.23598854759671E+00 -0.45317463073011E-03 -0.62836395106568E-17
     -0.79771334223064E-17  0.20543273853632E+00 -0.28605461858627E-01
      0.63519253321692E-02

 F =  0.21217202906824E-25

 C = -0.58129998768682E-20  0.89436352481144E-21  0.20736086980833E-06
     -0.77946793908268E-07  0.33018123685169E-06  0.20001798439750E-07
     -0.71132788548312E-07  0.67254666259869E-20 -0.35907479656316E-07
     -0.49651912359394E-07  0.46073402965487E-20  0.10904882264651E-06
     -0.20884862884158E-20 -0.84790043164797E-20  0.83128526284781E-09
     -0.49293613635371E-09  0.35773772832925E-09  0.71054273576010E-14
      0.51403326040145E-11 -0.17852386235973E-11 -0.34634033790215E-21
      0.33072211635954E-10  0.21167068098293E-10  0.39802325503391E-16

    THE PRINTING OF THE LAST ITERATION GIVES THE
    VALUES THAT ARE RETURNED BY SUBROUTINE VF02AD


---SOLUTION CONVERGED---
X =     -0.31113166253579E+01
    0.23830894092665E+01
    0.69908109877120E-20
   -0.31009703414240E+00
   -0.39273127003103E+00
   -0.20284578276292E-20
    0.15270000000000E+01
 0.839490890444448E-01
-0.703005907395950E-01
-0.558237674945740E-20
 0.533486322897410E+00
 0.736340492551290E+00
-0.799584338609320E-20
 0.782111329865740E+00
 0.190737880663490E+02
-0.757891208253790E-20
-0.156952063594680E-20
-0.656087621381910E+00
-0.235988547596710E+00
-0.453174630730110E-03
-0.628363951065680E-17
-0.797713342230640E-17
 0.205432738536320E+00
-0.286054618586270E-01
 0.635192533216920E-02
```

Appendix A GSHOOT's File Format

The input file "" for "GSHOOT" has a specific file format. The file must consist of exactly 14 lines. The variables read from this file have a specific order: MU, GO, ISP, THRUST, MO, AO, EO, WO, AD, ED, WD, TMAX, NGS, and NIX. All variables are of the type REAL except the last two, NGS and NIX, which are of the type INTEGER. An example file is listed below.

```
 Mu       = 1.00
 Go       = 1.00
 Isp      = 0.5673
 Thrust   = 0.5166
 Mo       = 10.0000
 ao       = 1.00000
 eo       = 0.000
 wo       = 0.000
 ad       = 1.285
 ed       = 0.219
 wd       = 0.000
 TMAX     = 0.000
 NGS      = 100
 NIX      = 3
```

On each line intended to supply a REAL variable, the FORTRAN FORMAT layout is (1X,A9,F30.15); for INTEGER variables, this statement is (1X,A9,I10). Therefore, each line starts with a blank space followed by nine characters, all of which are ignored. Only the numerical data following is used.

Appendix B The PAT2D and PAT3D File Formats

The PAT2D file format is used by MPMM2D and PAT2D. The PAT3D file format is only used by MPMM3D. They are called the PAT formats because all of the information supplied by the PAT2D format is used by PAT2D; only some of the information is used by MPMM2D and MPMM3D. Exactly what information is used by MPMM2D and MPMM3D is described in Chapter IV.

The PAT2D format is represented below:

```
TOL  = #
MU   = #
T    = #
GO   = #
ISP  = #
AO   = #
EXO  = #
EYO  = #
AF   = #
EXF  = #
EYF  = #
a    = #
ex   = #
ey   = #
NORB =  2
NODE =  3
SEL  =  1
index,x,y,u,v,m,lx,ly,lu,lv,lm,tf,g1,g2,g3,g4,g5,g6
  1, #, #, #, #, #, #, #, #, #, #, #, #, #, #, #, #, #,
  2, #, #, #, #, #, #, #, #, #, #, #, #, #, #, #, #, #,
  3, #, #, #, #, #, #, #, #, #, #, #, #, #, #, #, #, #,
  4, #, #, #, #, #, #, #, #, #, #, #, #, #, #, #, #, #,
a    = #
ex   = #
ey   = #
NODE =  3
SEL  =  2
index,x,y,u,v,m,lx,ly,lu,lv,lm,tf,g1,g2,g3,g4,g5,g6
  1, #, #, #, #, #, #, #, #, #, #, #, #, #, #, #, #, #,
  2, #, #, #, #, #, #, #, #, #, #, #, #, #, #, #, #, #,
  3, #, #, #, #, #, #, #, #, #, #, #, #, #, #, #, #, #,
  4, #, #, #, #, #, #, #, #, #, #, #, #, #, #, #, #, #,
a    = #
ex   = #
ey   = #
NODE =  3
SEL  =  3
INDEX,X,Y,U,V,M,TF,L1,L2
  1, #, #, #, #, #, #, #, #,
  2, #, #, #, #, #, #, #, #,
  3, #, #, #, #, #, #, #, #,
  4, #, #, #, #, #, #, #, #,
```

where the symbol "#" is used in place of digits. The first eleven lines give constants for the orbit transfer problem in type REAL. These have a fixed order: TOL, MU, T, GO, ISP, AO, EXO, EYO, AF, EXF, and EYF. Their descriptions follow:

TOL	THE SOLUTION TOLERANCE
MU	THE GRAVITATIONAL CONSTANT FOR THE CENTRAL BODY
T	THE THRUST LEVEL OF THE ROCKET MOTOR
GO	EARTH'S GRAVITATIONAL ACCELERATION AT SEA-LEVEL [ONLY USED FOR GET MOTOR FUEL CONSUMPTION]
ISP	SPECIFIC IMPULSE OF ROCKET MOTOR
AO	INITIAL ORBIT SEMIMAJOR AXIS
EXO	INITIAL ORBIT X-COMPONENT ECCENTRICITY
EYO	INITIAL ORBIT Y-COMPONENT ECCENTRICITY
AF	FINAL ORBIT SEMIMAJOR AXIS
EXF	FINAL ORBIT X-COMPONENT ECCENTRICITY
EYF	FINAL ORBIT Y-COMPONENT ECCENTRICITY

Note that these apply to the transfer as a whole, esp. when referring to the initial and final orbits. The FORTRAN FORMAT edit descriptors for each of these first eleven lines is (1X,A6,E27.20).

The PAT3D format up to this point is identical except that HXO, HYO, HZO, EXO, EYO, HXF, HYF, HZF, EXF, EYF replace AO, EXO, EYO, AF, EXF, and EYF. Their descriptions follow:

```
HXO .......... INITIAL ORBIT X-COMPONENT ANG. MOMENTUM
HYO .......... INITIAL ORBIT Y-COMPONENT ANG. MOMENTUM
HZO .......... INITIAL ORBIT Z-COMPONENT ANG. MOMENTUM
EXO .......... INITIAL ORBIT X-COMPONENT ECCENTRICITY
EYO .......... INITIAL ORBIT Y-COMPONENT ECCENTRICITY
HXF .......... FINAL ORBIT X-COMPONENT ANG. MOMENTUM
HYF .......... FINAL ORBIT Y-COMPONENT ANG. MOMENTUM
HZF .......... FINAL ORBIT Z-COMPONENT ANG. MOMENTUM
EXF .......... FINAL ORBIT X-COMPONENT ECCENTRICITY
EYF .......... FINAL ORBIT Y-COMPONENT ECCENTRICITY
```

For both PAT2D and PAT3D formats, the next line indicates how many intermediate transfer orbits there are. The variable NORB takes on this value. The FORTRAN FORMAT edit descriptors for this line is (1X,A6,I3). This same layout is used for the next two lines, both also containing INTEGER data. These lines specify data for the first burn. NODE is how many nodes, not counting the first one, are to be used for this burn. Specifying a "3" for NODE indicates that four lines of data will describe the burn.

The line after NODE's is for SEL. The variable SEL indicates which method should be used. Note that in the PAT2D representation above, three different values are given for SEL. A "1" indicates that the data below is in a multiple-point shooting format but Direct Collocation with Nonlinear Programming (DCNLP) should be used in the first attempt to obtain a solution. A "2" also indicates that the data below is in a multiple-point shooting format but that multiple-point shooting should be used in the first attempt to obtain a solution A "3" indicates that the data below is in a DCNLP format and DCNLP should be used in the first attempt to obtain a solution. The following table summarizes:

SEL	Guess Format	Method to try First
1	Multiple Shooting	DCNLP
2	Multiple Shooting	Multiple Shooting
3	DCNLP	DCNLP

No matter what format the data lines will be in, the line following SEL's line has the FORMAT edit descriptors (1X,A). The contents of this line are ignored.

Note that since MPMM3D cannot accept SEL=3, in PAT2D only SEL=1 or SEL=2 is acceptable.

The next NODE+1 lines are the guess data for that burn. The FORMAT edit descriptors are (1X,I3,A1,50(D27.20,A1) irrespective of which guess format is intended. Considering only PAT2D, the multiple-point shooting format has 18 elements in each line. These elements are in the following order: INDEX, X, Y, U, V, M, LX, LY, LU, LV, LM, TF, G1, G2, G3, G4, G5, G6. "INDEX" numbers each line; the first line represents the initial point for this burn and last line represents the final point for this burn. The lines for each burn are evenly spaced. "X, Y, U, V" are the Cartesian components of the 2D position and velocity vectors, respectively. "M" is the mass. "LX, LY, LU, LV, LM" are the values of the Lagrange multiplier functions/or costates, λ_r, λ_v, and λ_m, respectively. "TF" is the length of time the burn lasts. "G1, G2, G3" are the constant Lagrange multipliers, ν_f, associated with the final boundary conditions. "G4, G5, G6" are the constant Lagrange multipliers, ν_o, associated with the initial boundary conditions.

For PAT3D, the multiple-point shooting format has 26 elements in each line. These elements are in the following order: INDEX, X, Y, Z, U, V, W, M, LX, LY, LZ, LU, LV, LW, LM, TF, G1, G2, G3, G4, G5, G6, G7, G8, G9, G10. Their meanings are simple extensions of those from PAT2D.

The DCNLP format has 9 elements in each line. These elements are in the following order: INDEX, X, Y, U, V, M, TF, L1, L2. All of these are as described above, except "L1, L2" which are the Cartesian components in the inertial frame of the thrust direction unit vector.